TAMPERE UNIVERSITY OF TECHNOLOGY

TONI LÄHTEENSUO

LINEARITY REQUIREMENTS IN LTE-ADVANCED MOBILE TRANSMITTER

Master of Science Thesis

Examiner: Professor Mikko Valkama
Examiner and topic approved in the Computing and Electrical Engineering Faculty Council meeting on 3 October 2012

ABSTRACT

TAMPERE UNIVERSITY OF TECHNOLOGY
Master's Degree Programme in Electrical Engineering
LÄHTEENSUO, TONI : Linearity Requirements in LTE-Advanced Mobile Transmitter
Master of Science Thesis, 85 pages
May 2013
Major: Wireless Communications
Examiner: Professor Mikko Valkama
Co-Supervisor: Antti Piipponen
Keywords: Long Term Evolution, LTE-Advanced, linearity, radio, transmitter

LTE-Advanced (LTE-A) is an emerging wireless communication system, which builds on the foundation of Long Term Evolution (LTE), adding many unprecedented arrangements in utilization of radio resources. Most notably LTE-A allows allocating non-contiguous resources in frequency domain, which significantly enhances the flexibility of the multiple access scheme. Contiguous and non-contiguous carrier aggregation, both intra- and inter-band, are essential components of LTE-A. However, these features set very high requirements especially for mobile transmitters, which simultaneously should be cheap, small, linear and power efficient.

Linearity in particular is an important aspect because non-contiguous allocation is prone to produce severe intermodulation distortion, which will degrade transmit signal quality and cause interference to users operating on adjacent frequency ranges. Because variety of wireless systems have to coexist and interoperate in the scarce spectrum supply, there are stringent requirements for unwanted spectrum emissions.

There is an inherent trade-off between linearity and power efficiency. Therefore it is significantly difficult to fulfill regulatory spectrum emission requirements with current transmitter technology without sacrificing battery life when operating near the maximum output power. As a compromise LTE-A allows relaxations to maximum output power requirement according to the used submodulation, number of used resource blocks and possible coexistence situations. In practice the transmitter power amplifier (PA) input power is reduced which linearises the PA response. However, this forces the PA to operate less efficiently. This simultaneously constrains using larger constellations and/or higher coding rates because of degraded link budget. Therefore maximum power reduction (MPR) should be minimized.

In this thesis LTE and LTE-A are introduced and the models and effects of transmitter nonlinearity are discussed. Linearity requirements of mobile LTE-A transmitter are evaluated using both simulations and measurements in different transmission scenarios, including LTE and LTE-A releases from 8 to 12. The results of the analysis can be used in development of intelligent radio resource management algorithms, advanced MPR specifications and digital predistortion systems.

TIIVISTELMÄ

TAMPEREEN TEKNILLINEN YLIOPISTO
Sähkötekniikan koulutusohjelma
LÄHTEENSUO, TONI: Lineaarisuusvaatimukset LTE-Advanced mobiililähettimessä
Diplomityö, 85 sivua
Toukokuu 2013
Pääaine: Langaton tietoliikenne
Tarkastaja: Professori Mikko Valkama
Ohjaaja: Antti Piipponen
Avainsanat: Long Term Evolution, LTE-Advanced, lineaarisuus, radio, lähetin

LTE-Advanced (LTE-A) on Long Term Evolution:iin (LTE) perustuva kehittyvä langaton tietoliikennejärjestelmä, joka lisää monia uusia ominaisuuksia radioresurssien käyttömahdollisuuksiin. Erityisesti LTE-A:ssa voidaan allokoida resursseja epäjatkuvasti taajuustasossa, mikä lisää merkittävästi monipääsymenettelyn joustavuutta. Myös jatkuva ja epäjatkuva kantoaaltojen yhdistäminen (carrier aggregation) on olennainen osa LTE-A:ta. Nämä ominaisuudet asettavat kuitenkin tiukkoja vaatimuksia eritoten mobiililähettimille, joiden tulisi olla samanaikaisesti halpoja, pienikokoisia, lineaarisia ja energiatehokkaita.

Erityisesti lineaarisuus on tärkeä ominaisuus, koska epäjatkuva taajuusallokaatio on altis aiheuttamaan voimakasta intermodulaatiosäröä, joka heikentää lähetetyn signaalin laatua ja häiritsee ympäröivillä taajuusalueilla toimivia käyttäjiä. Koska useat langattomat järjestelmät joutuvat jakamaan rajallisen spektrin, ei-toivotuille häiriöille on asetettu tiukat rajoitukset.

Energiatehokkuus ja lineaarisuus ovat ristiriitaisia vaatimuksia. Nykyisellä lähetintekniikalla on hankalaa saavuttaa emissiorajoja, koska ei-toivotut häiriöt ovat voimakkaita toimittaessa lähellä suurinta sallittua lähetystehoa. Kompromissina LTE-A sallii lievennyksiä lähetystehovaatimukseen käytetyn modulaation, resurssilohkojen määrän ja vierekkäisten järjestelmien perusteella. Käytännössä lähettimen tehovahvistimen sisääntulotehoa lasketaan, mikä linearisoi vahvistimen vastetta. Tämä pakottaa tehovahvistimen toimimaan huonommalla hyötysuhteella samalla rajoittaen suurempien konstellaatioden ja/tai koodaussuhteiden käyttöä heikentyneen linkkibudjetin vuoksi. Täten lievennysten tarve pitäisi minimoida.

Tässä diplomityössä esitellään LTE- ja LTE-A-järjestelmät sekä käsitellään LTE-A-mobiililähettimen epälineaarisuuksien mallinnusta ja vaikutuksia. LTE-A-mobiililähettimen lineaarisuusvaatimuksia on tarkasteltu käyttäen sekä simulaatioita että mittauksia erilaisissa lähetystilanteissa, jotka kattavat LTE- ja LTE-A-versiot 8-12. Analyysin tuloksia voidaan hyödyntää älykkäiden radioresurssien hallinta-algoritmien, kehittyneiden tehovähennysmäärittelyiden sekä digitaalisten esivääristimien kehityksessä.

PREFACE

This Master of Science Thesis was written at the Department of Electronics and Communications Engineering at Tampere University of Technology during the winter 2012-2013.

I would like to thank all people who have supported me throughout the time I worked at the department. Vesa Lehtinen and Lauri Anttila with whom I shared the office room have made my stay pleasant and always patiently provided help with all things I have asked. The common coffee breaks of the department have helped me to get to know a lot of great people and made it possible to put my mind away from work for a moment during the days.

Especially I would like to thank Petri Vasenkari and Antti Piipponen from Nokia Corporation about interesting and challenging working tasks which have made me to learn a great deal of new things. Antti also provided inspiring and thoughtful insights while co-supervising this thesis.

Mikko Valkama has been my supervisor during the two years I have spent at the department. I would like to thank Mikko for offering me the opportunity to work at the department and the flexibility with all practical things. I would also like to thank Mikko for supervising this thesis.

Last but not least thanks to all my friends who have made studying at TUT a wonderful time in my life. And of course thanks to my family Seija, Harri, Matti, Tero and Pauliina for all the support I have gotten from you.

In Tampere 16.04.2013

Toni Lähteensuo

TABLE OF CONTENTS

1. Introduction 1
2. Overview of LTE 3
2.1 Third Generation Partnership Project 4
2.2 General Properties of LTE 5
2.3 LTE Downlink: OFDMA 9
2.4 LTE Uplink: SC-FDMA 13
3. Modelling of Transmitter Nonlinearities 16
3.1 Basics of I/Q Signals 17
3.2 Transmitter Performance Metrics 20
3.3 Transmitter Architectures 25
3.4 Power Amplifier Nonlinearity 28
3.5 Baseband I/Q Nonlinearity 35
3.6 Other Transmitter Nonidealities 36
4. LTE/LTE-A Standard Evolution and Impact on Mobile Transmitter Requirements 41
4.1 Release 8 and 9 (LTE) and Contiguous Allocation in Single Carrier . . 41
4.2 Release 10 (LTE-A) and Carrier Aggregation 46
4.3 Release 11 (LTE-A) and Non-contiguous Allocation in Single Carrier . 51
4.4 Release 12 (LTE-A) and Non-contiguous Carrier Aggregation 52
5. Simulation and Measurement Examples and Results 56
5.1 Simulation Model and Measurement Setup 56
5.2 Single Contiguous Transmission Block (rel. 8) 58
5.3 Contiguously Aggregated Carriers (rel. 10) 64
5.4 Non-contiguous Transmission in Single Carrier (rel. 11) 68
5.5 Intra-band Non-contiguous Carrier Aggregation (rel. 12) 71
5.6 Own Receiver Desensitization (rel. 11) 73
6. Conclusions 77
References 80

LIST OF ABBREVIATIONS

3GPP	3rd Generation Partnership Project
A-MPR	Additional Maximum Power Reduction
ACLR	Adjacent Channel Leakage Ratio
AM-AM	Amplitude-to-Amplitude
AM-PM	Amplitude-to-Phase
AN	Access Network
CC	Component Carrier
CIM3	Third-Order Counter-Intermodulation
CIM5	Fifth-Order Counter-Intermodulation
CNR	Carrier-to-Noise Ratio
CT	Core Network and Terminals
DC	Direct Current
DFT	Discrete Fourier Transform
DPD	Digital Predistortion
DUT	Device Under Test
E-UTRA	Evolved Universal Terrestrial Radio Access
EDGE	Enhanced Data rates for GSM Evolution
EPC	Evolved Packet Core
EVM	Error Vector Magnitude
FDD	Frequency Division Duplexing
FDMA	Frequency Division Multiple Access
GERAN	GSM EDGE Radio Access Network
GSM	Global System for Mobile Communications
HARQ	Hybrid and Automatic Repeat Request
HSDPA	High Speed Downlink Packet Access
HSPA	High Speed Packet Access
I/Q	In-Phase and Quadrature
ICI	Inter-Carrier Interference
IF	Intermediate Frequency
IIP3	Input Referred Third-Order Intercept Point
IMD3	Third Order Intermodulation
IP3	Third-Order Intercept Point
IRR	Image rejection ratio

ISI	Inter-Symbol Interference
LO	Local Oscillator
LTE	Long Term Evolution
LTE-A	Long Term Evolution Advanced
LTI	Linear and Time-Invariant
MBWPS	Measurement Bandwidth Power Spectrum
MIMO	Multiple-Input and Multiple-Output
MPR	Maximum Power Reduction
MU-MIMO	Multi-User Multiple-Input Multiple-Output
OFDMA	Orthogonal Frequency Division Multiple Access
OIP3	Output Referred Third-Order Intercept Point
PA	Power Amplifier
PAPR	Peak-to-Average Power Ratio
PHS	Personal Handy-phone System
PSD	Power Spectral Density
QAM	Quadrature Amplitude Modulation
QPSK	Quadrature Phase Shift Keying
RAN	Radio Access Network
RB	Resource Block
RMS	Root Mean Square
RRM	Radio Resource Management
SA	Service and System Aspects
SAE	System Architecture Evolution
SC-FDMA	Single Carrier Frequency Division Multiple Access
SEM	Spectrum Emission Mask
SNR	Signal-to-Noise Ratio
TDD	Time Division Duplexing
TDMA	Time Division Multiple Access
TSG	Technical Specifications Group
UE	User Equipment
UMTS	Universal Mobile Telecommunications System
UTRA	Universal Terrestrial Radio Access
VSA	Vector Signal Analyzer
VSG	Vector Signal Generator
WG	Working Group

1. INTRODUCTION

Wireless communication systems have been developing rapidly throughout the last few decades. The number of mobile-cellular subscriptions has had a six-fold increase during the last ten years and reached approximately 6 billions as illustrated in Figure 1.1. The demand for data transfer capacity in wireless networks is increasing accordingly as higher data rates have become available and affordable. An exponential growth in mobile traffic is expected resulting in 15- to 30-fold increase during the next five years and up to 1000-fold increase during the next decade. The predicted staggering growth is partly due to machine-to-machine communications which will increase remarkably as internet of things evolves from a concept to reality. There has been forecasts that thousand devices per each person will be using wireless communications in 2020. The challenge for mobile operators and manufacturers will be satisfying these data demands. [1; 2; 3]

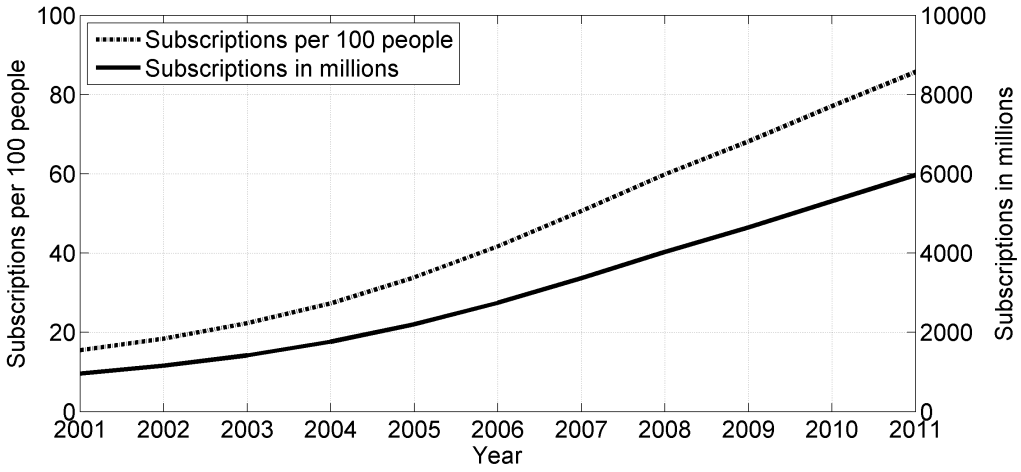

Figure 1.1. Mobile cellular subsriptions in the world during 2001-2011 [1].

The 3rd Generation Partnership Project (3GPP), a head organization for telecommunications standard development, is responding to this challenge by constantly developing enhancements to modern telecommunication systems like Long Term Evolution (LTE) and High Speed Packet Access (HSPA). Throughput is more than doubled in LTE when compared to HSPA peak data rate, being over 100 Mbps in downlink and 50 Mbps in uplink. At the same time round trip times have shortened significantly. Still further improvements are needed and they are introduced in new 3GPP LTE releases. [4; 5; 6; 7]

However, improvements aiming at higher capacity like more efficient spectrum usage and wider transmission bandwidths also set more stringent requirements for transceivers. Signal quality should be as good as possible to enable using high-order modulation and low coding rate to reach maximum throughput. Therefore interference levels must be kept in control. At the same time current consumption should not rise neither in base stations nor mobile devices. Especially challenging are mobile transmitters because they should be power efficient, cheap, small and linear all at the same time. There is a inherent trade-off between linearity and power efficiency, meaning that better linearity means worse power efficiency. Typically all the requirements for transmission power level and unwanted emissions are impossible to fulfill simultaneously and controlled relaxations are needed. In practice this means lower maximum transmission power to reach emission requirements. [8; 9]

This Master of Science thesis concentrates on linearity requirements in mobile LTE and LTE-Advanced (LTE-A) transmitters and their evolution through different LTE releases. The main idea is to illustrate how non-linearities in transmitter affect transmitted spectrum and how it has to be taken into account in system specifications. Different transmission scenarios are evaluated using primarily simulations and also measurements where appropriate. The main transmission schemes considered are multi-cluster transmission in single carrier (release 11) and in contiguously (release 10) as well as in non-contiguously (release 12) aggregated carriers. These are compared to the baseline which is contiguous allocation in single carrier (release 8). Results of the analysis can be used in further transmitter and especially power amplifier development and also in development of more intelligent radio resource management and scheduling algorithms.

In chapter two an overview of 3GPP standardization and LTE on overall is presented. In the third chapter nonlinear phenomena in transmitter and other transmitter impairments are discussed and their mathematical models are introduced. In the fourth chapter the development of LTE standard is discussed release-wise from the radio performance and transmitter requirements point of view. The Fifth chapter includes simulation and measurement results of different transmission scenarios. Finally conclusions are presented in chapter six.

2. OVERVIEW OF LTE

The development of LTE begun already in 2004 when 3GPP launched a study item on Evolved Universal Terrestrial Radio Access (E-UTRA). At that time Universal Mobile Telecommunications System (UMTS) was being intensively deployed and the deployment of High Speed Downlink Packet Access (HSDPA) was about to begin. The usage of mobile data was heavily increasing and it was already apparent that more performance and a more efficient system would be required to fulfill future demands. [4; 10]

The discussions and studies under the E-UTRA study item resulted in requirements for LTE. These requirements included reduced delay during connection establishment and transmission latency, increased user data rates, higher spectral efficiency and greater flexibility in spectrum usage both in new and already existing bands. The theoretical performance of LTE release 8 and HSPA release 7 are represented in table 2.1. It became also clear that whole network architecture would have to be simplified to reach these targets. [4; 11]

Table 2.1. Maximum theoretical performance values of LTE release 8 compared to HSPA release 7. [12]

	LTE release 8	**HSPA (release 7)**
Bandwidth	1.4 – 20 MHz	5 MHz
Peak transmission rate in downlink	300 Mbit/s	28 Mbit/s
Peak transmission rate in uplink	75 Mbit/s	11.5 Mbit/s
Peak spectrum efficiency in downlink	15 (bit/s)/Hz	5.6 (bit/s)/Hz
Peak spectrum efficiency in uplink	3.75 (bit/s)/Hz	2.3 (bit/s)/Hz
Latency	$<$ 10 ms	25 ms

In December 2008 the first LTE release (release 8) was frozen, meaning that its functionalities were no more modified. Release 8 has been the basis for the LTE-devices which are on the market at the time of writing this thesis (Spring 2013). However, the development of LTE, or other existing 3GPP technologies, has not ceased and new releases have already seen the daylight. Release 11 is already ready and release 12 specifications are in preparation.[13; 14]

In the following sections properties of LTE and LTE-A, which the system is called from release 10 onward, are described. First a look is taken on 3GPP standardization in general. Then properties of LTE and LTE-A are discussed followed by the specifics of LTE downlink and LTE uplink. However, a more detailed characterization of different releases regarding to transmitter requirements is done in chapter 4.

2.1 Third Generation Partnership Project

When compared to traditional transmission media such as copper lines or optical fibres wireless spectrum is a scarce resource which is shared with multiple different technologies which may interfere each other. Therefore regulatory bodies such as International Telecommunication Union, Radio Communication Sector (ITU-R) play a significant role in the evolution of radio technologies. They decide, together with national regulator, how much bandwidth and which part of the spectrum is available for a certain technology or service. Another key players are standard and technology developers, such as 3GPP and its organizational partners. As a whole the relationship between these authorities can be summarized as regulatory bodies (ITU-R and regional authorities) define the usable bandwidth and standards (3GPP and its partners) define the spectral efficiency. Total throughput of a system therefore depends on both parties. [4; 15]

Standardization work in 3GPP is divided between four different Technical Specifications Groups (TSG) and further between different Working Groups (WG) under TSGs. GSM EDGE Radio Access Network (GERAN) TSG works with Global System for Mobile Communications (GSM) and Enhanced Data rates for GSM Evolution (EDGE) radio access technologies. 3G and LTE issues belong to the Radio Access Network (RAN) TSG. Service and System Aspects (SA) TSG takes care of overall system architecture and services of 3GPP technologies. Finally Core Network and Terminals (CT) TSG handles terminal interfaces and capabilities and core network part of the systems.

LTE radio performance issues, which also this thesis deals with, and base station conformance testing belong the the RAN TSG and more specifically to the Radio Performance WG, typically denoted as RAN WG4. There are also four other WGs under RAN TSG. WG1 deals with physical layer of the radio interface. WG2 handles radio interface architecture and protocols, radio resource management (RRM) and upper layer services provided by the physical layer. WG3 works with universal terrestrial radio access (UTRA) and Evolved-UTRA (E-UTRA) network architectures and protocols. Finally WG5 is responsible for mobile terminal conformance testing.

Member companies of 3GPP participate in meetings where additions and modifications to the specifications are discussed and agreed on. Meeting documents are

publicly available and accessible through 3GPP website. New versions of specifications are published four times in a year. In addition to technical specifications 3GPP produces also technical reports which are intended for capturing background for specifications e.g. simulation and measurement results. [16; 17; 18]

Release Freezing Process

At a certain point a release is freezed, meaning that new features or functionalities are no more added. Later on the freezing is made permanent so that no modifications to existing features are made. This enables efficient device development and implementation because there is a point where no support for future features needs to be added. Since release 7 the trend has been to do the freezing in three separate stages. [14; 19]

A stage one freeze stands for freezing the functional content of what will be finalized in a certain release. In practise this means that some of the originally planned functionality may be transferred to a later release and no new functionalities can be introduced. From stage one freeze onwards work will concentrate on completing the missing parts and correcting detected errors. [4; 14]

In the second stage the protocol specifications are freezed and backwards compatibility is guaranteed. This means that the protocol versions can be used for commercial implementations. Older information is no more deleted but some extensions may still be included. Equipment based on the initial stage two freeze version will work but newer software versions can take advantage of the added extensions and therefore work more optimally. [4; 14]

In the final freeze stage no changes to specifications are allowed. Devices are out on the market and functionalities have been tested in real usage environment. Potential improvements will be done in later releases. Reasons for these improvements may be e.g. that some errors have not been detected before. Naturally the later releases will also include totally new features and continue the evolution of the system. [4; 14]

The freezing process described here is valid for a single release. However, several releases are developed parallel to each other. When a release has reached the first freeze stage studies concerning newer releases are already in good progress. This will guarantee a constant and continuing evolution and help to respond to the steadily growing demands. [14]

2.2 General Properties of LTE

A single LTE carrier can have six different bandwidths: 1.4 MHz, 3 MHz, 5 MHz, 10 MHz, 15 MHz and 20 MHz. These carriers can also be aggregated contiguously

(release 10) and non-contiguosly in a single band (expected in release 12). Non-contiguous carrier aggregation can be done even between different E-UTRA bands, either with single uplink carrier, i.e. transmission from mobile to base station, and two downlink carriers, i.e. transmissions from base station to mobile, active (release 10). Operation with two active uplink carriers, both within single band and separate bands, is expected in release 12. These capabilities are illustrated in Figure 2.1.

LTE is very flexible in frequency domain and can adapt to different deployment scenarios. Flexible carrier bandwidth also enables smooth migration from one radio access technology to another in a case where spectrum becomes gradually available. Resources can be also allocated flexibly in fixed size resource blocks in frequency domain within a single carrier. In Figure 2.1 it can be seen that carrier bandwidth is wider than the allocable region, leaving room for guard bands, which protect neighbouring channels from unwanted emissions. One mobile may transmit using only resources allocated to it, which are here called active resource blocks. In time domain resource allocation is done in 1 ms time intervals, which provides flexibility also in time domain. Modulations include quadrature phase shift keying (QPSK) and quadrature amplitude modulation (QAM) with constellation sizes of 16 and 64, though 64-QAM is optional in uplink. Coding rate can vary from 0.076 to 0.93. [4; 10; 11; 20]

LTE supports both frequency division duplexing (FDD) and time division duplexing (TDD) which are typically used in different geographical areas but can also coexist. The FDD mode of LTE enables full duplex operation, meaning that uplink and downlink can operate simultaneously using separate frequencies. In TDD mode uplink and downlink use the same frequencies but are not overlapping in time domain. In both FDD and TDD modes a single mobile can use certain frequency and time resources which are allocated by the network and may or may not utilize the whole transmission channel bandwidth. The multiple access scheme is discussed more thoroughly in section 2.3. FDD mode is more challenging for the mobile because uplink transmission can interfere downlink reception. This issue has been considered in chapter 5.6. [4; 21; 22]

To minimize retransmission overhead LTE uses hybrid and automatic repeat request (HARQ) with soft combining and incremental redundancy. This means that when cyclic redundancy check of a transmission block does not match, the packet is stored in the receiver and a repeat request is sent. The retransmitted block has different coding bits compared to the original one and it is combined with the old one. It is possible that none of the blocks has arrived without errors but the combination can still be correctly decoded. [4; 11]

To optimize spectral efficiency and terminal power efficiency LTE uses an asymmetric multiple access scheme. Orthogonal Frequency Division Multiple Access

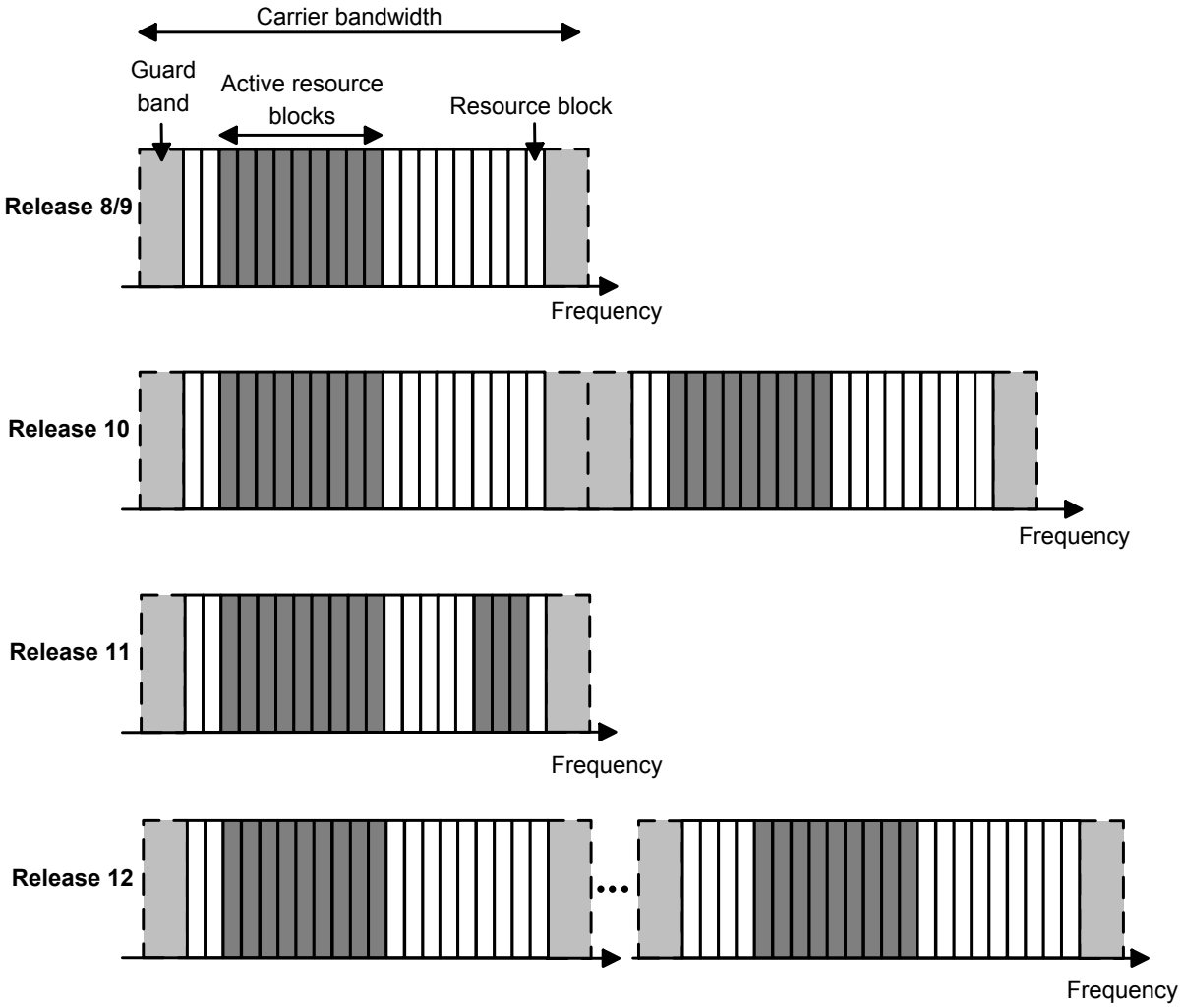

Figure 2.1. Uplink transmission configuration in releases 8 – 12.

(ODFMA) is used in downlink and Single Carrier Frequency Division Multiple Access (SC-FDMA) in uplink. SC-FDMA was chosen for the uplink transmission because it offers significantly lower peak-to-average power ratio (PAPR) than ODFMA with little additional calculation complexity. This leads to better efficiency and lower current consumption in mobile terminals, which in practice means longer battery life. Properties of LTE downlink and uplink are discussed more thoroughly in chapters 2.3 and 2.4. [4; 10; 11; 22]

Multiple-input and multiple-output (MIMO) is an integral feature of LTE. In release 8 MIMO is used to improve reception by using a diversity antenna in mobile receiver and also for space-time coding, a diversity method where two antennas send a single precoded data stream. Consecutive data symbol pairs having different precoding are sent on successive time instants. In the receiver the symbols can be decoded and combined with the help of linear algebra. Interference is suppressed in this process. In addition to space-time coding also space-frequency block coding can be used. The idea is same as in space-time coding, but instead of different

time instants different subcarriers are used. MIMO is also used for obtaining higher throughput by transmitting independent data streams in 2-by-2 or 4-by-4 antenna configuration, i.e. for spatial multiplexing. Spatial multiplexing can be open-loop or closed-loop. In the open loop approach no channel state information is used whereas in the closed-loop version channel state information is used to enhance precoding. In release 8 five different mobile terminal categories have been defined only the lowest category terminals not supporting spatial multiplexing in downlink. From release 10 onward spatial multiplexing is also supported in uplink. [11; 22]

LTE uses also multi-user MIMO (MU-MIMO) to improve cell capacity. In general the idea is to use same time-frequency resources for many users. In downlink the transmission scenario is point-to-multipoint. When spatial multiplexing cannot be used when transmitting to a specific mobile due to highly correlating spatial channels the same time-frequency resource can be still used to send data to another mobile. This increases cell capacity even though a single mobile does not get any boost to the data speed. In uplink MU-MIMO is used to allow more mobiles to transmit in the same cell simultaneously. The uplink scheme is called multiple access MU-MIMO. The idea is to use pre-coding to enable two transmitters to use overlapping resource elements when receiver capabilities allow it. In practise the receiver must have as many antennas as there are independent data streams to be received. In theory MU-MIMO doubles the cell capacity. It is possible to send also the reference signals used in channel estimation in overlapping resources, but in practice orthogonal resources are used. Using MU-MIMO becomes advantageous when there are a lot of users and cell capacity is almost fully utilized. [4; 11; 30]

Network Architecture Evolution

Overall the system architecture has been optimized for packet switched transmission. The need for higher end user bit rates and lower latencies resulted in simplified and flatter network structure when compared to HSPA. Comparison of network architectures between different 3GPP releases is presented in Figure 2.2. Radio Resource Management features have been brought from radio network controller directly to the base station, which is therefore called evolved NodeB or *eNodeB* in LTE. All radio protocols towards the mobile, which is usually called *user equipment* (UE) in case of LTE, are terminated at the eNodeB. This has made it possible to get a significant improvement in radio bearer establishment delays and round trip times. If transmissions contain only small amounts of data lower latency greatly improves the user experience. [4; 23]

ENodeBs are also largely responsible for the mobility management. Radio signal level measurements are made in the eNodeB and also the measurements made by the UE are controlled and analysed in the eNodeB. All eNodeBs are connected to

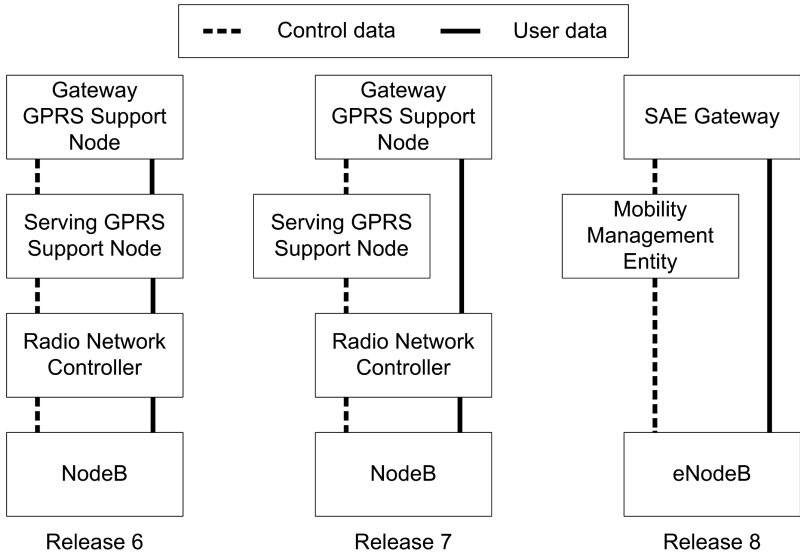

Figure 2.2. Comparison of RAN architectures between 3GPP releases.

neighboring ones and make the decision on a handover between cells. Also when a new mobile is activated eNodeB is responsible for updating the routing information to core network. [4; 11; 24]

The interoperability of different 3GPP access networks (AN) has been under consideration also. All ANs now connect to the Evolved Packet Core (EPC) which enables optimized interworking and is the main component of System Architecture Evolution (SAE), the core network architecture of LTE. In practice this is seen as smooth handovers between 3GPP technologies. Therefore e.g. traffic offloading from LTE to UMTS under heavy network load can be performed. The interworking of different ANs becomes increasingly important when the penetration of LTE grows. [4; 25]

2.3 LTE Downlink: OFDMA

LTE downlink uses OFDMA as a multiple access scheme. In contrast to UMTS and legacy systems OFDMA is a multicarrier scheme. In traditional single carrier transmission data is modulated to a single carrier, adjusting its amplitude, frequency, phase or a combination of these. Different users are separated in time, frequency or code domain. When a different data rate is needed, symbol rate, constellation size and/or coding rate has to be changed. Noise and interference limit the usable constellation size which leads to increasing the symbol rate to obtain a higher data rate. This results in using wider bandwidths and higher inter-symbol interference (ISI), which also complicates the reception of the signal. [11; 26]

In multicarrier systems data is modulated to several narrowband carriers simultaneously. In LTE orthogonal subcarriers are positioned 15 kHz from each other and

the number of subcarriers may vary from 72 to 1200 according to the bandwidth of the LTE carrier. Each of these subcarriers carries an independent data stream. The subcarrier orthogonality is illustrated in Figure 2.3. In practise subcarriers are allocated to users as non-overlapping blocks of 12 contiguous subcarriers, called resource blocks (RB). The independence of subcarrier data streams means also that narrowband interference will affect only a small amount of transmitted symbols whereas in single carrier transmission it affects all symbols simultaneously. Therefore multicarrier systems are more tolerant of narrowband interference than single carrier systems. This increases the feasibility of multicarrier transmission when a wider bandwidth is considered. [11; 22]

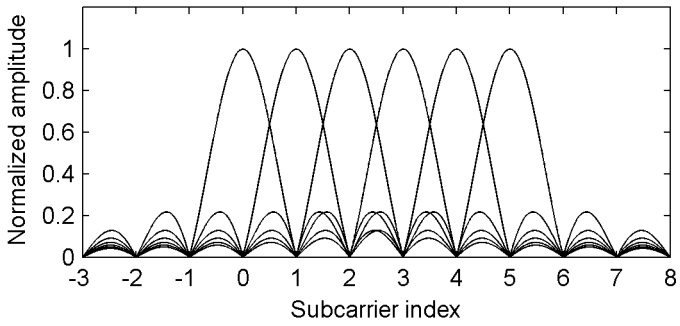

Figure 2.3. Spectra of orthogonal subcarriers. [4]

Subcarriers having a poor signal-to-noise ratio (SNR) may be left unused or the data may be recoverable using coding data transmitted on other subcarriers. Adaptive modulation and coding can be used to optimize data throughput under frequency selective fading. Theoretically modulation and coding rate can be chosen independently for each subcarrier making it possible to adapt both in time and frequency domain. In LTE the modulation is same within each resource block (RB) i.e. a block of 12 contiguously placed subcarriers. Otherwise the signaling overhead would be too large. [4; 11]

Effects of delay spread in the transmission channel can be easily avoided by using a cyclic prefix. This means that a part of the symbol is copied from the end to the beginning of the symbol creating a cyclic extension to the beginning. The length of the cyclic prefix should be longer than the delay spread. When this condition is fulfilled there should be no ISI after removing the cyclic prefix in receiver. The drawbacks in using a cyclic prefix is that it introduces overhead in time domain. It can be also said that overhead is introduced in frequency domain in a sense that the overall symbol rate gets lower but bandwidth usage stays the same. [4; 11; 27]

OFDMA makes the channel equalization simple on the receiver side. Time domain equalization would be very complex because time dispersion of the signal, i.e. frequency selective fading, is very probable due to the wide bandwidth. However,

there should be no ISI present after removing the cyclic prefix and it is possible to perform the equalization in frequency domain. This is because every narrowband subcarrier can be considered to be affected only by flat fading. In practice frequency domain equalization means that each symbol is multiplied with a complex coefficient which equalizes both the phase and the amplitude of the signal. Overall this is significantly less complex and calculation-wise more efficient way to equalize the channel compared to time domain filtering. However, also some signal processing along time axis has to be done because reference symbols are spaced sparsely in time and frequency domain, as shown in Figure 2.4. In practice consecutive frequency domain channel estimates are interpolated in frequency domain but only in the direction of time axis between different multicarrier symbols. [11; 27; 28]

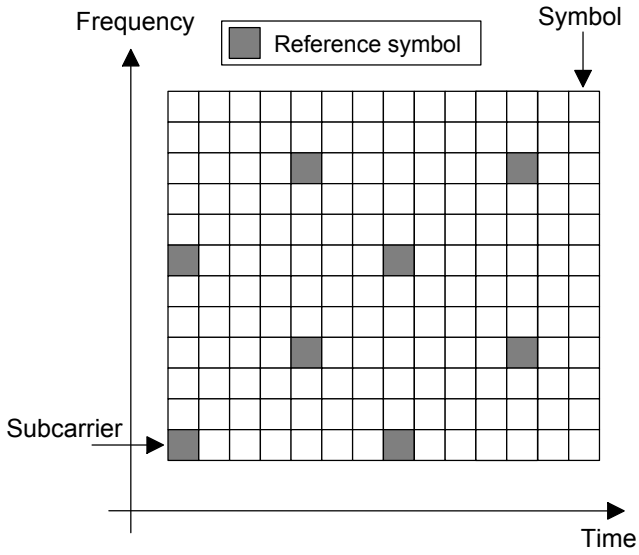

Figure 2.4. Reference symbols in one resource block. Time and frequency axes depict subcarriers and symbols. [10]

Multicarrier transmission has also drawbacks when compared to single carrier. Due to the small center frequency difference between subcarriers phase noise causes inter-carrier interference (ICI) which can have a severe impact on SNR. Therefore subcarrier spacing has been thoroughly considered together with requirements for phase noise performance. Also if the subcarrier spacing is too narrow Doppler spread may introduce problems. Because several independent symbols are transmitted simultaneously large amplitude variations may appear in time domain signal i.e. signal has a high PAPR defined as

$$PAPR = \frac{P_{peak}}{P_{avg}}, \tag{2.1}$$

where P_{peak} and P_{avg} are the peak and average signal power, respectively. [11; 27]

High PAPR leads to high linearity requirements in transmitter power amplifier

(PA) because the PA should behave linearly with all signal amplitudes. High linearity means lower transmitter power efficiency meaning that current consumption will rise. Also the cost of a linear PA is higher. Another option is to use lower average power, but it would lead to degradation of transmission range. Because power efficiency is an important issue in mobile terminals multicarrier transmission is better suited for downlink than uplink. [8; 9; 11; 29]

The actual multiple access is implemented as a combination of frequency division multiple access (FDMA) and time division multiple access (TDMA). In frequency domain subcarriers are allocated as RBs. In time domain resource allocation is done in 1 ms time intervals with the exception that if only control data is transmitted, the allocation can be shorter down to 1 symbol. One RB allocated for 1 ms therefore creates a single resource unit. Resource units are allocated to different users in such a way that allocations do not overlap in time or frequency domain. This means that resource units form a time-frequency grid illustrated in Figure 2.5. It can be also seen that bandwidth and time allocation per user is not constant. Flexible time and frequency utilization allows to take advantage on channel state information in both time and frequency domain whereas in e.g. UMTS only time domain information can be utilized. [4; 7; 10; 11; 22]

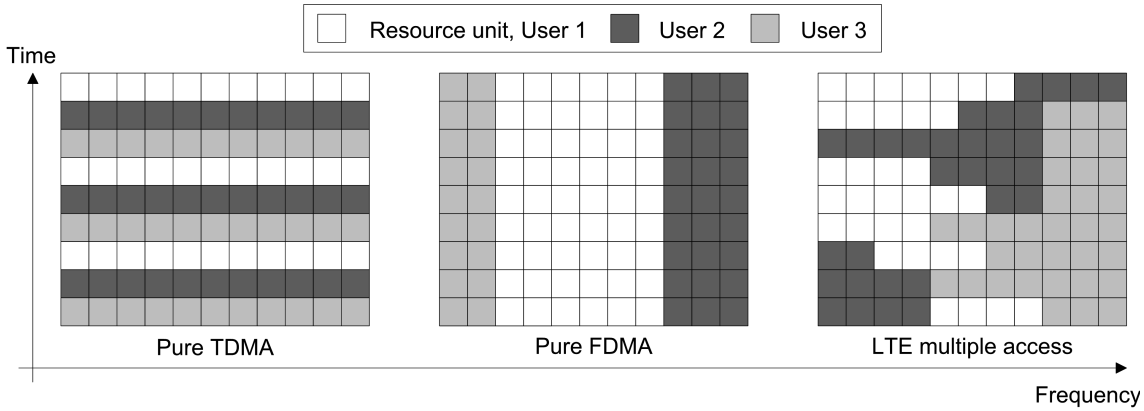

Figure 2.5. Comparison of different multiple access methods. [11]

OFDMA Signal Generation

Baseband OFDMA signal generation is illustrated in Figure 2.6. Transmitted bits are originated from the data source and modulated to symbols with a standard QAM-modulator. Symbols are divided to individual subcarriers first using N-point serial to parallel transform and then mapping symbols to the wanted subcarriers. These subcarriers are then fed to M-point inverse discrete Fourier transform (IDFT) block. IDFT is typically implemented as inverse fast Fourier transform (IFFT). IDFT generates time domain signals which are then summed together using parallel

to serial transform. Finally a cyclic prefix is inserted by copying part from the end of the OFDM to the beginning of the symbol. [4; 27; 30]

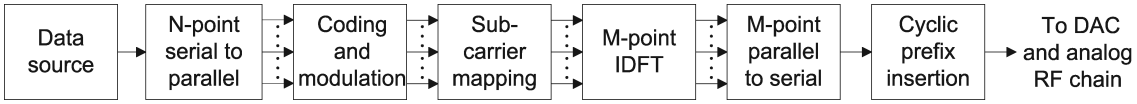

Figure 2.6. Generation of the baseband OFDMA signal from the implementation point of view. [10; 11]

To implement the IDFT efficiently using IFFT the length of the IDFT should be a power of two. In practice this means that the IFFT has more inputs than there are subcarriers. Therefore the IFFT input is zero-padded meaning that unused subcarriers are set to zeros. A mathematical representation of the OFDMA signal is shown in Equation (2.2). [4; 11]

$$x_n = x(nT_s) = \sum_{k=0}^{N-1} a'_k e^{j2\pi k\Delta f n T_s} = \sum_{k=0}^{N-1} a'_k e^{j2\pi kn/N} \tag{2.2}$$

where

$$a'_k = \begin{cases} a_k & \text{if subcarrier is populated} \\ 0 & \text{otherwise} \end{cases} \tag{2.3}$$

Baseband OFDMA signal x_n is formed from the IDFT of N subcarriers which have a frequency separation of Δf. However, only part of these subcarriers are modulated with a complex symbol a_k, others being zero. Sampling rate is the reciprocal of symbol time and a multiple of subcarrier spacing, that is $f_s = 1/T_s = N\Delta f$. For example with a 20 MHz carrier there are 1200 subcarriers. This leads to an IFFT size of $2^{11} = 2048$. With 15 kHz LTE subcarrier spacing this corresponds a sampling rate $f_s = N\Delta f = 30.72$ MHz. [11; 27; 30]

Real implementation of OFDMA in LTE requires using additional low-pass filtering because otherwise IFFT will produce too powerful sidelobes and it would be impossible to fulfill spectrum emission requirements. It should be noted that any filtering used in the transmitter reduces the time window where, under ideal channel conditions, perfect OFDMA symbol can be captured i.e. filtering corrupts a part of the cyclic prefix. [11; 27]

2.4 LTE Uplink: SC-FDMA

Because of the requirements which high PAPR of the OFDMA signal sets for the transmitter linearity it is not well suited for uplink transmission. Therefore SC-FDMA was selected to be used in LTE uplink. SC-FDMA is a transmission scheme where pre-coding is combined with OFDMA signal generation principles. In case

of LTE, discete Fourier transform (DFT) is used as a precoding matrix. From the SC-FDMA signal generation block diagram presented in Figure 2.7 it can be seen that DFT is the only additional block compared to the OFDMA signal generation presented in Figure 2.6. [4; 10; 11; 30]

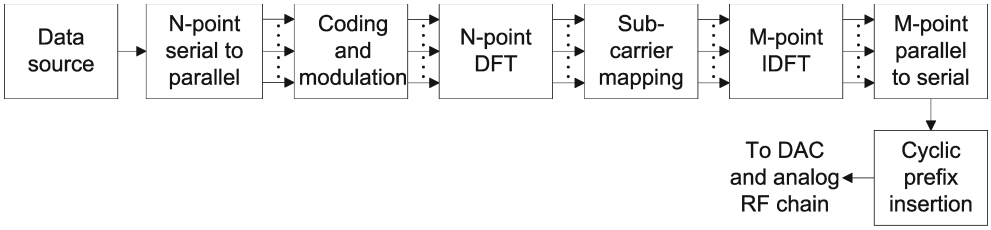

Figure 2.7. Generation of the baseband SC-FDMA signal from the implementation point of view. [10; 11; 30]

In practise using DFT means that only a single QAM-symbol is transmitted in time domain at a time. DFT output is the spectrum of symbol block consisting of N QAM-symbols which are only partly overlapping in time domain. Therefore most of the instantaneous pulse energy comes from a single symbol. Therefore SC-FDMA has a single carrier like time domain characteristics and the PAPR of the signal is significantly lower than the one of OFDMA. Instead, PAPR is now more dependent on the constellation size. The spectrum is mapped to the wanted subcarriers and transformed back to time domain. To maximise the computational efficiency typically FFT and IFFT are used in real implementations. Cyclic prefix is added between each block of symbols which simplifies the channel equalization in the receiver. However, because cyclic prefix is between each block of symbols instead of each symbol, cyclic prefix cannot eliminate all ISI. Channel equalization can still be done using a single complex valued multiplier for each subcarrier, because frequency domain equalization removes the remaining ISI between QAM-symbols. [4; 11; 30]

Because of the multicarrier-like signal generation SC-FDMA has the same flexibility in time and frequency domain as OFDMA. Therefore also the multiple access in uplink uses the same principles as downlink meaning that the smallest user data allocation is 1 RB for 1 ms. Release 8 and 9 use only localized transmission scheme, meaning that the transmission is contiguous in frequency domain. In the signal generation this means that DFT output is mapped to consecutive IDFT inputs. From release 10 onwards different distributed transmission schemes are also supported, i.e. DFT output is no more mapped to consecutive IDFT inputs and the term *multicluster allocation* is used with it. This kind of multicluster signal no more has true single carrier properties. Different baseband subcarriers face different phase shifts when the originally contiguous spectrum is divided into pieces. This means that when subcarriers are summed together in time domain, there will be more additive and destructive summations present than in the original signal leading into increase

in higher PAPR and stricter requirements for the RF chain. Terminology associated with different multicluster and carrier aggregation schemes is introduced together with the corresponding schemes in chapter 4. [4; 11]

3. MODELLING OF TRANSMITTER NONLINEARITIES

Accurate simulation and analysis of a nonlinear system, such as a mobile transmitter, requires using nonlinear models. Therefore it is essential to understand how the nonlinear system behaviour is modelled and how it differs from a linear system. In this chapter the mathematical models for the most important transmitter nonlinearities and their effects on transmitted signal and its spectrum are introduced.

A linear system or function fulfils two principles: homogeneity and additivity. Homogeneity means that if the argument of a homogeneous function is scaled with a constant also the result or output is scaled with the same constant. Additivity means that inputting the sum of the arguments yields the same output as summing the outputs obtained from each argument separately. These principles can be combined into a single formula and written as

$$f(ax + by) = af(x) + bf(y), \tag{3.1}$$

where a, b, x and y are constants and f is a linear function. [31; 32]

A nonlinear function does not fulfill the condition presented in Equation (3.1). In practice this means that the output of a nonlinear function is more difficult to predict because certain changes in input arguments may generate different changes in the output depending on the starting point. A saturating PA is a good example of this kind of behaviour. When a PA is working within its linear region an increase in input power leads to a corresponding increase in wanted output power also. However, when PA is driven to saturation, increasing input power causes more distortion and unwanted emissions rather than an increase in wanted output power. PA nonlinearity is discussed more thoroughly in section 3.4. Whereas linear effects are often noteworthy simple to model, compensate and cancel, the nonlinear ones are significantly more complicated in all aspects. A linear filter, for example, may distort the signal amplitude and phase, but it generates no new frequency components and the effect can be cancelled out with an inverse filter. This is not the case with nonlinear distortion. [31; 32; 33]

A non-linear device can generate new signal components residing at harmonic frequencies of the original signal or on top of and adjacent to the original frequency

band. This results in self-interference and also interference to the users on adjacent channels. Harmonics are typically sufficiently easy to suppress and are not as big a problem as interference near the wanted channel. In addition to interference, part of the transmitted power is allocated to signal components which carry no useful information. This is naturally unwanted and a lot of effort has been put into understanding where and why new signal components are born, how they respond to changes in input signal and how they can be cancelled. When the nonlinear behaviour has been modeled one method to compensate its effect is digital predistortion (DPD). The idea in DPD is modifying the digital baseband signal in a way that when passing through the transmitter chain the total response will be as close to linear as possible. [32; 34; 35; 55]

This thesis concentrates on transmitter nonlinearities and this chapter introduces the mathematical models for those. First in-phase and quadrature (I/Q) signals are introduced in general. Then a look is taken on transmitter performance metrics, meaning how transmitter and signal quality is evaluated. Next the transmitter architectures are considered, giving on overlook on the whole transmitter. After that the transmitter blocks where non-linearities are generated are inspected more specifically. First a look is taken on PA non-linearity and then on baseband non-linearity. Finally other transmitter non-idealities are discussed.

3.1 Basics of I/Q Signals

Modern communications radio transceivers have widely adapted the usage of complex-valued I/Q signal processing in both analog and digital domain. Even though all realized waveforms are real-valued, they can be described using a corresponding complex-valued lowpass equivalent. Therefore real-valued bandpass signals can be modelled and analysed using the baseband equivalent signal. The complex-valued signal models are also preferred in this thesis. Terms baseband equivalent signal, complex envelope and low-pass equivalent signal are used interchangeably. [31; 33]

The motivation behind using complex-valued baseband equivalent signal models is that they are modulation and implementation independent in a sense that the same signal model is valid for all modulations. The baseband equivalent model does not depend on the center frequency of the real bandpass signal. Complex representation leads to efficient mathematical notation and calculations and at the same time provides some insights which cannot be directly seen from real-valued signal models. For example the connection between time domain signal and its spectrum is easy to grasp in case of e.g. conjugation of the complex signal. [31; 33; 36]

The baseband I/Q signal model can be derived starting from a general real-valued

bandpass signal which can be expressed as follows

$$x_{BP}(t) = 2\mathrm{Re}\{x(t)e^{j\omega_C t}\} = x(t)e^{j\omega_C t} + x^*(t)e^{-j\omega_C t}. \tag{3.2}$$

Using Euler's identity

$$e^{jt} = \cos(t) + j\sin(t) \tag{3.3}$$

equation 3.2 can be further modified

$$\begin{aligned} x(t)e^{j\omega_C t} + x^*(t)e^{-j\omega_C t} &= 2x_I(t)\cos(\omega_C t) - 2x_Q(t)\sin(\omega_C t) \\ &= 2A(t)\cos(\omega_C t + \phi(t)). \end{aligned} \tag{3.4}$$

Now the baseband equivalent signal is

$$x(t) = A(t)e^{j\phi(t)} = A(t)\cos(\phi(t)) + jA(t)\sin(\phi(t)) = x_I(t) + jx_Q(t), \tag{3.5}$$

where $x(t)$ is the complex-valued baseband signal consisting of two real-valued signals $x_I(t)$ and $x_Q(t)$ sometimes called in-phase (I) and quadrature (Q) components. ω denotes angular frequency, which can be also written as $2\pi f_C$, f_C being the carrier frequency. In addition j denotes the imaginary unit for which $j^2 = -1$. $A(t)e^{j\phi(t)}$ is the complex envelope having the amplitude and phase components $A(t)$ and $\phi(t)$, respectively. Complex conjugate of a signal is denoted by $(\cdot)^*$ and it means changing the sign of the imaginary part. The connection between the complex envelope and quadrature and in-phase signals can be summarized as follows

$$\begin{aligned} x_I(t) &= A(t)\cos(\phi(t)) \\ x_Q(t) &= A(t)\sin(\phi(t)). \end{aligned} \tag{3.6}$$

Now if $A(t)$ and $\phi(t)$ are solved from the Equation (3.6) we get

$$\begin{aligned} A(t) &= \sqrt{x_I(t)^2 + x_Q(t)^2} \\ \phi(t) &= \arctan\frac{x_Q(t)}{x_I(t)}. \end{aligned} \tag{3.7}$$

These equivalences allow practical transformations between different forms to represent complex-valued baseband signals. [31; 33; 36].

Frequency translation

Benefits of complex-valued signals are especially well seen in frequency domain representation i.e. by taking the Fourier transform of a signal. Real-valued signals

reside symmetrically as mirror images on both negative and positive frequencies, as seen on Figure 3.1 (a). Mathematically this Hermitian symmetry can be expressed as

$$X(-f) = X^*(f), \tag{3.8}$$

where $X(f)$ is Fourier transform of $x(t)$, a real-valued time domain signal. However, complex-valued signals do not have this kind of symmetrical property. The spectra of real-valued bandpass signal and its complex envelope is presented in Figure 3.1 together with the effect of conjugation. [31; 33; 35]

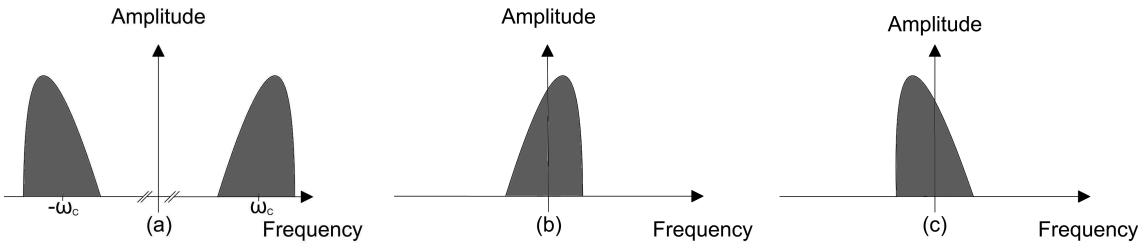

Figure 3.1. Spectra of a real-valued bandpass signal (a), complex-valued baseband signal (b) and the effect of conjugation of the complex-valued baseband signal (c). [35]

Frequency translation can be done asymmetrically in complex domain by multiplying the signal with a complex exponential. It can be directly seen from the Equation (3.2) and from the Figure 3.1 that the bandpass signal has the baseband equivalent signal mixed to center frequency ω_C and the complex conjugate of the baseband equivalent mixed to center frequency $-\omega_C$. Both components contain all the information the baseband signal has and therefore it does not matter whether receiver captures the component on negative or positive frequencies. [36]

The principle of frequency translation helps to understand the relationship between baseband equivalent signal and real-valued bandpass signal. The connection is further illustrated in Figure 3.2. It should be noted that the frequency translation presented in Figure 3.2 results in symmetric frequency translation i.e. a real-valued signal. Purely complex mixing requires four real mixers as both I and Q branches have to be multiplied with a complex exponential. A complex signal at a center frequency f_C is also called an analytic signal and it has the same spectral same as the baseband equivalent. Purely complex frequency translation using real-valued signals and the spectrum of the resulting analytic signal is presented in Figure 3.3. [36]

Even though the terminology regarding complex signals may appear difficult to grasp at first, the actual complex-valued mathematics and models are significantly simpler and more efficient than their real-valued counterparts. It should be kept in mind that the complex representation is nothing more than two real values tied together with the imaginary unit. The real-valued signals can always be restored by

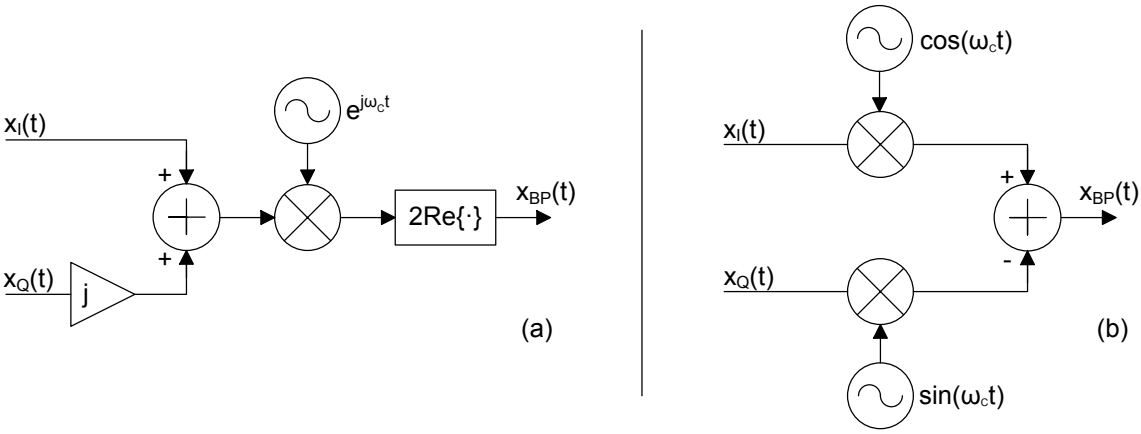

Figure 3.2. Relationship between complex-valued baseband signal and real-valued bandpass signal as a form of block diagram using complex-valued signals (a) and real-valued signals (b). [37]

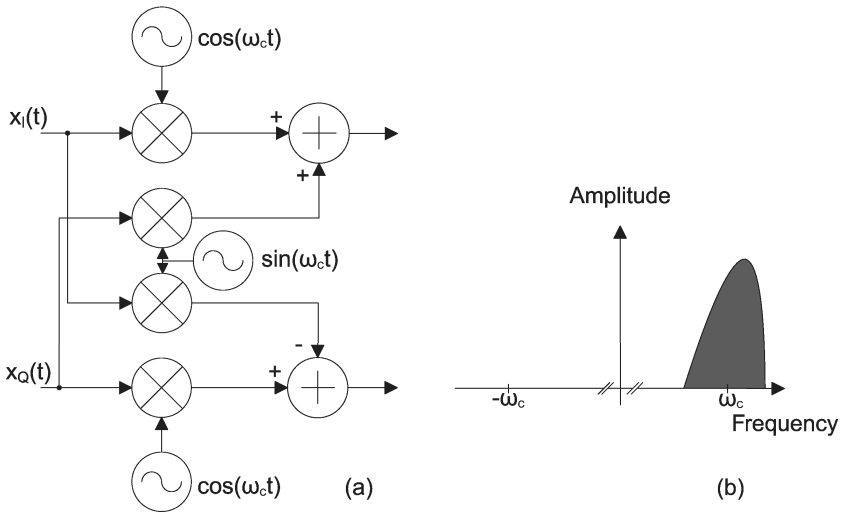

Figure 3.3. Pure complex mixing implemented using real mixers (a) resulting in an analytic signal the spectrum of which is shown in (b). [38]

taking the real and imaginary part of the complex signal. [36]

3.2 Transmitter Performance Metrics

Performance level of a transmitter can be evaluated using several different metrics. In practice a transmitter should be able to provide controlled and high enough output power without degrading the quality of the signal, causing interference to others or consuming too much energy. Basically all the performance metrics are meant to describe one or more of these quality attributes. In this section some widely used performance metrics are introduced. [11; 39]

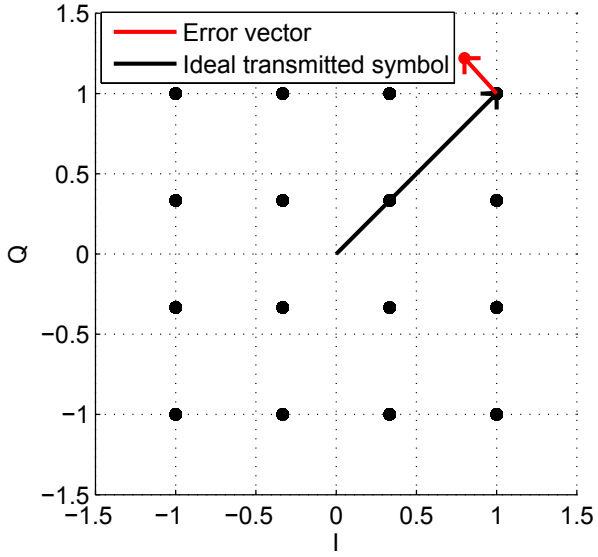

Figure 3.4. Visualization of EVM. [40]

Transmit Signal Quality

One of the most important things is the quality of the transmitted signal. With modern digitally modulated signals this is typically measured using error vector magnitude (EVM), which also has a close relationship to SNR and carrier-to-noise ratio (CNR). The I-Q plane constellation of a signal sent by an ideal transmitter would have all the symbols exactly at the optimal constellation points. However, due to nonidealities the actual sent symbols differ from the ideal ones. Now an error vector can be formed between the ideal constellation point and the actual transmitted point. This principle is illustrated in Figure 3.4. EVM is the ratio between root mean square (RMS) error power and the RMS power of the reference. Using dB-values it is therefore defined as

$$EVM_{dB} = 10log_{10}\frac{P_{error}}{P_{ref}} \tag{3.9}$$

where P_{error} is the RMS error power and P_{ref} is the RMS reference power. EVM is also used as a percentage value, which is defined as

$$EVM_{\%} = \sqrt{\frac{P_{error}}{P_{ref}}} \cdot 100\%. \tag{3.10}$$

In case of LTE, EVM is measured after the removal of the cyclic prefix, frequency synchronization and zero-forcing equalization which must result in certain spectrum flatness to make the measurement of EVM valid. With QPSK the maximum allowed EVM is 17.5 % and with 16-QAM 12.5 %. The main contributors to EVM include carrier leakage to transmitter output and PA and IQ-nonlinearity, which all are

considered more thoroughly in sections 3.4 – 3.6. [4; 11; 40; 41]

Whereas EVM is used with constellations, SNR and CNR are more commonly used with analogue signals. SNR is the ratio between the signal power, i.e. the actual information signal power, and unwanted noise power caused by background noise and imperfections in the signal chain. Using dB-values this can be written

$$SNR_{dB} = 10log_{10}\frac{P_{signal}}{P_{noise}} \tag{3.11}$$

where P_{signal} and P_{noise} are the signal and noise powers, respectively. SNR is typically used with baseband signals whereas CNR is used with modulated passband signals. If there is no reason to make a distinction between these two, SNR is often used in both cases. Similarly as SNR, CNR is defined as the ratio between modulated carrier signal power to noise power. Using dB values this can be written as

$$CNR_{dB} = 10log_{10}\frac{P_{carrier}}{P_{noise}}, \tag{3.12}$$

where $P_{carrier}$ is the modulated carrier signal power. [40]

If the error is additive white Gaussian noise, then the relationship between SNR and EVM can be written

$$EVM_{dB} = 20log_{10}\left(\frac{1}{\sqrt{SNR}}\right) = -10log_{10}(SNR) = -SNR_{dB}. \tag{3.13}$$

From (3.9), (3.10) and (3.13) it can be calculated that the EVM limits for LTE correspond approximately 15 dB and 18 dB SNR with QPSK and 16-QAM, respectively. Transmission channel and receiver imperfections add additional noise to the signal. In practise successful reception is possible even with negative SNRs. [20; 42].

Interference to Other Users

Interference to other users, both within the same channel and at adjacent channels, is caused by unwanted emissions from the transmitter in FDMA systems. In code division multiple access the same frequencies are shared between all users and therefore all transmissions cumulate the interference on top of the wanted channel. Coding is also used to separate users in LTE uplink control channel. Unwanted emissions are caused by the imperfections of the transmitter and include carrier leakage, baseband and PA nonlinearity and IQ-image. To make sure that the interference stays at an acceptable level within the own channel there are limits for the maximum allowed carrier leakage and IQ-image level relative to carrier power. Elsewhere certain spectrum emission masks have to be fulfilled i.e. transmitter can only emit a limited amount of power to a certain measurement bandwidth. [4; 11; 20]

Spectrum emission masks are typically defined for three separate regions: in-band, out-of-band and spurious region. Within these regions different measurement bandwidths, emission limits and filtering within measurement bandwidths can be used. Masks may be absolute or relative to the carrier power and in practise define the upper limit of the allowed power in the measurement bandwidth. The measurement bandwidth power spectrum (MBWPS) can be obtained as a convolution between power spectrum density (PSD) and the Fourier transform of the wanted window function. Therefore the MBWPS can be generally written as

$$S_{MBW}(f) = S_x(f) * G_{window}(f), \tag{3.14}$$

where S_{MBW} is measurement bandwidth power spectrum, $S_x(f)$ is PSD, f is frequency, $*$ denotes convolution and G_{window} is the Fourier transform of the window function. Windowing equals (weighted) averaging in the frequency domain.

When the unwanted emission measurement is done on the channels adjacent to the own transmission, measurement bandwidth being the adjacent channel bandwidth, a metric called adjacent channel leakage ratio (ACLR) is obtained. ACLR is the ratio between the transmitted power on the wanted channel and on the adjacent channel. This is illustrated in Figure 3.5. ACLR can be written as

$$ACLR = 10log10\frac{P_{wanted}}{P_{Adjacent}}, \tag{3.15}$$

where P_{wanted} and $P_{Adjacent}$ are the transmitted powers on the wanted channel and the adjacent channel, respectively. When the transmitted signal is contiguous in frequency domain most of the unwanted emissions will be on top the own transmission and adjacent channels. Being a relative measure, ACLR also limits the unwanted emission throughout the power control range. Therefore ACLR is a very important performance metric. [20]

Power Efficiency

In a mobile power efficiency is a very essential thing, because degradation of battery life will negatively affect user experience and usability of the mobile. Therefore also the power efficiency of the transmitter is an important factor. The actual transmission power also has certain limitations. The transmitter has to be able to provide high enough output power with certain accuracy and emissions should be at a very low level when nothing is transmitted. There is also a time mask which defines how quickly a specific power level has to be achieved when transmission begins or ends. [20]

PA is typically the most power hungry component in the transmitter chain and

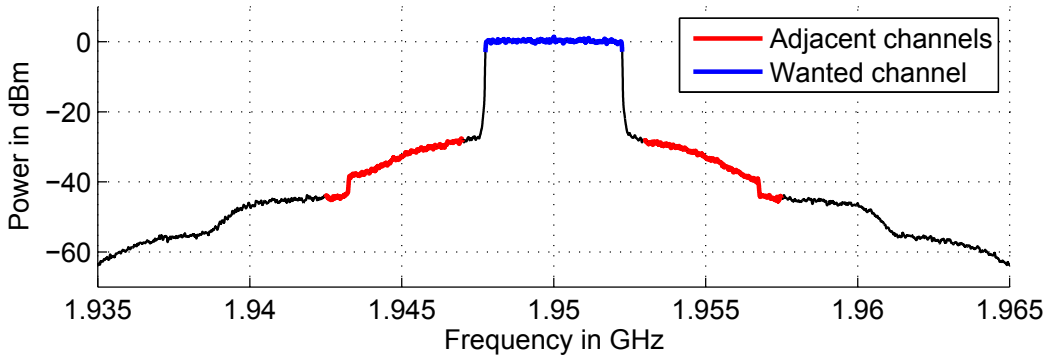

Figure 3.5. Visualization of wanted channel and adjacent channels. ACLR is the ratio between the integrated power of blue curve divided with the integrated power of one of the red curves.

therefore especially its efficiency is interesting. It is inherent to the current transmitter technology that the power efficiency degrades when transmission power is lowered. This means that power efficiency should always be told together with the measured output power level. There are three often used measures for power efficiency: drain efficiency, power-added efficiency and total efficiency. [8; 29]

Drain efficiency is the most simplest one of these measures. It tells how much direct current (DC) power is converted to RF power. Drain efficiency can be written as

$$\eta_{drain} = \frac{P_{RFout}}{P_{DC}}, \tag{3.16}$$

where η_{drain} is the drain efficiency, P_{RFout} is the RF output power and P_{DC} is the DC power entering the PA. Drain efficiency does not take into account the input RF power, which can be substantial if the gain of the amplifier is low. [43]

Power-added efficiency takes the RF input power into account. In practise this means that higher gain results in better power-added efficiency. Power-added efficiency is defined as follows

$$\eta_{PAE} = \frac{P_{RFout} - P_{RFin}}{P_{DC}} = \left(1 - \frac{1}{G}\right)\eta_{drain}, \tag{3.17}$$

where η_{PAE} is the power-added efficiency, P_{RFin} is the RF input power and G is the gain of the amplifier. It can be seen in Equation 3.17. that theoretically power-added efficiency equals drain efficiency when the gain is infinite. [8; 44]

Total efficiency or overall efficiency also considers the input and output powers as total values. Therefore total efficiency is the most traditional efficiency measure in a thermodynamic point of view. Total efficiency is defined as

$$\eta_{total} = \frac{P_{RFout}}{P_{DC} + P_{RFin}}, \tag{3.18}$$

where η_{total} is the total efficiency. Even though it would be intuitive to use total efficiency, power-added efficiency is the most often quoted efficiency measure. [45]

3.3 Transmitter Architectures

Traditional super-heterodyne transmitter architecture has been used in communications transceivers for decades. It was the dominant architecture for a very long time because of its ability to offer good spectral localization because unwanted emission can be filtered at both intermediate frequency (IF) and RF and high gain because active mixers can introduce gain to the signal. In 1995 it was estimated that approximately 98% of radio devices used the super-heterodyne architecture. However, super-heterodyne architecture has some drawbacks regarding to integrability and power efficiency. Direct-conversion architecture has been able to amend these problems and is nowadays also the reference architecture used by 3GPP. Still it has some issues of its own. In this section super-heterodyne and direct-conversion architectures are introduced and compared. [46; 47]

Super-heterodyne transmitter uses an IF in addition to RF. This means that the analog baseband signal coming from the digital-to-analog converter (DAC) is first upconverted to the IF, typically using quadrature mixing. Then the branches are summed together and the signal is upconverted to the RF. RF-image and harmonics produced in the mixing are filtered away. Finally the signal is amplified to the wanted power level and driven to the antenna through band-select filter. Several IF-stages can also be used, each requiring an own additional local oscillator (LO). After each upconversion there has to be also a filter to suppress the unwanted mixing products, such as harmonics and image components. Super-heterodyne architecture is shown in Figure 3.6. [48]

In super-heterodyne transmitter the IF LOs operate at a constant and relatively low frequency offering good quadrature modulation accuracy. The transmitter can be tuned to different RF by changing only the RF LO frequency. High gain can be achieved with the help of having several active components. However, increased number of active components also leads to increased current consumption. IF-stage can be also digital which means that after DAC there is a bandpass filter and only a single upconversion. LO leakage is not a problem, because neither of the LOs operates at the wanted RF frequency. Therefore RF filters help in suppressing the leakage. [48; 49]

The biggest issues with super-heterodyne architecture are that filters and LOs are difficult to integrate. This leads to using external components and different

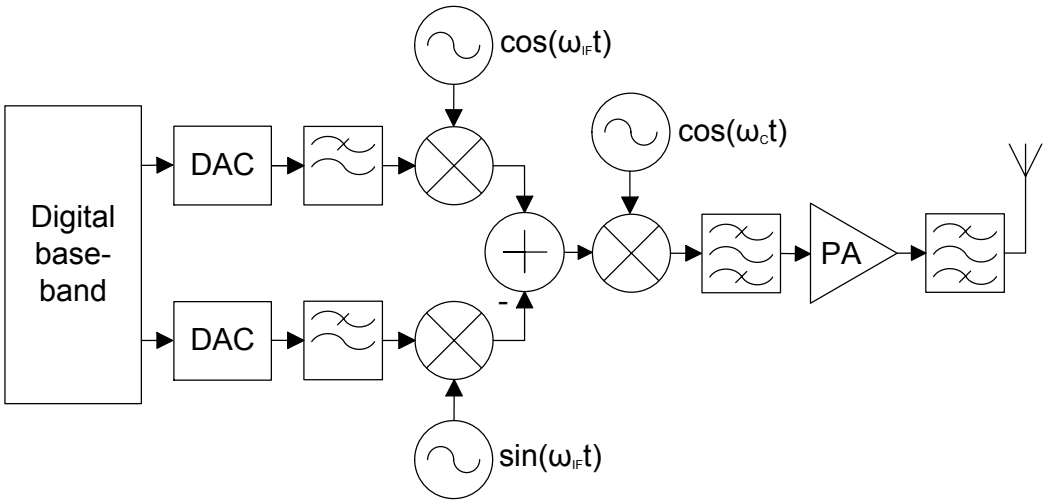

Figure 3.6. Super-heterodyne transmitter architecture with a single complex analog IF-stage. [48]

submodules in the circuit-level implementation. Typically a 50 Ω impedance matching is used between submodules and therefore current levels are high and thermal power dissipation increases, meaning worse efficiency. In addition, external components may cause additional unwanted signal leakage due to parasitic coupling effects which further decreases efficiency. LO signal leakages and harmonics must be controlled because they may result in unwanted mixing products and spurious outputs. Naturally several submodules and external components also require more space on the circuit board. [48; 50]

Direct-conversion Architecture

Due to the problems of the super-heterodyne architecture a simpler architecture with better integrability has been desirable. Direct-conversion (also known as homodyne and zero-IF) principle, i.e. upconversion from baseband directly to RF, has been known since 1930's but there has been implementation challenges which have prevented it from gaining popularity. Lately these challenges have been overcome and direct-conversion transmitter is the de facto architecture used in mobile devices. Direct-conversion transmitter architecture is presented in Figure 3.7. [39; 46; 47]

Direct-conversion architecture solves many of the issues that super-heterodyne has. Because there are neither IF-filters nor separate LOs for IF, direct-conversion architecture is simpler and allows better integrability than super-heterodyne. Also current consumption is lower. There is a lower number of components which results in lower probability of signal leakage away from the wanted signal path via parasitics. On the other hand, unwanted signals leak more easily through the wanted signal path to the output. [39; 46; 48]

Direct-conversion also has some issues of its own. Filters and mixers are never

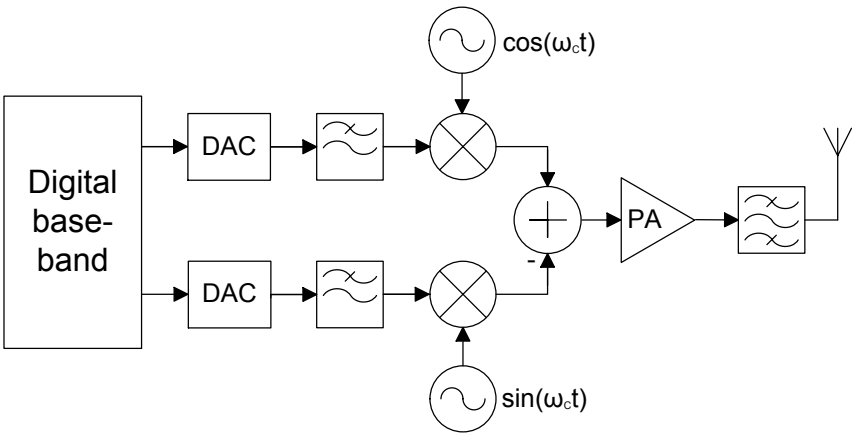

Figure 3.7. Direct-conversion transmitter architecture.

exactly alike in I- and Q-branches and also the phase shift between oscillators is not exactly 90°. This means that there are always some gain and phase mismatches, which introduces the IQ-image in the output spectrum. In super-heterodyne the image component is of low power, because quadrature signal generation is easier at a lower frequency. [35; 39; 46]

The low number of components makes it easier for the LO-signal to leak to the output. Because the LO is operating at the wanted RF, the leakage component will appear in the middle of the transmission channel. Another issue is the LO pulling. It means that the large signal generated by the PA can interfere the LO by coupling. This results in changes in the LO frequency. LO pulling is a problem especially in direct-conversion transmitters, because LO operates exactly at the wanted RF. [39; 46; 48]

To sum up, good modulation accuracy and low EVM are harder to achieve with direct-conversion than super-heterodyne architecture. However, the better integrability and efficiency of direct-conversion architecture are such important factors, that using it has been a very attractive option. The gains from small size, cheap price and easy mass-producibility further push towards using direct-conversion architecture, despite its performance issues. Due to technical development there are now solutions to cope with these issues, and direct-conversion architecture is nowadays extremely popular in mobile devices. Development in transmitter architectures is expected to continue when envelope tracking PAs become feasible. The idea of envelope tracking is to modulate the supply voltage according to the signal amplitude to achieve better efficiency. In the following sections from 3.4 to 3.6 the mathematical modelling of direct-conversion transmitter impairments is discussed. [35; 39; 46; 48]

3.4 Power Amplifier Nonlinearity

PA nonlinearity has the most significant impact on the transmitter output spectrum. Therefore it is extremely important to be able to model it accurately. Generally the goal is to be able to describe the passband nonlinearity as accurately as possible with a baseband model. PA models can be divided into different categories depending on which nonidealities they take into account. The simplest nonlinear models are generic behavioral models, which describe the nonlinear behaviour of a certain type of PA. One example of these is Rapp-model for solid state PA. These models typically only describe PA gain conversion properties and are not considered in this thesis. More accurate and interesting models are based on measurements taken from a specific PA. [29; 32; 51; 52; 53]

A measured PA model can be memoryless, quasi-memoryless or with memory. Memoryless model is the simplest of these and only describes gain behaviour. Quasi-memoryless model also takes the phase behaviour into account. The output of a model with memory can be formed of the sum of several differently delayed and distorted copies of the original input signal. Here the concentration is mostly on quasi-memoryless modeling but also the memory effects are discussed. First the effects of intermodulation stemming from the nonlinear response are discussed and then a closer look is taken into the actual modelling. [32; 51; 53; 54; 57]

Intermodulation Distortion

Intermodulation distortion is a type of nonlinear distortion which appears when a signal having two or more separate frequency components passes through a nonlinear device. Whereas linear distortion only affects the phase and amplitude of the signal and does not depend on the input amplitude, intermodulation distortion generates new frequency components and depends greatly on input amplitude. Therefore intermodulation cannot be modeled with a linear time-invariant system, such as a linear filter. [32; 55]

The simplest way to demonstrate intermodulation is the two-tone test. Two tones are fed into the PA and output spectrum is examined. When the input power is increased, new frequency components can be seen to appear in the output spectrum both above and below the original input tones and with the same frequency separation that the original input tones had. Mathematically this can be expressed using a power series where the input is the sum of two real tones. Now the input signal is

$$x(t) = A_1 \cos(\omega_1 t) + A_2 \cos(\omega_2 t) \tag{3.19}$$

where t is time and ω_1 and ω_2 are the angular frequencies of the input signal. For simplicity the power series used as the nonlinear transfer function is truncated after

the third-order term. Therefore the output is

$$\begin{aligned} y(t) &= \sum_{i=1}^{3} C_i x(t)^i = C_1 x(t) + C_2 x(t)^2 + C_3 x(t)^3 \\ &= C_1(A_1 \cos(\omega_1 t) + A_2 \cos(\omega_2 t)) + C_2(A_1 \cos(\omega_1 t) + A_2 \cos(\omega_2 t))^2 \\ &\quad + C_3(A_1 \cos(\omega_1 t) + A_2 \cos(\omega_2 t))^3 \end{aligned} \tag{3.20}$$

where C_i are power series coefficients describing how strong is the contribution of each power. Larger coefficient means that the term is more dominant and has a greater effect on the output. [32; 55]

Now the power series can be expanded and then simplified using well-known trigonometric identities

$$\cos^2(x) = \frac{1}{2}(1 + \cos(2x)) \tag{3.21}$$

$$\cos^3(x) = \frac{1}{4}(\cos(3x) + 3\cos(x)) \tag{3.22}$$

$$\cos(x)\cos(y) = \frac{1}{2}(\cos(x+y) + \cos(x-y)) \tag{3.23}$$

In Equations (3.21) – (3.23) it can be directly seen that nonlinear distortion generates new frequency components. All the resulting signal components are gathered in table 3.1.

It can be seen from the table 3.1 that second order nonlinearity only generates frequency components which do not overlap with the wanted signal. On the other hand third order nonlinearity generates components on top of the wanted signal, adjacent channels and harmonic frequencies. It applies generally that only odd-order distortion will generate frequency components to the proximity of the wanted signal. These odd-order components can be seen in Figure 3.8. Even-order distortion components can be filtered away with the band selection filter. Therefore it is enough to model the effect of odd-order distortion. [32; 55]

Generally the input to the power amplifier model is the complex baseband signal $A(t)e^{j\phi}$. This means that instead of separate tones the input has a certain bandwidth. The bandwidth of the intermodulation distortion components is the original signal bandwidth multiplied with the order of the distortion. This comes from the fact that multiplication in time domain equals convolution in frequency domain. Because the distortion components overlapping the wanted signal are wider, they cause *spectral regrowth* i.e. spreading of the power spectrum around the wanted signal. Spectral reqrowth is illustrated in Figure 3.9. [32; 55]

Every PA has some limited maximum output power which it can produce. Increasing the input power does not result in corresponding increase in the output

Table 3.1. All signal components resulting from third-order polynomial transfer function with two-tone input.

Origin	Amplitude	Center frequency
$x(t)$	$C_1 A_1$	ω_1
	$C_2 A_2$	ω_2
$x(t)^2$	$\frac{C_2}{2}(A_1^2 + A_2^2)$	0
	$C_2 A_1 A_2$	$\omega_1 + \omega_2$
	$C_2 A_1 A_2$	$\omega_1 - \omega_2$
	$\frac{C_2 A_1^2}{2}$	$2\omega_1$
	$\frac{C_2 A_2^2}{2}$	$2\omega_2$
$x(t)^3$	$\frac{3C_3}{2}(\frac{A_1^3}{2} + A_1 A_2^2)$	ω_1
	$\frac{3C_3}{2}(\frac{A_2^3}{2} + A_1^2 A_2)$	ω_2
	$\frac{3C_3}{4} A_1^2 A_2$	$2\omega_1 - \omega_2$
	$\frac{3C_3}{4} A_1^2 A_2$	$2\omega_1 + \omega_2$
	$\frac{3C_3}{4} A_1 A_2^2$	$2\omega_2 - \omega_1$
	$\frac{3C_3}{4} A_1 A_2^2$	$2\omega_2 + \omega_1$
	$\frac{C_3 A_1^3}{4}$	$3\omega_1$
	$\frac{C_3 A_2^3}{4}$	$3\omega_2$

power when operating near the maximum power. Instead the gain gets lower and the output power starts to saturate to its maximum level. This phenomenon is called *gain compression*. Typically the gain compression properties of a PA are told using *1 dB compression point*, i.e. the point where the true output level differs 1 dB from a perfectly linear response. [8; 32; 55]

Another traditional measure of nonlinearity is the third-order intercept point (IP3) which can be referred either to input (IIP3) or output (OIP3) power. IP3 is the power level where third order intermodulation (IMD3) product would be as powerful as the linear component. This output/input power would typically be so large, that it would damage the device under test (DUT). Therefore IP3 is defined using the linear extensions of the linear and IMD3 components when the PA is still in its linear operating range. IP3 is illustrated in Figure 3.10. It is assumed that the slope of the IMD3 component is three times larger than the slope of the linear component. This is theoretically correct when the IMD3 is analyzed separately, but in practice all higher order intermodulation distortion components contribute to the

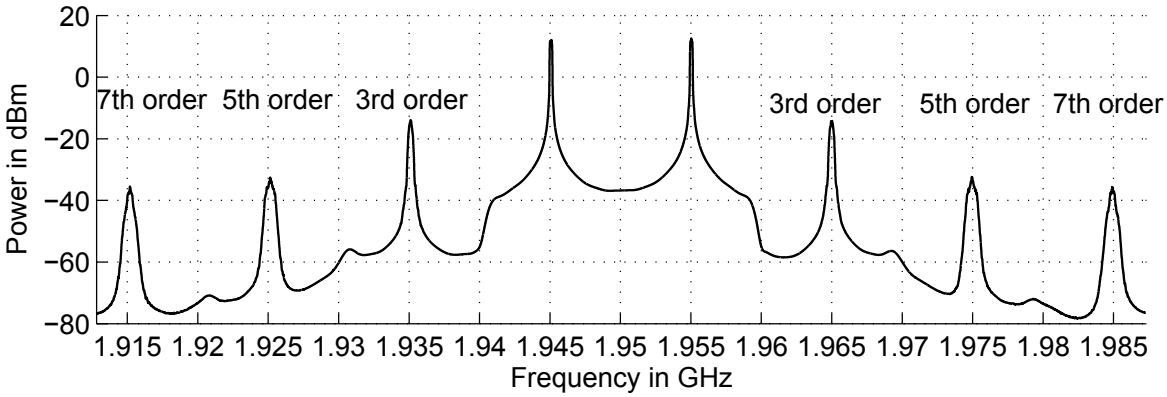

Figure 3.8. Odd-order intermodulation products around fundamental signal components spaced 10 MHz from each other.

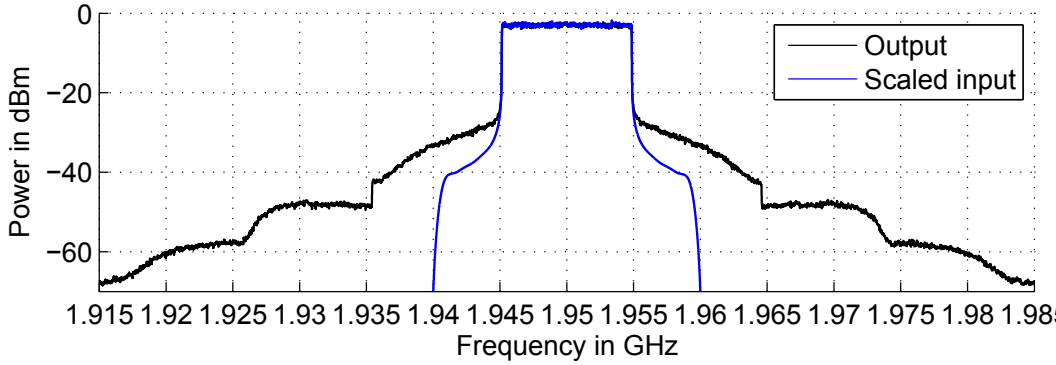

Figure 3.9. Spectral regrowth can be seen as spreading of the power spectrum.

power level also. [32]

When the real gain compression properties are measured, the power series model for PA nonlinearity can be obtained by fitting a polynomial to the gain curve. However, this model does not take the phase response into account at all. To include the dependence between the input power and phase shift into the model, a complex polynomial has to be used. PA model which considers both gain and phase conversion properties is called a quasi-memoryless model. [32; 52; 54; 56]

Quasi-Memoryless Power Amplifier Model

A quasi-memoryless PA model describes the amplitude-to-amplitude (AM-AM) and amplitude-to-phase (AM-PM) conversion properties of the PA, i.e. how output power and phase shift in the DUT change as a function of input power. These parameters are simple to extract from a vector network analyzer and therefore a quasi-memoryless model is widely used. [54; 56]

Typically the AM-AM and AM-PM responses are measured using a sinusoidal signal and sweeping the input power. The PA which is used in measurements can be unpackaged, meaning that it has low mass. This may lead into significant changes

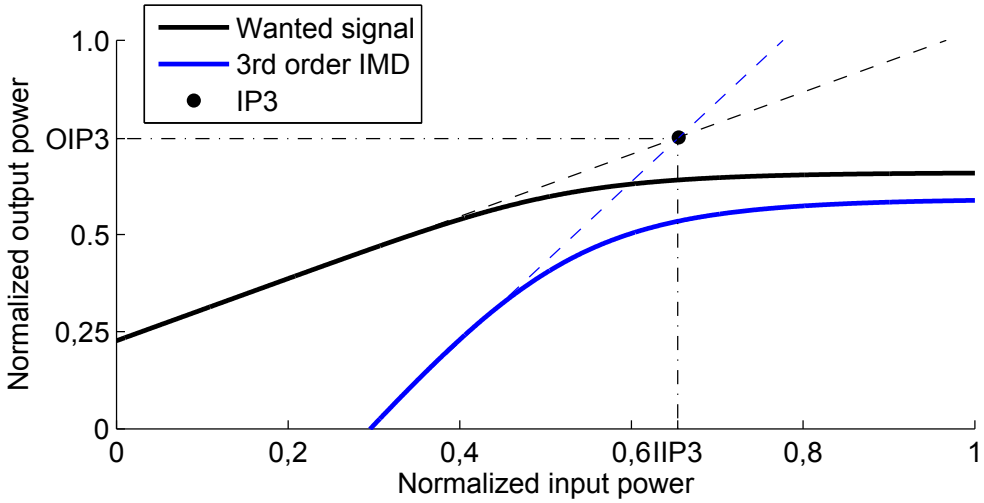

Figure 3.10. Third-order intercept point.

in operating temperature during the measurement which may result in erroneous results. Therefore a modulated measurement signal with higher PAPR may lead into more accurate results. The average power is lower, meaning less heat, but the signal also has high power levels and the performance in saturation can be also evaluated. One example of AM-AM and AM-PM curves is shown in Figure 3.11. [54; 56]

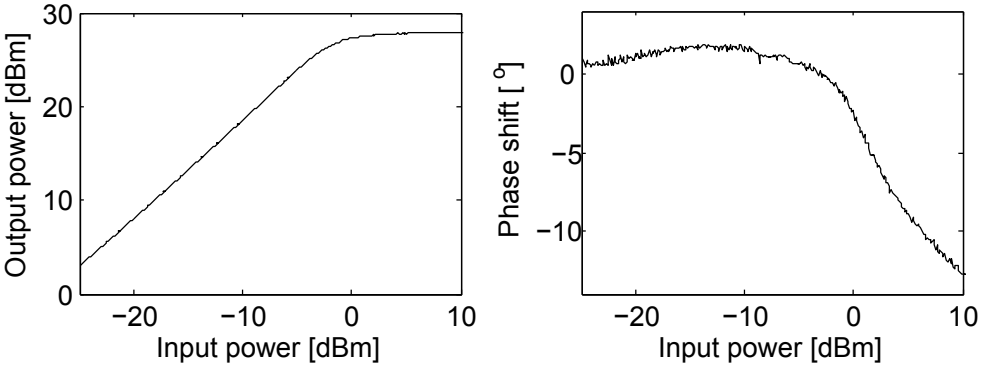

Figure 3.11. Example of AM-AM and AM-PM characteristics measured on a single operating frequency.

The amplitude and phase response can be used separately, but they can also be combined into a complex polynomial. When the measurement data is fitted the actual fitting method can be freely chosen. The absolute value (amplitude) and phase (angle) of each complex input sample is mapped to a corresponding output. Because this is done to each sample separately there is no real memory in the model. However, phase shift takes into account the varying delay in the PA which is essentially a memory effect. The model is thus called quasi-memoryless. [52]

The complex polynomial which defines the quasi-memoryless PA model can be written in general as follows

$$y(t) = x(t) \sum_{k=0}^{K} a_{2k+1} |x(t)|^{2k} = \sum_{k=0}^{K} a_{2k+1} [x(t)]^{k+1} [x^*(t)]^k, \tag{3.24}$$

where a_k are the complex polynomial coefficients. Now the AM-AM response is the relationship between absolute values

$$|y(t)| = |x(t)| \left| \sum_{k=0}^{K} a_{2k+1} |x(t)|^{2k} \right| \tag{3.25}$$

and the AM-PM response is the difference between output and input phase

$$\angle y(t) - \angle x(t) = \angle \sum_{k=0}^{K} a_{2k+1} |x(t)|^{2k}, \tag{3.26}$$

where $\angle$ denotes the phase of the phasor in IQ-plane. [52]

When the AM-AM and AM-PM conversion measurements are conducted with a modulated signal, the result is not two smooth curves. Instead the same input data samples may result in several different output power levels and phase shifts. This happens because also preceding samples affect the PA behaviour, i.e. there is memory in the PA. One reason to this kind of behaviour is thermal memory, i.e. the PA internals are in different temperature due to preceding low or high signal level. The memory effects become more and more important when the transmission bandwidth gets wider because symbol time is shorter when compared to the internal memory of the PA. Memory effects cause frequency selective nonlinear behavior and lead to frequency selectivity and asymmetric emission spectrum. [57; 58]

Modeling Memory Effects

One way to model the different frequency responses is to measure AM-AM and AM-PM response in different center frequencies. However, this kind of model does not take the thermal memory into account. Therefore the are also more complex behavioral PA models which include memory effects. The most well-known ones are Wiener and Hammerstein models, which can also be combined into Wiener-Hammerstein model. The basic structures of these models is are shown in Figure 3.12. [57; 58]

The Wiener model consists of a linear and time-invariant (LTI) system, i.e. a linear filter, followed by a memoryless or a quasi-memoryless nonlinearity. In practice this means that several delayed and scaled copies of the original signal are distorted by the nonlinearity. The Hammerstein model has the same building blocks but the order of them has been reversed: original signal goes through a nonlinearity and then into a LTI system. Therefore the distorted signals are delayed, scaled and summed

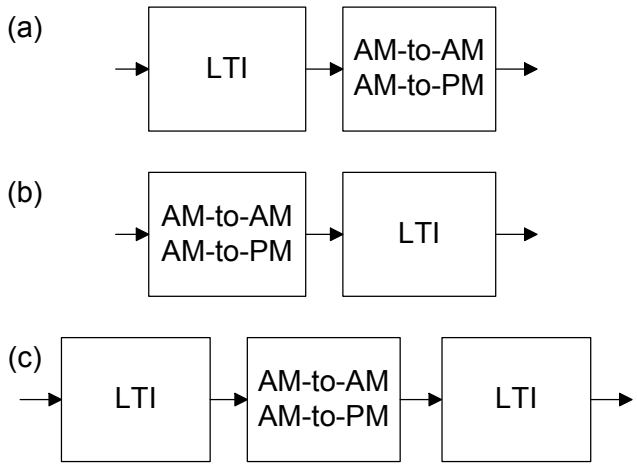

Figure 3.12. Principles of Wiener (a), Hammerstein (b) and Wiener-Hammerstein (c) PA models. [57]

together. The Wiener-Hammerstein model has linear filters both before and after the nonlinearity. [57]

In Wiener, Hammerstein and Wiener-Hammerstein models the signal goes through only one nonlinearity, which is same for all signal components. These models can be extended to parallel versions, where the original signal is copied and then the copies are passed through different nonlinearities and summed together. This allows e.g. signal components having a different delay to face different nonlinear behavior in the model. A block diagram of parallel Hammerstein PA model is depicted in Figure 3.13. [57]

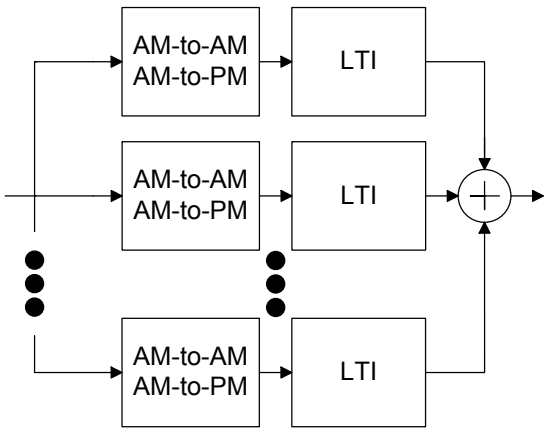

Figure 3.13. Parallel Hammerstein model. [57]

Using a more complex model may lead into more accurate results. However, the parameter extraction becomes more difficult at the same time. Erroneous parameters will not improve the accuracy of the model. Also calculation time when using the model increases correspondingly. Therefore one should always think which model

to use depending on the signal bandwidth, available time, calculation capacity and required accuracy. If the main interest is the power spectrum near the wanted signal the needs are very different from e.g. pre-distortion or other kind of cancellation of non-linear effects. [57; 58]

3.5 Baseband I/Q Nonlinearity

Nonlinear phenomena happen also in analog baseband part of the transmitter, though they are weaker due to the lower signal level. However, if additional unwanted signal components are generated in the baseband, they also go through PA and its nonlinearity, which will amplify their effects significantly. Therefore also baseband nonlinearities have to be carefully considered in transmitter design. In 3GPP especially effects of third- and fifth-order baseband nonlinearities have been considered. In 3GPP documents they are called third-order (CIM3) and fifth-order counter-intermodulation (CIM5). Simulated spectrum with third- and fifth order baseband nonlinearities is shown in Figure 3.14. The used simulator is described in chapter 5. It should be noted that if the original signal is a pure baseband signal centered at DC then all the baseband nonlinearity components will also be centered at DC, though being spread in frequency domain.

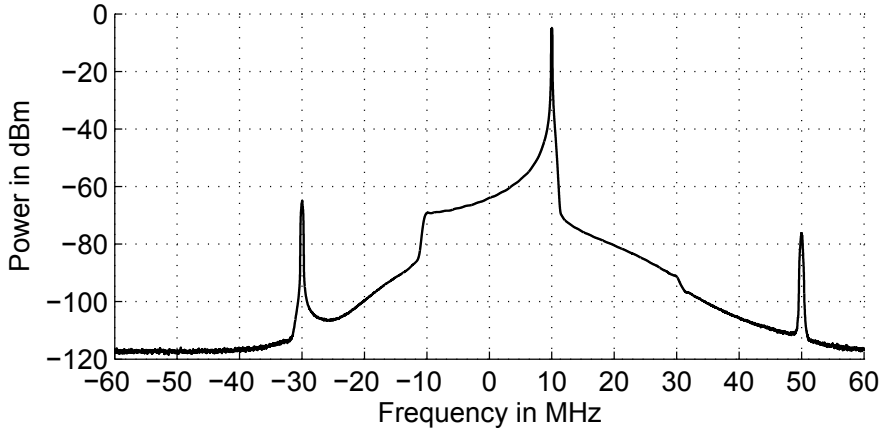

Figure 3.14. Spectrum of the baseband signal showing the fundamental signal at 10 MHz and CIM3 and CIM5 components at -30 MHz and 50 MHz, respectively.

Mathematically the biggest difference to PA nonlinearity is that now nonlinearities are in I and Q branch separately. For third order nonlinearity this can be written as

$$y_3(t) = \mathrm{Re}\{x(t)\}^3 + j\mathrm{Im}\{x(t)\}^3 = \left(\frac{x(t) + x^*(t)}{2}\right)^3 + j\left(\frac{x(t) - x^*(t)}{j2}\right)^3, \quad (3.27)$$

where $y_3(t)$ is the result of third-order baseband nonlinearity and $x(t)$ is the original input signal. $\mathrm{Re}\{\cdot\}$ and $\mathrm{Im}\{\cdot\}$ refer to real and imaginary part of the signal,

respectively. Now when the last form of Equation (3.27) is simplified we get

$$y_3(t) = \frac{3}{4}|x(t)|^2 x(t) + \frac{1}{4}x^*(t)^3. \tag{3.28}$$

It can be seen that third-order baseband nonlinearity generates components on top of the original signal and also centered at frequency $-3f$, f being the original baseband frequency. This component can be clearly seen also in the Figure 3.14.

The same analysis can be also performed to the fifth-order nonlinearity as follows

$$\begin{aligned} y_5(t) &= \mathrm{Re}\{x(t)\}^5 + j\mathrm{Im}\{x(t)\}^5 \\ &= \left(\frac{x(t) + x^*(t)}{2}\right)^5 + j\left(\frac{x(t) - x^*(t)}{j2}\right)^5 \\ &= \frac{5}{8}|x(t)|^4 x(t) + \frac{5}{16}|x(t)|^2 x^*(t)^3 + \frac{1}{16}x(t)^5. \end{aligned} \tag{3.29}$$

It can be seen that fifth-order nonlinearity will generate additional components to the same frequencies as third-order nonlinearity and also at $5f$. The fifth-order nonlinearity component can be clearly seen in Figure 3.14 also.

3.6 Other Transmitter Nonidealities

Other significant transmitter nonidealities which can be seen in the output spectrum are carrier leakage and IQ-imbalance. Carrier leakage means that LO leaks into the output of the transmitter. In direct-conversion transmitter this means that an additional tone will be present at the same frequency range as the wanted signal is. In super-heterodyne the leakage will not affect the wanted signal, because LO operates at a different frequency.

Carrier leakage can be modelled simply by adding a tone to the signal in the mixer model. In baseband model carrier is located at zero frequency. It should be also noted that carrier leakage will cause additional intermodulation components to appear when it goes through PA. The effect of carrier leakage is demonstrated in the Figure 3.15.

IQ-imbalance is caused by differences between analog I- and Q-branches. Random variations in physical characteristics of analog components are unavoidable with current implementation techniques and lead into amplitude and phase mismatches. These mismatches result in imperfect quadrature frequency conversion which means that IQ-imbalance component will appear at the mirror frequency. This mirror image component may cause interference to both own transmission and others. [35; 59]

Frequency independent IQ-imbalance in direct-conversion transmitter can be modelled simply by adding a gain and phase contributions to either of the analog branches. Typically the mismatch is modelled as gain and phase offset of the LO.

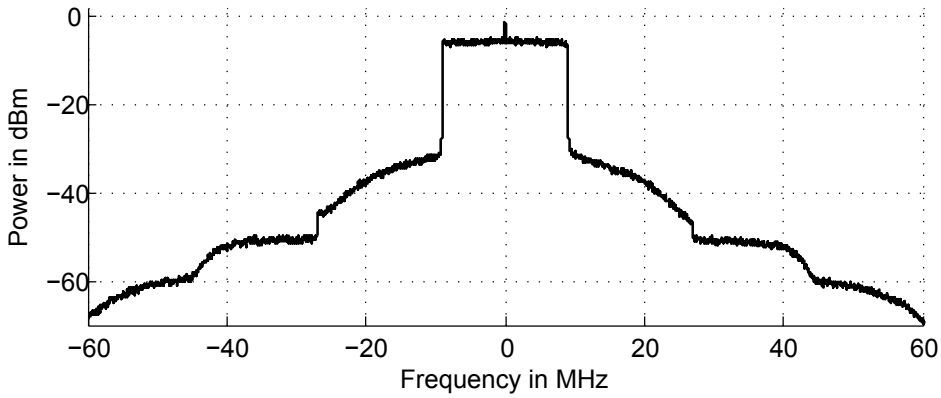

Figure 3.15. Carrier leakage at zero frequency.

Frequency dependance can be added to the model by including also a filter. The imbalance model structure is shown in Figure 3.16. [35]

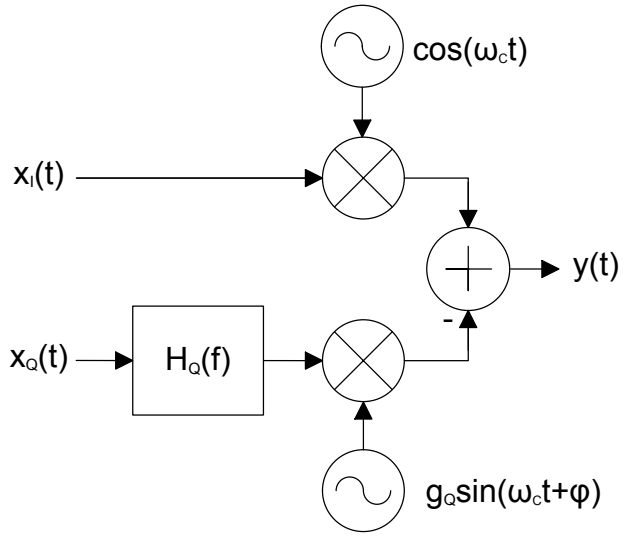

Figure 3.16. Block diagram model of frequency selective IQ-imbalance. [35]

Mathematically the frequency selective imbalance can be now expressed as follows

$$y_{BP}(t) = x_I(t)\cos(\omega_C t) - g_Q h_Q(t) * x_Q(t)\sin(\omega_C t + \phi) \tag{3.30}$$

where $h_Q(t)$ is the impulse response of the frequency selective filter. Now trigonometric identity

$$\sin(a+b) = \sin(a)\cos(b) + \cos(a)\sin(b) \tag{3.31}$$

can be used to simplify the Equation (3.30) further

$$\begin{aligned} y_{BP}(t) &= x_I(t) - g_Q \sin(\phi)(h_Q(t) * x_Q(t)) \cos(\omega_c t) \\ &= (g_{Q1}(t) * x(t) + g_{Q2}(t) * x^*(t))e^{j\omega_c t} \\ &\quad + (g_{Q1}(t) * x(t) + g_{Q2}(t) * x^*(t))^* e^{-j\omega_c t}. \end{aligned} \tag{3.32}$$

The imbalance filters $g_{Q1}(t)$ and $g_{Q2}(t)$ are defined as

$$\begin{aligned} g_{Q1}(t) &= \frac{1}{2}(\delta(t) + g_Q e^{j\phi} h_Q(t)) \\ g_{Q2}(t) &= \frac{1}{2}(\delta(t) - g_Q e^{j\phi} h_Q(t), \end{aligned} \tag{3.33}$$

where $\delta(t)$ denotes an impulse.

From Equation (3.32) it can be seen that the baseband equivalent of $y_{BP}(t)$ is

$$y(t) = g_{Q1}(t) * x(t) + g_{Q2}(t) * x^*(t). \tag{3.34}$$

$y(t)$ is a widely-linear transformation of the original baseband signal $x(t)$ and in frequency domain it can be written as

$$Y(f) = G_{Q1}(f)X(f) + G_{Q2}(f)X^*(-f), \tag{3.35}$$

where the mirror-frequency component can be clearly seen. If there is no imbalance, i.e. $g_Q = 1$, $\phi = 0$ and $h_Q(t) = \delta(t)$ we end up with $y(t) = x(t)$ as it also should be. [35; 59]

The mirror-frequency attenuation is typically measured using image rejection ratio (IRR), which is defined as

$$IRR(f) = \left| \frac{G_{Q1}(f)}{G_{Q2}(f)} \right|^2. \tag{3.36}$$

The effect of IQ-imbalance on the transmitted spectrum is demonstrated in Figure 3.17. When the wanted signal is centered at zero-frequency the image component will fall on top of the own signal causing self-interference. It can be seen that other users may suffer from the mirror-frequency interference if they operate at those frequencies. The interference may have a significant effect especially if the interfering transmitter operates at a higher power level as the interfered one. [35]

If the mirror-frequency interference falls on top of the own signal it has effects on the constellation. Gain imbalance will cause expansion or contraction of the constellation and phase imbalance will cause skewing. These effects are demonstrated in Figure 3.18. [35]

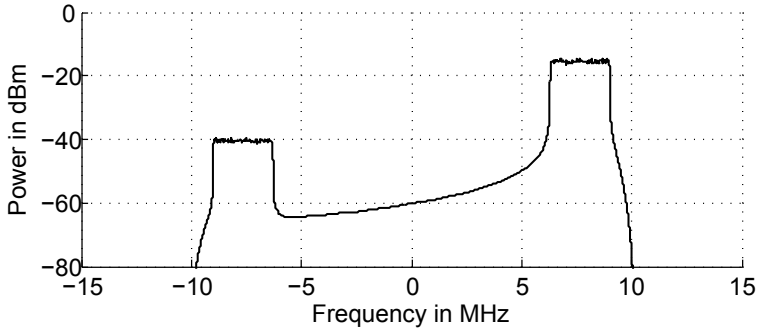

Figure 3.17. Spectrum of complex IF signal where the effect of IQ-imbalance is clearly visible.

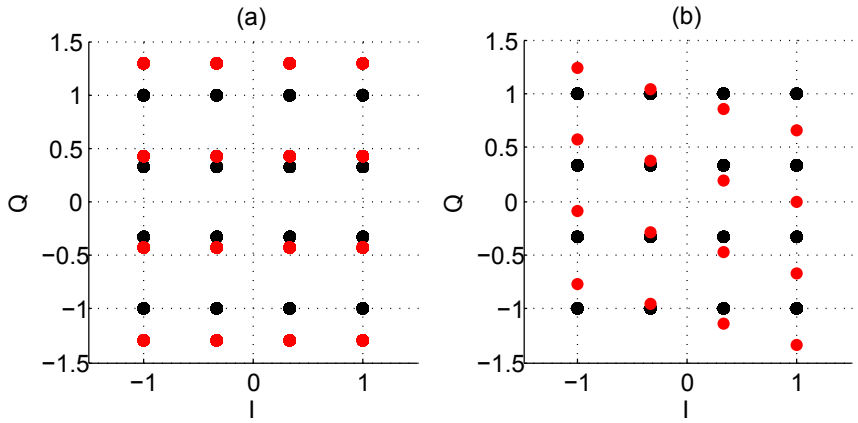

Figure 3.18. Effect of gain imbalance (a) and phase imbalance (b) on constellation of a baseband single carrier signal. [35]

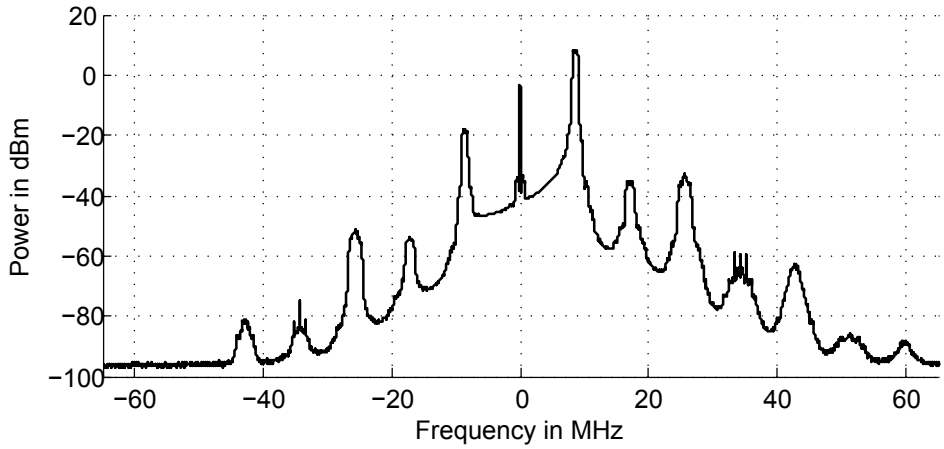

Figure 3.19. Spectrum of a signal which is impaired by carrier leakage, IQ-imbalance and baseband nonlinearity and then passed through a nonlinear PA.

When all the nonlinearities and -idealities are present in the signal chain a lot of new frequency components are generated in the spectrum. Because of the large number of different impairments the analytical analysis of the whole signal chain is difficult and laborious. Therefore transmitter performance is often studied using simulations. A simulated signal spectrum having all the impairments introduced in

this chapter is presented in Figure 3.19.

In this chapter modelling of transmitter nonlinearities and -idealities was considered. It was seen that nonideal transmitter suffers from many impairments, which generate additional components in the transmitted spectrum causing interference to both own transmission and users operating at adjacent frequency regions. In the following chapters 4 and 5 the unwanted emissions from the transmitter are considered from an LTE-specific point of view. In chapter 4 the standard development and the effects of new features on transmitter requirements and performance are discussed. Then in chapter 5 simulation and measurement result examples of the transmitter performance are presented.

4. LTE/LTE-A STANDARD EVOLUTION AND IMPACT ON MOBILE TRANSMITTER REQUIREMENTS

In this chapter evolution of LTE and LTE-A standard is considered from the mobile radio performance point of view. LTE has adopted many new features which complicate the operation of mobile radio transmitter and reaching limits for unwanted emissions. The main features in this context are introduced together with the corresponding releases and the impact of them on transmitter performance is discussed. However, LTE spectral emission limits are introduced first because transmitter performance is evaluated in contrast to these limits. The emission limits also have differences between releases and therefore the changes to the release 8 baseline are introduced together with each release.

4.1 Release 8 and 9 (LTE) and Contiguous Allocation in Single Carrier

Generally spectral emissions can be divided into three different classes depending on if they appear in in-band, out-of-band or in spurious region. In this thesis in-band emission requirements are considered only for carrier leakage and IQ-image. Out-of-band emissions are limited by spectrum emission mask (SEM) and ACLR. In addition a spurious emissions limit is defined for the spurious region. Out-of-band region is measured as an offset from channel bandwidth edges. This takes the different channel bandwidths into account better than specifying the requirements in reference to the carrier frequency. For 1.4 MHz and 3 MHz channel bandwidths out-of-band region is twice as wide as the channel bandwidth. For wider channel bandwidths it is the channel bandwidth + 5 MHz. The out-of-band emission regions and limits for general SEM can be seen from table 4.1. In table 4.1 *Meas. BW* is the bandwidth over which the PSD is integrated as shown in Equation 3.14. In addition to the general SEM additional requirements are set for certain geographical areas because of national requirements and coexisting technologies. [20; 60]

ACLR requirements include three different measurement regions: $\text{UTRA}_{\text{ACLR1}}$, $\text{UTRA}_{\text{ACLR2}}$ and $\text{E-UTRA}_{\text{ACLR}}$. $\text{UTRA}_{\text{ACLR}}$ are meant to protect two adjacent UMTS channels. Therefore $\text{UTRA}_{\text{ACLR1}}$ and $\text{UTRA}_{\text{ACLR2}}$ are measured using a 3.84

Table 4.1. General spectrum emission mask for transmission in single carrier. [20]

Δ f_{OOB}	**Spectrum emission limit (dBm) / Channel BW**						**Meas.**
(MHz)	1.4 MHz	3 MHz	5 MHz	10 MHz	15 MHz	20 MHz	**BW**
± 0-1	-10	-13	-15	-18	-20	-21	30 kHz
± 1-2.5	-10	-10	-10	-10	-10	-10	1 MHz
± 2.5-2.8	-25	-10	-10	-10	-10	-10	1 MHz
± 2.8-5		-10	-10	-10	-10	-10	1 MHz
± 5-6		-25	-13	-13	-13	-13	1 MHz
± 6-10			-25	-13	-13	-13	1 MHz
± 10-15				-25	-13	-13	1 MHz
± 15-20					-25	-13	1 MHz
± 20-25						-25	1 MHz

MHz raised root cosine filters with 0.22 roll-off, centered at 2.5 MHz and 7.5 MHz offsets from the channel edges. This equals the spectral convolution, i.e. windowing the power spectrum, presented in section 3.2, window function being the frequency response of the measurement filter. However, there is no $\text{UTRA}_{\text{ACLR2}}$ requirement for 1.4 MHz or 3 MHz carriers. [20]

$\text{E-UTRA}_{\text{ACLR}}$ measurement bandwidth is the own channel bandwidth without guard bands, which are unused regions placed symmetrically at the outer edges of the channel before out-of-band region begins. Guard bands are 160 kHz with 1.4 MHz carrier and 5% of the channel bandwidth in other cases. $\text{EUTRA}_{\text{ACLR}}$ is measured using a rectangular filter centered at an offset of half the channel bandwidth from the outer edge of own channel. ACLR emission limits are relative to the transmitted power within the wanted channel and are presented in table 4.2. Measurement regions for spectral emissions are visualized in Figure 4.1. [20]

Table 4.2. ACLR emission requirements. [20]

$\textbf{UTRA}_{\textbf{ACLR1}}$	$\textbf{UTRA}_{\textbf{ACLR2}}$	$\textbf{E-UTRA}_{\textbf{ACLR}}$
33 dB	36 dB	30 dB

Spurious emission requirements are defined according to ITU's recommendations for different frequency ranges as shown in table 4.3. Additional requirements for spurious emissions have also been defined to protect other E-UTRA downlink and TDD bands and coexisting technologies. [20; 60]

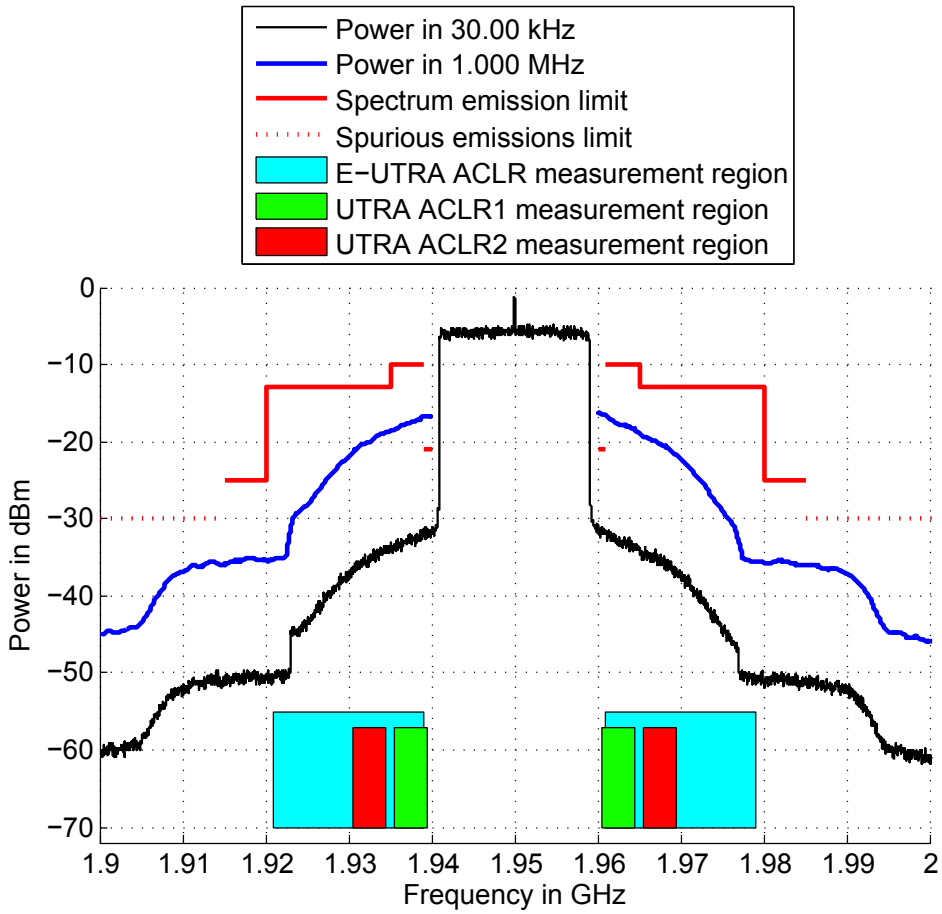

Figure 4.1. Spectrum emission limits and ACLR measurement regions with fully allocated 20 MHz carrier.

In-band emission requirements are defined for all nonallocated RBs, IQ-image and carrier leakage. No requirement is set for guard bands. Considering nonallocated RBs and IQ-image the emissions are measured as an average over 1RB and evaluated against average power in corresponding region in transmission bandwidth. Carrier leakage is evaluated against total output power. To avoid distortion caused by carrier leakage the subcarriers are frequency shifted by ±7.5 kHz so that no subcarrier is centered at DC. The inband emission limit for nonallocated RBs is dependent on the offset from the allocated RBs, number of allocated and total number of RBs, and EVM. The release 8 limits for carrier leakage and IQ-image are presented in table 4.4. [20; 61]

In addition to the many different emission requirements also the terminology associated with and the structure of the own transmission channel is essential to know. The channel bandwidth which includes also the guard bands is measured in MHz. However, resource allocation is done using RBs. The maximum number of resource blocks within each channel bandwidth is called *transmission bandwidth configuration*. Furthermore, the active RBs are separated from the ones used by

Table 4.3. Spurious emissions requirements. [20]

Frequency range	Emission limit	Measurement bandwidth
9 kHz – 150 kHz	-36 dBm	1 kHz
150 kHz – 30 MHz	-36 dBm	10 kHz
30 MHz – 1000 MHz	-36 dBm	100 kHz
1 GHz - 12.75 GHz	-30 dBm	1 MHz

Table 4.4. Minimum requirements for carrier leakage and IQ-image when transmission power is over 0 dBm. [20]

Output power	Carrier Leakage	IQ-image
> 0 dBm	-25 dBc	-25 dB

other UEs. The active RBs within transmission bandwidth configuration are the actual *transmission bandwidth*. The channel bandwidths and transmission bandwidth configuration are shown in table 4.5 and the channel structure is visualized in Figure 4.2.

Table 4.5. Channel bandwidths and transmission bandwidth configurations. [20]

Channel bandwidth / Transmission bandwidth configuration					
1.4 MHz	3 MHz	5 MHz	10 MHz	15 MHz	20 MHz
6 RB	15 RB	25 RB	50 RB	75 RB	100 RB

LTE releases 8 and 9 support only traditional contiguous frequency domain allocations within a single carrier. Therefore the most significant differences to UMTS and wideband code division multiple access are slightly bigger PAPR and more flexible bandwidth usage and wider maximum bandwidth of SC-FDMA. [62]

The tradeoff between linearity and efficiency has been taken into account in LTE specifications also, meaning that the maximum output power requirement of 23 dBm is relaxed in scenarios which are difficult from the linearity point of view. The relaxation parameter is called maximum power reduction (MPR). MPR is allowed depending on the used modulation, allocation size and channel bandwidth. MPR for contiguous transmission in single carrier is shown in table 4.6. Also additional maximum power reduction (A-MPR) is defined and used when there are additional emission requirements. A-MPR is added on top of MPR. [20]

To put MPR in context of more familiar transmitter metrics, MPR and OIP3 can be compared. An approximation is made that 3rd order nonlinearity is the

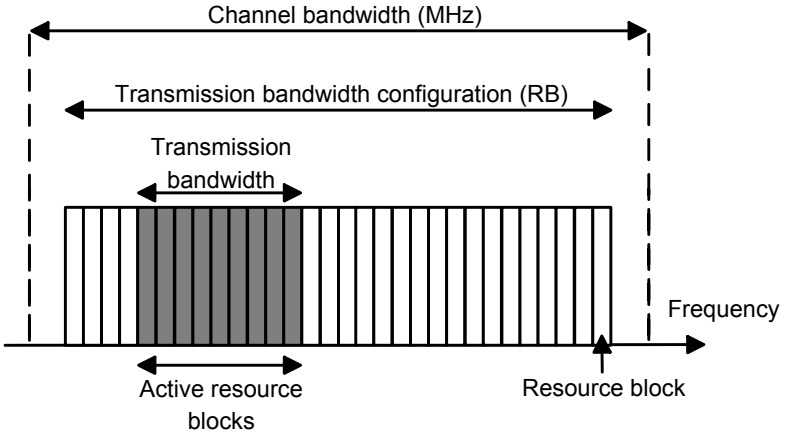

Figure 4.2. The structure of the own transmission channel. [20]

gating factor and IMD3 power changes 3 dB when wanted power changes 1 dB. If emission requirements can be reached by applying 1 dB of MPR then 1.5 dB higher OIP3 compared to the original would mean that no MPR is needed. With this approximation applying x dB MPR corresponds generally to an increase of $1.5x$ dB in OIP3.

Table 4.6. MPR for contiguous transmission in single carrier. [20]

Modulation	**Channel BW / Transmission BW (RB)**						**MPR**
	1.4 MHz	3 MHz	5 MHz	10 MHz	15 MHz	20 MHz	**(dB)**
QPSK	> 5	> 4	> 8	> 12	> 16	> 18	≤ 1
16-QAM	≤ 5	≤ 4	≤ 8	≤ 12	≤ 16	≤ 18	≤ 1
16-QAM	> 5	> 4	> 8	> 12	> 16	> 18	≤ 2

It can be seen from table 4.6 that with QPSK MPR is allowed when allocation is wide enough and with 16-QAM there is always at least 1 dB MPR. In practise this means that transmitter is calibrated and especially power amplifier is biased to work according to these power and linearity requirements. Typically in simulations which try to cover the worst case situation the PA operation point is chosen so that $\text{UTRA}_{\text{ACLR1}}$ is 33 dB and all general emission requirements are fulfilled with fully allocated QPSK-modulated carrier and 22 dBm output power. 1 dB MPR allowed with large allocation size is also used here. [56; 63]

All the general spectrum emission requirements can be fulfilled with the help of MPR defined in table 4.6. The power levels of intermodulation components generated from contiguous allocation are low and ACLR requirements are most often the gating factor. However, when additional emission requirements are present those low-powered intermodulation components become problematic. For example in E-

UTRA band 13 where the uplink is between 777 MHz – 787 MHz additional requirement *NS_07* can be signalled by the eNodeB, causing the requirement presented in table 4.7 to come into effect. It can be seen that at only 2 MHz offset from the channel edge the requirement is tightened significantly. -57 dBm in 6.25 kHz corresponds -35 dBm in 1 MHz and the original limit was -13 dBm in 1 MHz. Also the spectrum emission mask differs slightly from the general case and is shown in table 4.8.

Table 4.7. NS_07 additional emission requirement. [20]

Frequency (MHz)	**Spectrum emission limit (dBm)**	**Meas. BW**
769 – 775	-57	6.25 kHz

Table 4.8. Spectrum emission mask for band 13.

Δ f_{OOB} (MHz)	**Spectrum emission limit (dBm) / Channel BW**		**Meas. BW**
	5 MHz	10 MHz	
± 0-1	-15	-18	30 kHz
± 1-2.5	-13	-13	100 kHz
± 2.5-2.8	-13	-13	1 MHz
± 2.8-5	-13	-13	1 MHz
± 5-6	-13	-13	1 MHz
± 6-10	-25	-13	1 MHz
± 10-15		-25	1 MHz

To reach these requirements up to 12 dB A-MPR is allowed in specifications. Depending on the allocation, intermodulation between wanted signal, IQ-image and carrier leakage may fall on the protected frequency range. Also baseband nonlinearity gives its own contribution and has to be considered. Simulation results for this scenario are presented in chapter 5.2 showing that even though the transmission is contiguous in frequency domain it is not enough to look only at traditional spectral regrowth around the wanted signal. [20]

4.2 Release 10 (LTE-A) and Carrier Aggregation

Release 10 is the first release where the technology is called LTE-Advanced. Release 10 brings two major updates to the uplink transmission scenarios: Carriers

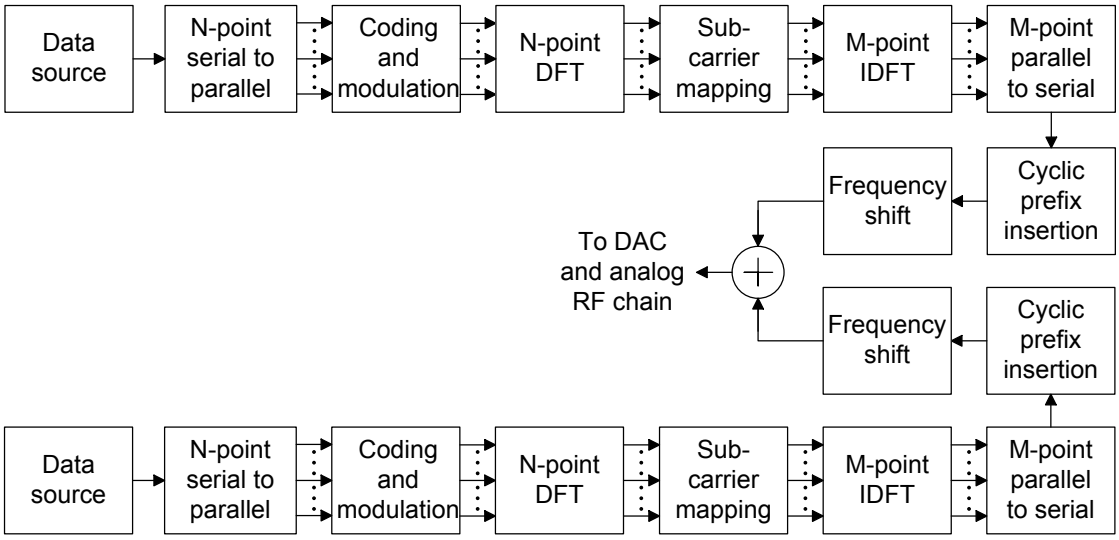

Figure 4.3. Baseband signal generation from the implementation point of view for contiguous carrier aggregation.

can be contiguously aggregated and non-contiguous resource allocation is allowed within contiguously aggregated carriers. Contiguous carrier aggregation means that adjacent release 8 carriers, now called component carriers (CC), can be transmitted simultaneously from the same mobile and they are considered as a single transmission. Terminology is updated so that channel bandwidth is replaced with *aggregated channel bandwidth* and transmission bandwidth configuration with *aggregated transmission bandwidth configuration*. Theoretically up to five carriers can be aggregated but at the moment radio aspects have been considered only for two CCs. [11; 20]

These two CCs are independent in a sense that they have their own digital baseband chains. The same traditional direct conversion architecture is used, but now the digital signal generation consists of two independent baseband signals, which are digitally aggregated, i.e. frequency shifted and summed together, before DACs. The baseband signal generation is illustrated in Figure 4.3. Therefore carrier aggregation destroys the single carrier nature of the SC-FDMA and increases PAPR. This makes the waveform more challenging to the transmitter even if contiguous allocation is used. Therefore release 10 MPR for contiguous allocation allows 1 dB more MPR compared to release 8 specifications when the number of allocated RBs exceeds the number of RBs in the narrower component carrier as shown in table 4.9. The component carriers are aggregated before analog RF parts, meaning that only a single quadrature mixer and PA is used. Carrier leakage will now appear between these two carriers if the CCs have the same bandwidth and fall on top on the own transmission in other cases. Distortion caused by carrier leakage is avoided similarly as in release 8 i.e. by ± 7.5 kHz frequency shift. [11]

The wider transmission bandwidth has two major impacts on the emission re-

Table 4.9. MPR for contiguously aggregated carriers. [20]

Modulation	**BW configuration / Transmission BW (RB)**			**MPR**
	50 RB + 100 RB	75 RB + 75 RB	100 RB + 100 RB	**(dB)**
QPSK	> 12 and ≤ 50	> 16 and ≤ 75	> 18 and ≤ 100	≤ 1
QPSK	> 50	> 75	> 100	≤ 2
16-QAM	≤ 12	≤ 16	≤ 18	≤ 1
16-QAM	> 12 and ≤ 50	> 16 and ≤ 75	> 18 and ≤ 100	≤ 2
16-QAM	> 50	> 75	> 100	≤ 3

quirements. First the width of out-of-band region is now the nominal bandwidth of the transmission +5 MHz. Nominal bandwidth is the total bandwidth of the two CCs, which are spaced according to the 300 kHz channel raster requirement between aggregated EUTRA component carriers. 300 kHz is the smallest common factor of 15 kHz subcarrier spacing and 100 kHz carrier spacing and orthogonality between subcarriers in aggregated carriers is therefore maintained. This change means that 3rd order intermodulation still falls within SEM region and therefore the requirements do not become stricter when compared to release 8. Instead more emissions are allowed compared to the situation that release 8 SEM would be placed around the transmission. [20]

Another change is that CA E-UTRA$_{\text{ACLR}}$ is used instead of E-UTRA$_{\text{ACLR}}$. CA E-UTRA$_{\text{ACLR}}$ is measured using a rectangular filter, the width of which is the same as the width of the aggregated channel bandwidth without guard bands, centered at the adjacent corresponding aggregated channel bandwidth with nominal channel spacing. Guard bands in contiguous carrier aggregation are as wide as the guard band of the wider CC. Wanted power is the sum of the power in aggregated carriers. The limit is the same 30 dB as it were for the E-UTRA$_{\text{ACLR}}$ also. This means that the linearity requirement is tightened compared to release 8, because the measurement bandwidth is increased. This also contributes to the increased MPR. The general emission requirements and ACLR measurement regions are visualized in Figure 4.4. [20]

Wider bandwidth combined with multicluster allocation means that intermodulation products will be stronger and fall further away in the spectrum. In worst case scenario where two 1 RB clusters are allocated at the opposite outer edges of the component carriers, fifth order intermodulation will fall on the strictly protected spurious region still being strong, because the power of the original transmission is concentrated on a very narrow bandwidth. It is clear that the MPR specified for contiguous allocation is not sufficient for a non-contiguous transmission scheme. It

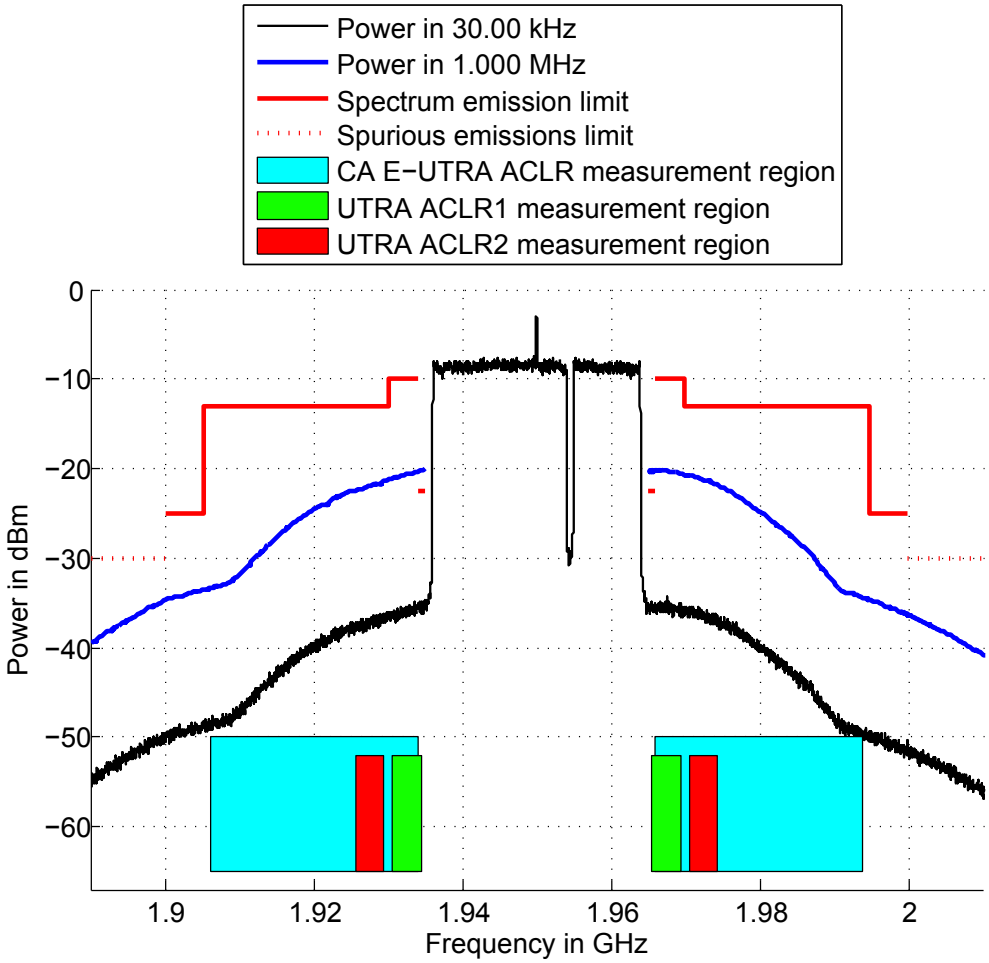

Figure 4.4. Spectrum emission limits and ACLR measurement regions with aggregated and fully allocated 20 MHz and 10 MHz carriers.

is also possible to have a difference in PSD between carriers, which leads to asymmetrical emission spectrum. Another issue with non-contiguous transmission is that the number of different possible allocations is extremely large and going through all of them is practically impossible. Therefore it is not straightforward to choose how MPR for non-contiguous allocation should be specified. [64]

Different methods for specifying multicluster MPR were considered in 3GPP. These included the maximum gap between clusters, minimum distance to channel edge and the differences between sizes of outermost clusters, among others. 3GPP selected to define MPR for non-contiguous allocation using a single variable called *allocation ratio*. Allocation ratio was able to provide least excess MPR from the studied methods and is also very simple to calculate. Allocation ratio is the ratio between allocated RBs and total number of RBs in the transmission configuration as shown in Equation (4.1).

$$A = \frac{N_{RB,alloc}}{N_{RB,agg.}}, \tag{4.1}$$

where $N_{RB,alloc}$ is the number of allocated RBs and $N_{RB,agg.}$ is the total number of RBs in the aggregated transmission configuration. A linear function of the allocation ratio defines the actual MPR. MPR for multi cluster transmission in contiguously aggregated carriers is specified as follows

$$MPR = \lceil \{M_A, 0.5\} \rceil, \tag{4.2}$$

where

$$\begin{aligned} M_A = {} & 8.2 && ; 0 \leq A < 0.025 \\ & 9.2 - 40A && ; 0.025 \leq A < 0.05 \\ & 8 - 16A && ; 0.05 \leq A < 0.25 \\ & 4.83 - 3.33A && ; 0.25 \leq A < 0.40 \\ & 3.83 - 0.83A && ; 0.40 \leq A \geq 1 \end{aligned} \tag{4.3}$$

and $\lceil \{M_A, 0.5\} \rceil$ means rounding upwards to nearest 0.5 dB. The MPR mask is presented in Figure 4.5 as a function of allocation ratio. [20; 64]

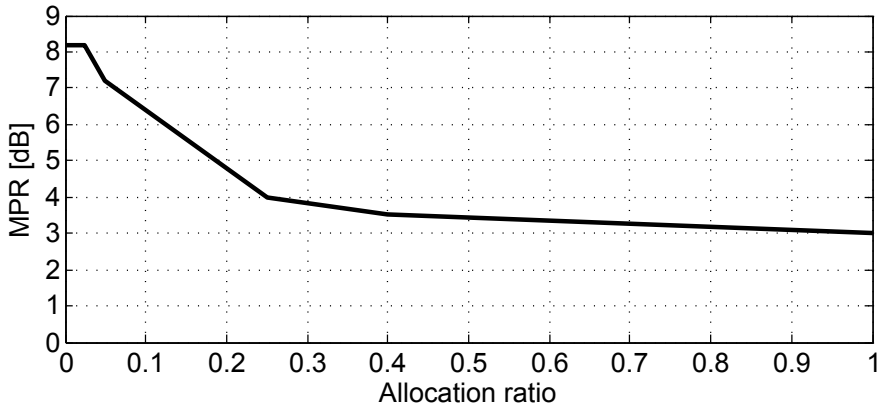

Figure 4.5. MPR mask for multicluster transmission in contiguously aggregated carriers as a function of allocation ratio.

In Figure 4.5 it can be seen that with low allocation ratio over 8 dB MPR is allowed to reach emission requirements and the amount of allowed MPR gets lower when allocation ratio increases. This behaviour is the opposite from release 8 MPR, where more MPR was allowed when the number of allocated RBs increased. Depending on the allocation ratio 1 – 6 dB more MPR is required compared to the maximum MPR with corresponding modulation in release 8. Therefore all new transmission scenarios presented in release 10 require better linearity than release 8. Different scenarios with multicluster transmission are considered in section 5.3. Also the benefits and drawbacks of the allocation ratio method are discussed.

4.3 Release 11 (LTE-A) and Non-contiguous Allocation in Single Carrier

Multicluster transmission in single carrier is introduced in release 11. At the time of writing (spring 2013) the MPR specifications have not yet been frozen because there have been proposals about using more efficient, and therefore also more nonlinear, PA modules. From the linearity point of view the difference between multicluster transmission in single carrier or in contiguously aggregated carriers is very small. Low-order intermodulation will not reach as far as with carrier aggregation, but release 8 emission limits are used with the exception that when operating below 1 GHz IQ-image and carrier leakage requirements are tightened to -28 dB. Also the border between out-of-band and spurious region is the same as in release 8. [20]

In the current specifications MPR for multi cluster transmission in single carrier is defined as follows

$$MPR = \lceil \{M_A, 0.5\} \rceil, \tag{4.4}$$

where

$$\begin{aligned} M_A = 8.0 - 10.12A \quad & ; 0 < A \leq 0.33 \\ 5.67 - 3.07A \quad & ; 0.33 < A \leq 0.77 \\ 3.31 \quad & ; 0.77 < A \leq 1.0. \end{aligned} \tag{4.5}$$

This mask is presented together with MPR mask for multicluster transmission in contiguous aggregated carriers in Figure 4.6. It can be seen that the mask for single

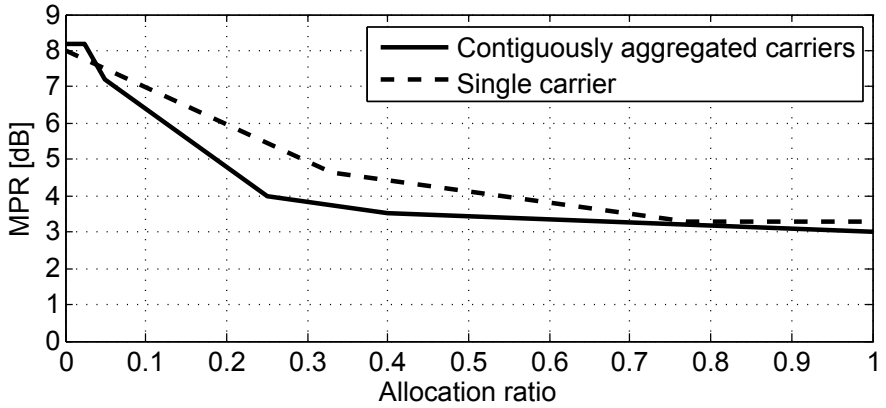

Figure 4.6. MPR mask for multicluster transmission in single carrier together with MPR mask for multicluster transmission in contiguously aggregated carriers as a function of allocation ratio.

carrier allows more MPR than is allowed for carrier aggregation. The main reason for this is that the same allocation ratio is achieved with a lower number of RBs, meaning that PSD is still higher and intermodulation components are stronger. This

is one of the drawbacks of using allocation ratio and leads to allowing MPR in excess with wider carrier bandwidths. [20]

Multicluster MPR for single carrier with additional emission requirements has not yet been included in 3GPP specifications. However, it seems clear that a significant drop in transmission power is needed in these cases, even though the spectrum emission limits are equal to release 8. Therefore the release 11 waveform requires significantly higher linearity from the transmitter. Lower transmission power may limit data throughput, because coding rate and constellation size are limited by link budget. However, contiguous single carrier transmission can still be used as in release 8. Simulation examples and results considering additional emission requirements are provided in section 5.4.

4.4 Release 12 (LTE-A) and Non-contiguous Carrier Aggregation

Release 12 introduces two major updates which significantly complicate radio performance: Intra-band non-contiguous carrier aggregation and inter-band carrier aggregation. Carrier aggregation in a single band is considered non-contiguous when the center frequency spacing of the two carriers is larger than the nominal spacing. Because the gross bandwidth can be equal to the total bandwidth of the used E-UTRA band and significantly wider as before, also the reference transmitter architecture is modified. Reference transmitter architecture for intra-band carrier aggregation is illustrated in Figure 4.7. [65]

The main practical differences between the transmitter architecture in Figure 4.7 and traditional direct-conversion transmitter is that now each carrier has its own upconversion chain. The result is that each carrier will have its own IQ-image and carrier leakage. The carriers are aggregated before PA setting high requirements for the PA because high gain and wide bandwidth are difficult to achieve simultaneously. When the gap between carriers increases already third order intermodulation will fall very far from the original frequencies meaning that high linearity is needed even more than before. [65; 66]

With non-contiguous carrier aggregation also emission requirements have been updated, because in the past there has been no gap in the middle of the transmission. Also the terminology has been redefined taking into account that in the future more carriers can be part of the aggregation scheme. The transmission now consist of sub-blocks which contain release 8 carriers. In future contiguously aggregated carriers may form one sub-block. Between sub-blocks is the sub-block gap which consist of out-of-band and also spurious region depending on the gap bandwidth. Also the nature of the emission limits is slightly different, because before the transmission

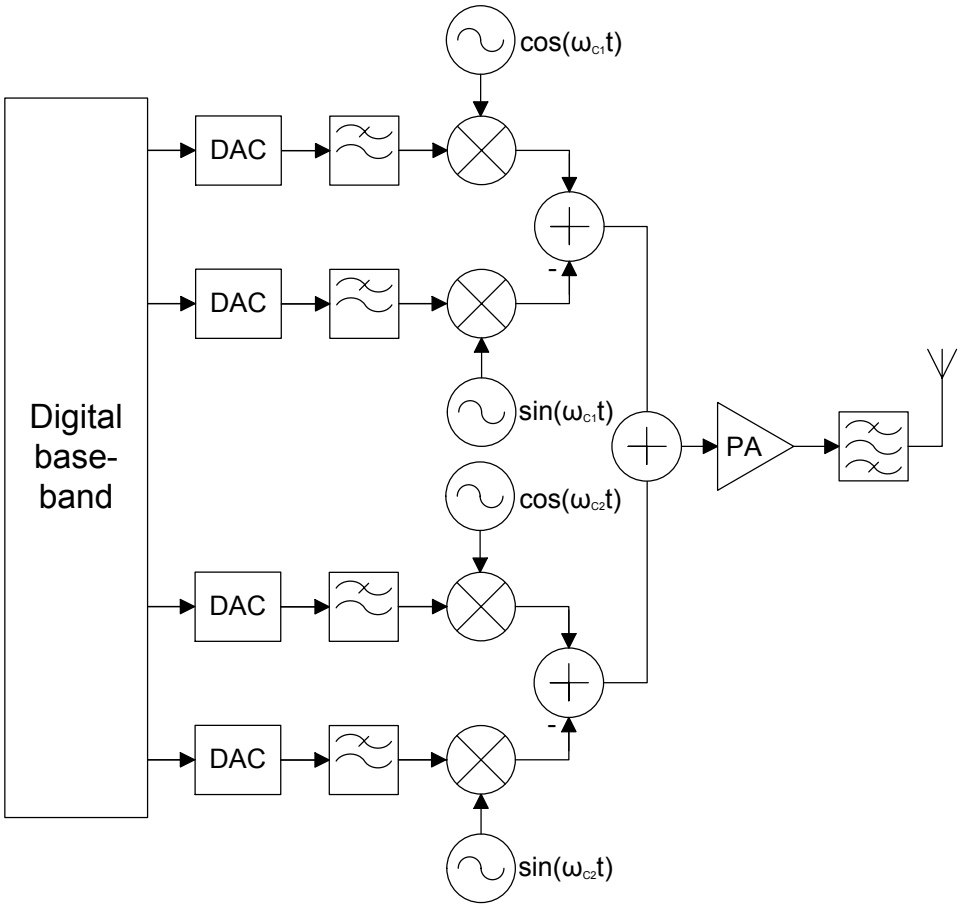

Figure 4.7. Reference transmitter architecture for intra-band carrier aggregation [65]

has been considered as a single entity. However, now the transmission, and also the emission limits, are considered as a composite of several sub-blocks. [66]

Out-of-band region for each sub-block is defined similarly as in release 8. If SEMs overlap in the sub-block gap the one allowing higher PSD will be in force. Also if SEM around one sub-block is overlapping another sub-block it will omitted from the overlapping region. Other frequency regions than sub-blocks or out-of-band regions are spurious regions. ACLR is measured around each sub-block similarly as in release 8. However, the power of the wanted channel is the summed power of all sub-blocks. If sub-block gap is less than 5 MHz $\text{UTRA}_{\text{ACLR1}}$ is not measured For $\text{UTRA}_{\text{ACLR2}}$ the corresponding limit is 15 MHz. $\text{E-UTRA}_{\text{ACLR}}$ is measured for each sub-block if the measurement region fully fits into the sub-block gap. Scenarios with overlapping measurement regions and very wide sub-block gap are visualized in Figures 4.8 and 4.9. [66; 67]

In Figure 4.8 it is clearly visible that emission are approximately 15 dB stronger than allowed even with the full allocation. When the number of allocated RBs in sub-blocks diminishes PSD will rise and the situation will get worse. Currently there has been no decisions on how MPR and A-MPR will be specified in case of

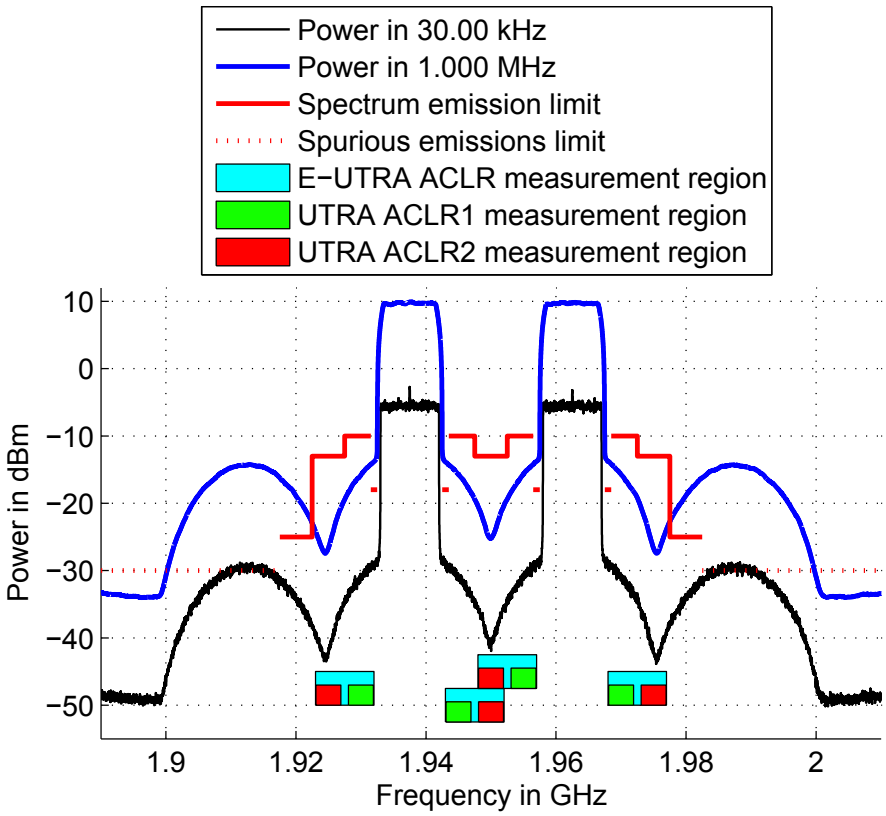

Figure 4.8. Emission requirements for intraband non-contiguous carrier aggregation with two fully allocated 10 MHz carriers and 15 MHz sub-block gap bandwidth. Measurement regions can be seen overlapping in the sub-block gap. Power in 1 MHz measurement bandwidth in spurious emission region is over 15 dB too high.

non-contiguous intraband transmission.

Another issue with non-contiguous intraband transmission is that with wide sub-block gaps intermodulation will fall on top of own downlink band and desensitize own receiver. In previous releases the duplex gap is the same as center frequency separation between uplink and downlink subtracted by the (aggregated) channel bandwidth. For example in band 25 uplink and downlink frequencies are 1850 MHz – 1915 MHz and 1930 MHz – 1995 MHz, respectively. When release 8 and release 12 are compared with 5 MHz channels the duplex gap will taper from 75 MHz in release 8 down to 15 MHz in release 12 when the sub-block gap is at its widest. The situation is problematic even if only one uplink is active, because downlink side uses the same sub-block separation and the active uplink can be the one closer to downlink. The effect is illustrated in Figure 4.10. This sets high requirements for the isolation between transmitter and receiver chains. Simulations and measurements considering non-contiguous intraband carrier aggregation including also the impact on own receiver will be presented in sections 5.5 and 5.6. [68; 69]

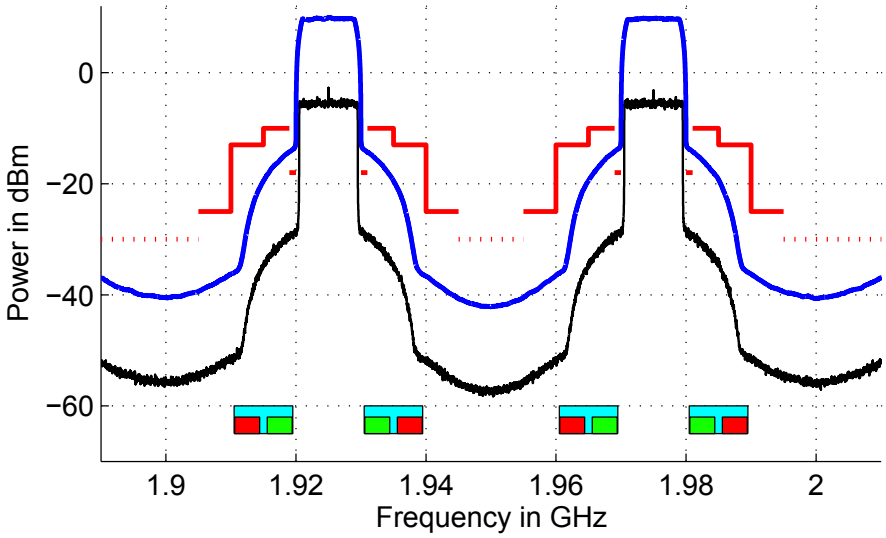

Figure 4.9. Emission requirements for intraband non-contiguous carrier aggregation with two fully allocated 10 MHz carriers and 40 MHz sub-block gap bandwidth. Strongest intermodulation components are out of the frequency range of the figure.

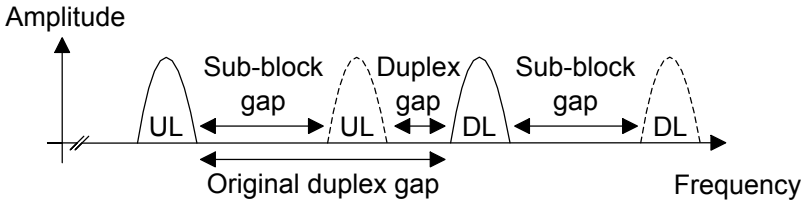

Figure 4.10. The impact of sub-block gap on duplex gap. [68]

Interband carrier aggregation will face all the same problems. However, two PAs will be used even though these can be placed in the same enclosure. Therefore it becomes important to control the leakage between the PAs. Depending on the bands intermodulation can also fall in the middle of the carriers, which does not happen with intra-band carrier aggregation. Interband carrier aggregation has not been considered on the simulations and measurements section of this thesis.

5. SIMULATION AND MEASUREMENT EXAMPLES AND RESULTS

In this chapter simulation and measurement results of different transmission scenarios introduced in chapter 4 are presented. The results do not completely cover all possible cases neither they are intended to do so. The idea is to showcase and discuss the effects of new features brought into LTE(-A) in different releases on the radio transmitter linearity requirements. The main method to compare different scenarios is how much the PA has to be backed off, i.e. how much MPR and A-MPR is needed, to fulfill all emission requirements.

First the simulation model for the transmitter is introduced and the accuracy and complexity of the models for different impairments are shortly discussed. Then different scenarios are considered in a release-wise order starting from release 8 up to release 12. The results are based mostly on simulations but also some measurements are included when appropriate.

5.1 Simulation Model and Measurement Setup

The simulation results are generated with a baseband LTE UE RF simulator, i.e. a simulator using a modeling RF transmission with a baseband equivalent model, which models both transmit and receive functionalities of an UE. No bit error or similar link level analysis can be made, but metrics like EVM and SNR can be examined. Here the main interest is the spectrum of the transmitted signal. The signal generation and measurement features are designed according to 3GPP technical specifications 36.211, Evolved Universal Terrestrial Radio Access (E-UTRA); Physical channels and modulation and 36.101 Evolved Universal Terrestrial Radio Access (E-UTRA); User Equipment (UE) radio transmission and reception. Reference signals are time-multiplexed with data symbols in SC-FDMA signal generation process. However, no separation has been done between physical uplink shared channel and physical uplink control channel, because they are alike from the radio performance point of view.

The signal flow follows the baseband signal generation and direct-conversion transmission models presented already in Figures 2.7 and 3.7. Analog RF chain is discussed here because all of the impairments are generated in this part of the transmitter. When the signal enters DAC it is a perfect baseband signal. In DAC

model no quantization is performed and the signal is upsampled from baseband rate to the final output rate. Then the signal is filtered with a DAC filter, which in these cases is a Chebyshev with 0 dB gain and introduces only linear distortion in form of passband ripple.

After DAC the signal enters an imperfect quadrature mixer, which has limited image and carrier suppression. 25 dB suppression is used according to requirements in 3GPP specification 36.101. Also third and fifth order baseband nonlinear components are generated and added to the signal at this point. Attenuations are 60 dB and 300 dB for CIM3 and CIM5, respectively. The attenuation for CIM5 is in practice almost infinite. An exception is the case of own receiver desensitization where CIM5 has been taken into account with 80 dB attenuation.

From quadrature mixer the signal goes to PA. PA is modelled using a quasi-memoryless model i.e. AM-AM and AM-PM responses which have been measured from a real mobile RF PA module. In PA model also -135 dBm/Hz background noise is added to the signal. Because PA backoff is the main method to conform to emission requirements it is important to define from where the backoff is made. The maximum required output power in LTE is 23 dBm. In all of the simulation cases PA input level is chosen so that with a fully allocated 100 RB QPSK signal $\text{UTRA}_{\text{ACLR1}}$, $\text{UTRA}_{\text{ACLR2}}$ and $\text{E-UTRA}_{\text{ACLR}}$ requirements are fulfilled with a minimum margin. Then the PA gain is chosen so that the output power is 22 dBm, i.e. 1 dB MPR is used as allowed by the specifications. To be able to select the gain freely, normalized AM-AM and AM-PM data are used. This means that the linear gain component is subtracted from the AM-AM response and it only describes the nonlinearity. It should be noted that real PAs typically perform better than this, because in the calibration process ACLR is forced to the limit but in real implementations some safety margin is always used. The calibration result is shown in Figure 5.1 together with measured performance values. SEM and spurious margins are positive when measurement bandwidth spectrum is below the limit and show the minimum difference between the limit and simulated spectrum.

After PA comes the duplex filter, which is modelled simply as 4 dB attenuation. This means that in practise the PA output level has to be 27 dBm to reach the specified maximum output power of 23 dBm at the antenna port. After duplex filter the signal is analysed. The spectrum of the signal is calculated using a FFT with good spectral resolution. The power of individual FFT bins in the measurement bandwidth is summed together to get the power in measurement bandwidth. In simulation scenarios where required backoff is searched the PA input power is lowered until all emission requirements are fulfilled. The simulated signals consist of four subframes, one subframe being 1 ms long. This selection is a compromise between simulation time and accuracy. Using longer signals means that the statistics of the

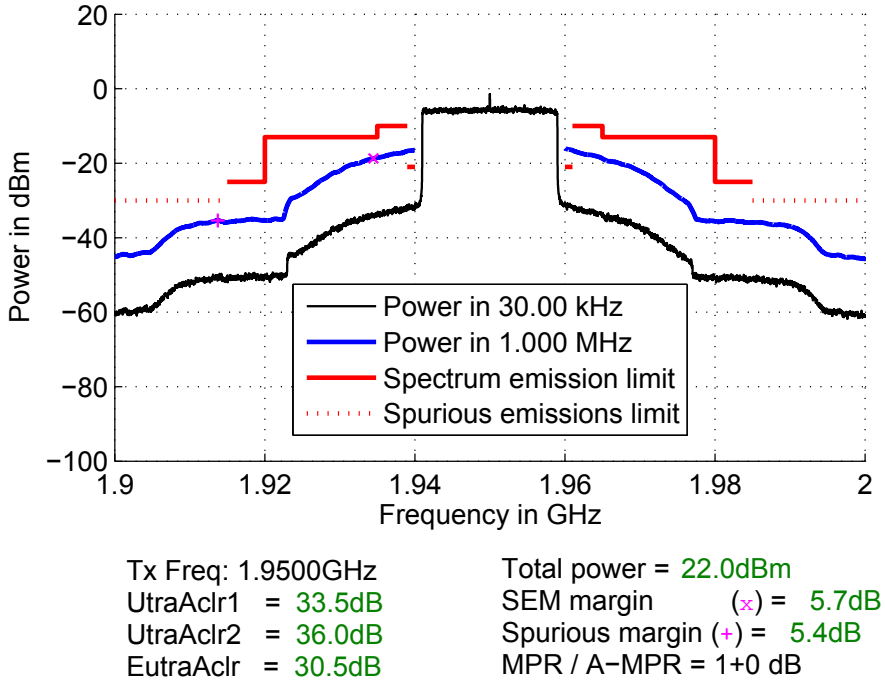

Figure 5.1. Result of PA calibration. Analysis results are shown below the spectrum.

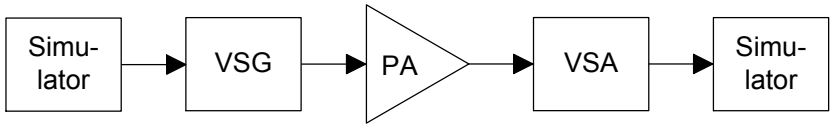

Figure 5.2. The measurement setup.

random signal are closer to expected values and variations between signal realizations are smaller. On the other hand simulation time increases correspondingly.

The used measurement setup includes a vector signal generator (VSG), PA module and a vector signal analyzer (VSA). A cyclic signal is used, i.e. a signal with no discontinuities. The cyclic signal is extracted from the simulator before going through the PA model and fed into the VSG. VSG is connected to PA module and the PA output is connected to VSA. In VSA the PA output is digitized and then fed back into the LTE UE RF simulator. Therefore all LTE-specific analysis can be made in the simulator. The measurement setup is visualized in Figure 5.2.

5.2 Single Contiguous Transmission Block (rel. 8)

Release 8 allows only contiguous transmission in frequency domain within a single carrier and it works as the baseline where other results are compared. First fulfilling general emission requirements, i.e. general SEM, spurious emissions and ACLRs, is studied. The worst case scenario is that the transmitted RBs are placed at the edge of the carrier. This means that unwanted emissions will reach as far from the carrier

frequency as possible where also the emission requirements are stricter. Simulated and measured spectrums of 20 MHz carrier with one RB allocated at the lower edge are shown in Figures 5.3 and 5.4, respectively.

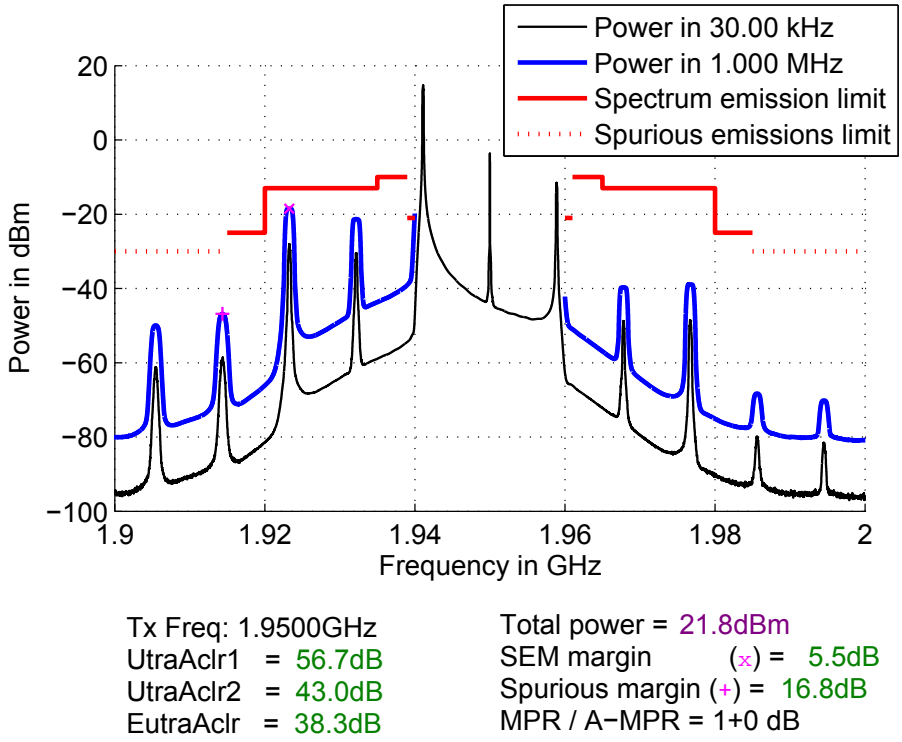

Figure 5.3. Simulated spectrum of 1 RB allocated at the lower edge of 20 MHz carrier. Used modulation is 16-QAM which allows using 1 dB MPR.

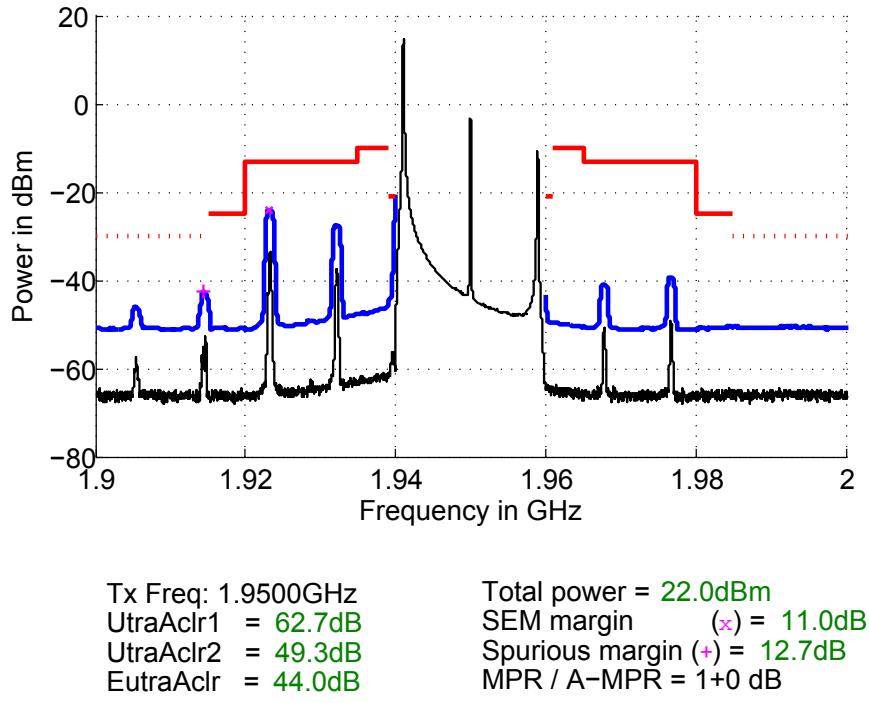

Figure 5.4. Measured spectrum of 1 RB allocated at the lower edge of 20 MHz carrier. Used modulation is 16-QAM which allows using 1 dB MPR.

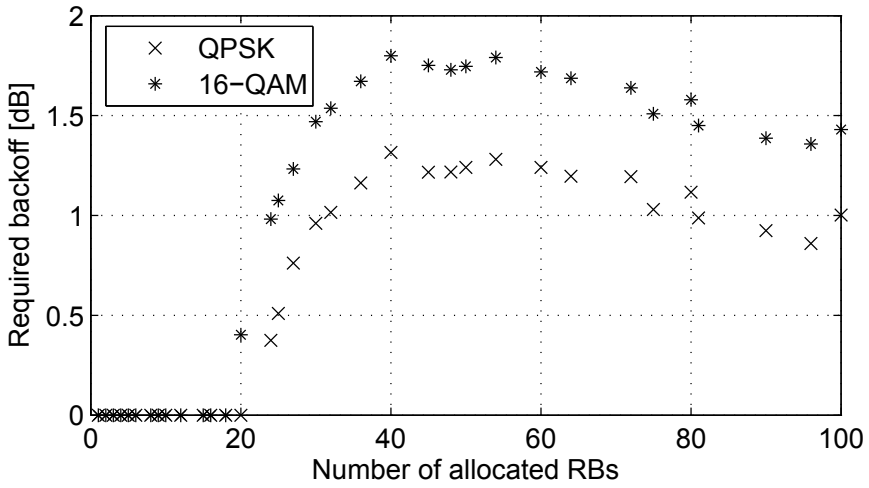

Figure 5.5. Required backoff for contiguous transmission in 20 MHz carrier as a function of number of allocated resource blocks.

It can be seen in Figures 5.3 and 5.4 that even with the narrowest possible allocation, where the power is maximally localized, intermodulation components do not reach the emission masks. Therefore it can be concluded that in release 8 transmission power is limited by ACLR requirements. In the measured signal ACLR performance is better, because the PA is not pushed to the ACLR limit in the calibration. Also the SEM margin is better but spurious margin is worse, i.e. third order intermodulation is stronger and fifth order intermodulation weaker in the simulated spectrum. However, in the measured spectrum high noise floor contributes to the spurious margin also. Now allocation size is increased so that the lower edge of the allocated RBs will always be as near to the carrier edge as possible. Required backoff is searched for all allocation sizes using both QPSK and 16-QAM. The results are presented in Figure 5.5.

From Figure 5.5 it can be seen that the results are well in line with the specification shown in table 4.6. For 20 MHz carrier 1 dB MPR is allowed for QPSK when allocation size is greater than 18 RBs. This is approximately the same point where some backoff is also required. With full allocation the match is also very good. It can be seen also that the difference between QPSK and 16-QAM is about 0.5 dB in all cases. Therefore 1 dB more MPR for 16-QAM is well justified. With allocation sizes between 30 and 80 QPSK transmission exceeds MPR specification with approximately 0.3 dB. In practice this means that some safety margin to the specifications is needed in real implementations.

It should be noted that MPR specifications are in most cases done according to worst case assumption. For example if the transmission bandwidth would be placed in the middle of the channel bandwidth instead of the edge, results would be different. This is intuitive when looking at the shape of the spectrum e.g. in

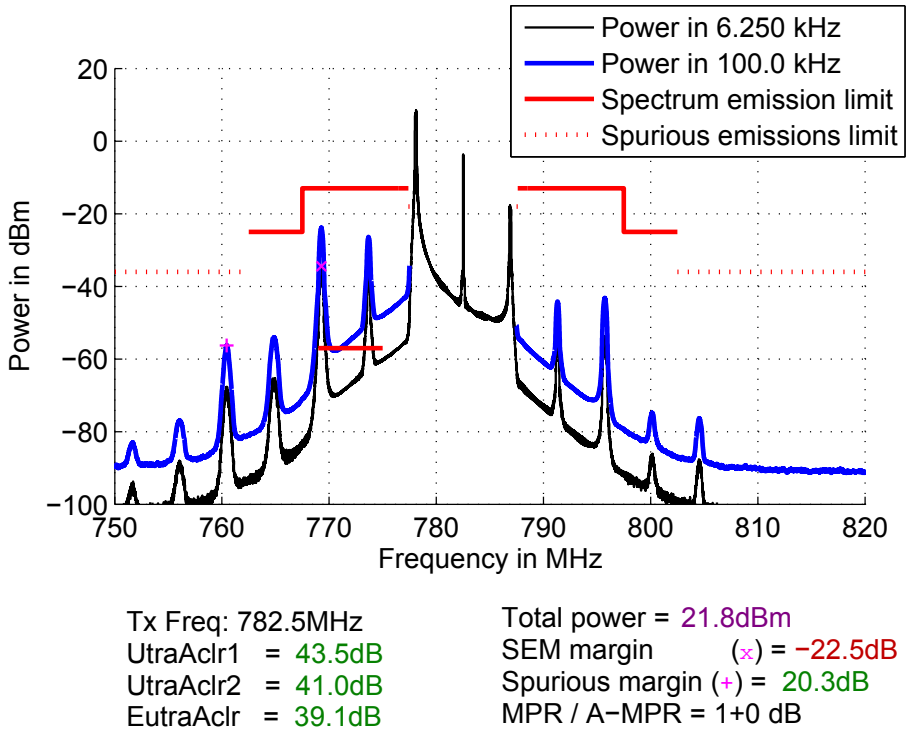

Figure 5.6. 1 RB allocated at the lower edge of 10 MHz carrier. Used modulation is 16-QAM which allows using 1 dB MPR.

Figure 5.1. This means that the linearity performance is not dependent only on transmission bandwidth but also on its position within the carrier. If the allocation is moved away from the edge of the carrier the required backoff will be lower. This means that large simulation and measurement campaigns would be needed to go through all possible allocations and the specifications would become more complex if different allocation positions would be taken into account. However, when there are additional emission requirements e.g. only on one side of the channel bandwidth then also the positions of active RBs have been taken into account.

Effect of Additional Emission Requirements

The effect of additional spectrum requirements is studied using band 13 as an example. Compared to the general emission requirements SEM requirement is 3 dB tighter within 1 - 10 MHz offset from the channel edge and there is also strictly protected frequency region which is related to public safety communication system. Within the protected region of 769 MHz - 775 MHz the emission limit is -57 dBm in 6.25 kHz measurement bandwidth. First a signal similar to the one shown in Figure 5.3 having 1 RB at the lower edge of the carrier is used. The result is illustrated in Figure 5.6.

It can be seen that the limit is not reached and the margin is -22.5 dB. The limiting component in this case is the third order intermodulation between the allocated re-

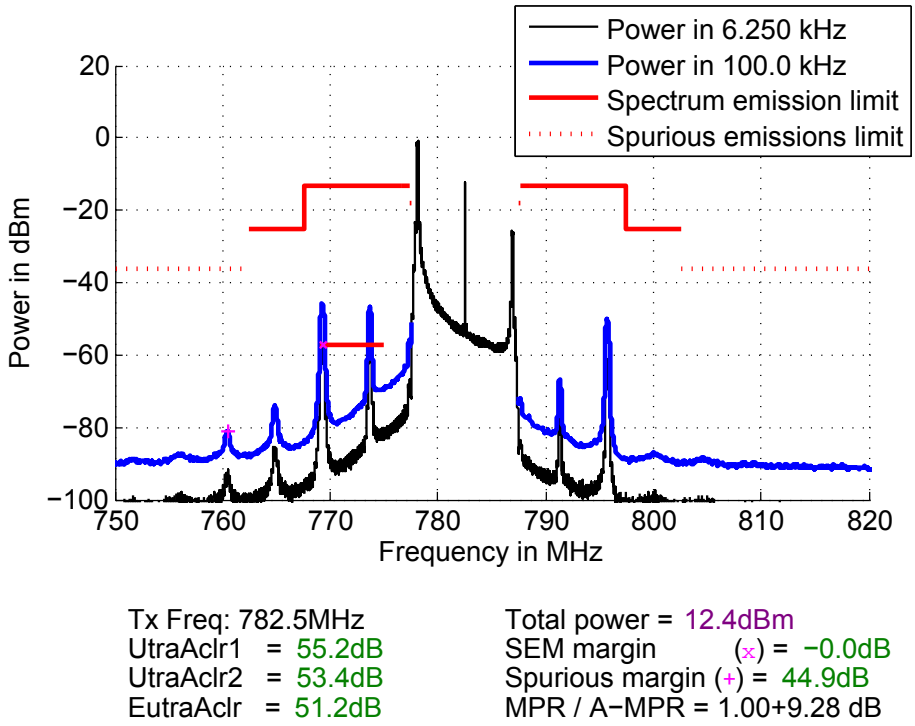

Figure 5.7. 1RB 16-QAM signal at the lower edge of the carrier with 1 dB MPR and 9.28 dB A-MPR to reach emission requirements.

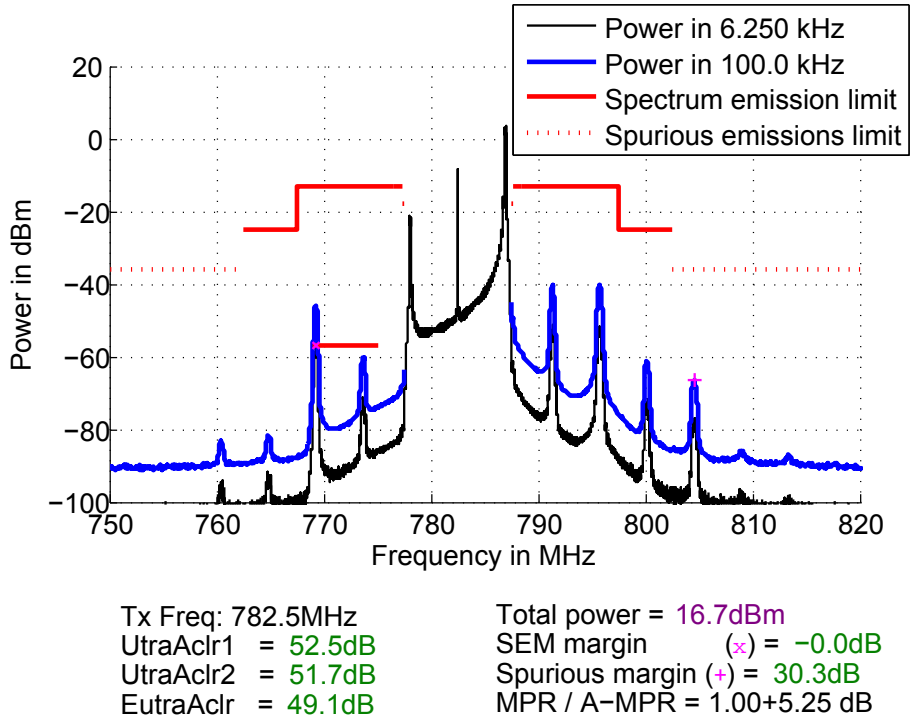

Figure 5.8. 1RB 16-QAM signal at the higher edge of the carrier with 1 dB MPR and 5.25 dB A-MPR to reach emission requirements.

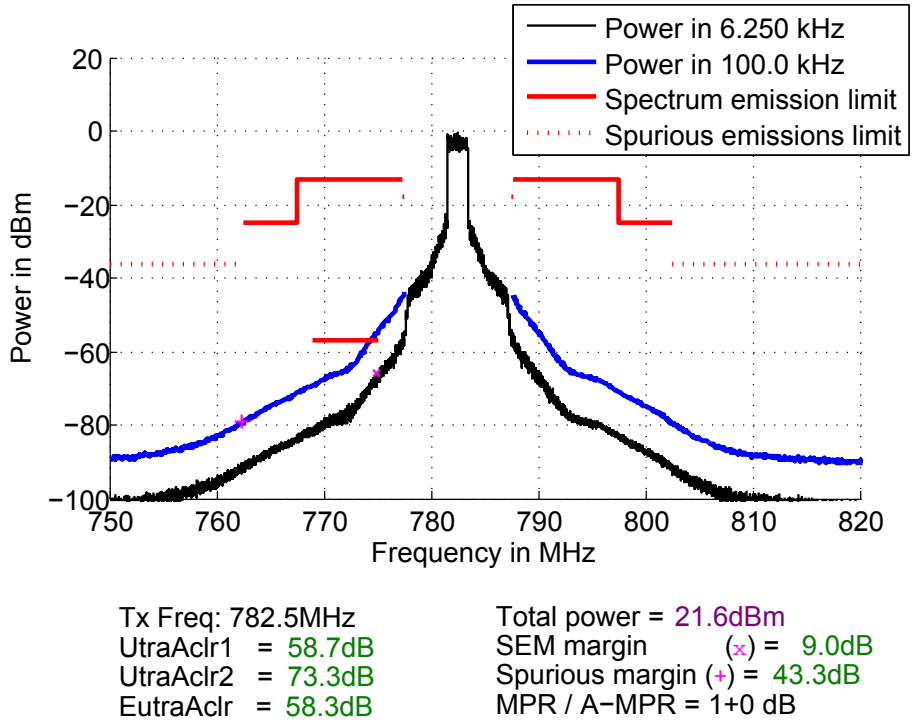

Figure 5.9. 10RB 16-QAM signal placed in the middle of the band 13 requires no A-MPR.

source block and its IQ-image. If the allocation would be at the other edge of the carrier then CIM3 would be the gating factor. The required MPR and A-MPR in these situations are shown in Figures 5.7 and 5.8.

It can be seen that total of approximately 10.3 dB and 6.3 dB backoff were needed to reach the requirement in Figures 5.7 and 5.8. This means that less than one tenth of the maximum output power is used in the first scenario. In absolute values this means a drop from 200 mW below 20 mW. If the interference level in the cell is assumed to be constant this also leads to 10 dB lower SNR compared to transmitting at maximum power, which may lead to using smaller constellation and coding rate and therefore limit data throughput. Also cell coverage is affected. An often used approximation for free space path loss is

$$FSPL_{dB} = 20\log_{10}(d) + 20\log_{10}(f) + 32.44, \tag{5.1}$$

where d is the distance in kilometers and f is the center frequency in MHz. To get 10 dB lower free space path loss the distance has to diminish by 68 %. This means that 10 km cell range will drop to roughly 3 km and cell coverage to one tenth of the original using this approximation. However, in real implementation the situation is better. Control channels can be placed so that they require low MPR and mobiles near the base station can be allocated to resources requiring high MPR. Therefore there will only be minor effect in coverage and capacity. [28].

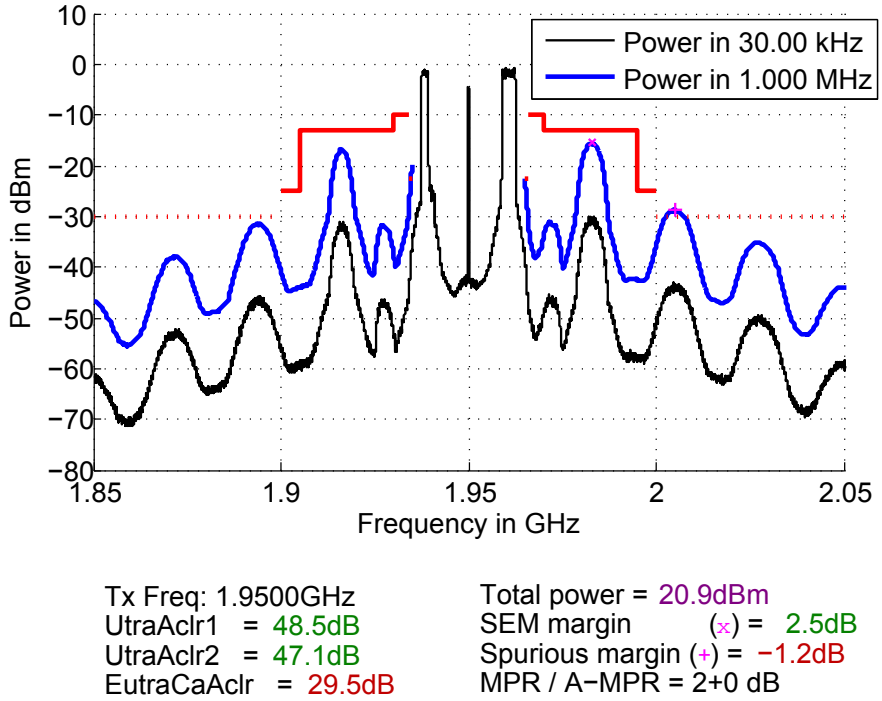

Figure 5.10. Release 10 spectrum where first CC has ten and second CC 20 active RBs with MPR specified for contiguous allocation. Requirements for spurious emissions and CA E-UTRA$_{\mathrm{ACLR}}$ are not met.

The impact of the position of the allocation can be also clearly seen. Different amount of backoff is required depending on which component will fall on top of the additional requirement. From figure 5.6 it can be seen that only third order intermodulation components are strong enough to breach the limit and therefore when the active RBs are in the middle of the band no A-MPR is required. This is illustrated in Figure 5.9.

5.3 Contiguously Aggregated Carriers (rel. 10)

Contiguous carrier aggregation and non-contiguous allocation within contiguously aggregated carriers are introduced in release 10. MPR requirements have been specified separately for contiguous and multicluster allocation. Multicluster allocation is more challenging of these scenarios and the major part of the results also concern multicluster transmission. First fulfilling general emission requirements is considered briefly. Then results for both multicluster and contiguous allocation are presented in case of *CA_NS_01* additional requirement. In all cases 15 MHz + 15 MHz configuration is used. An example spectrum of multicluster transmission having 2 dB MPR, which is specified for contiguous allocation with same number of active RBs, is shown in Figure 5.10. [20]

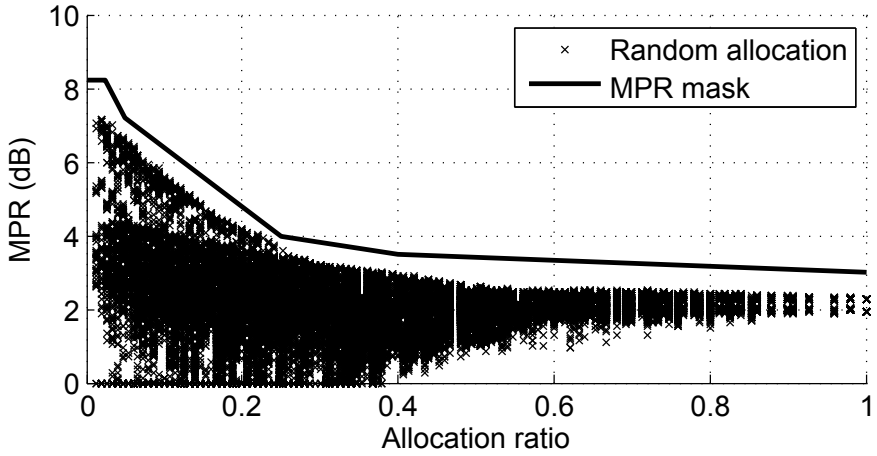

Figure 5.11. Required MPR for multicluster transmission in contiguosly aggregated carriers.

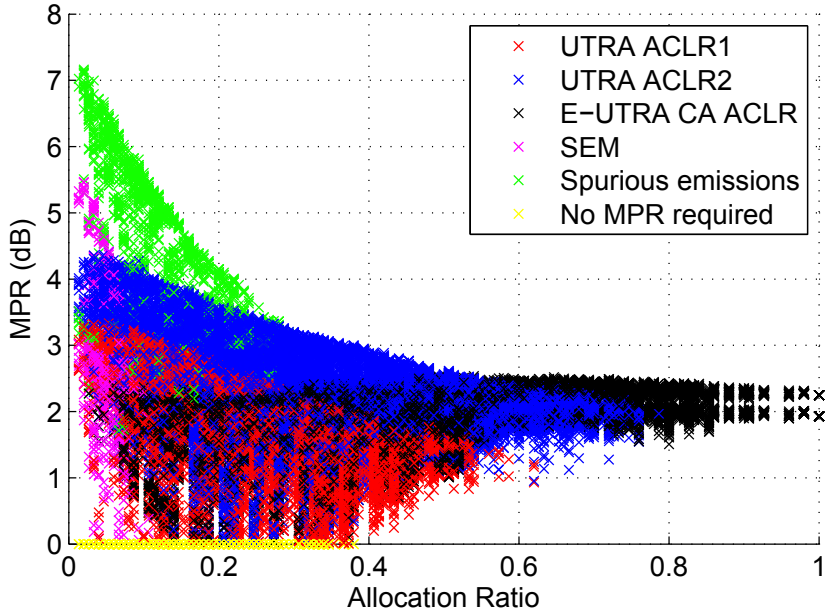

Figure 5.12. Gating factors for MPR in multicluster transmission in contiguously aggregated carriers.

It can be seen from Figure 5.10 that the MPR for contiguous allocation is not enough for multicluster transmission. To find out how much MPR is needed a group of 40000 randomly chosen allocations having one cluster in each CC were created and the required MPR was searched. Both QPSK and 16-QAM modulations were used with even distribution. The required MPR for each signal plotted as a function of allocation ratio are presented in Figure 5.11 together with the MPR mask in Equation 4.3.

It can be seen from Figure 5.11 that the results are well in line with the specifications. The greatest backoff is required with small allocation ratios because in

those cases the transmission power is localized to narrow bandwidths. The active RBs are at the outer edges of the CCs and fifth order intermodulation will fall on spurious region as seen also in Figure 5.10. When allocation size increases PSD will become lower and also lower MPR satisfies the requirements. When the allocation ratio increases even further no single IMD component breaches emission limits and ACLR limits become the gating factor. The gating factors for MPR are presented in Figure 5.12.

When additional emission requirements are present multicluster transmission becomes very challenging from linearity point of view. This is demonstrated with CA_NS_01 requirement in band 1, whose uplink is 1920 MHz – 1980 MHz. CA_NS_01 is signalled in Japan where legacy Personal Handy-phone System (PHS) operates below band 1. Also E-UTRA band 34 above band 1 has to be protected simultaneously. In addition to general emission requirements the limits presented in Table 5.1 are in force.

Duplexer attenuation to band 34 is assumed to be 15 dB in total. This includes the 4 dB insertion loss and therefore the simulations have been performed with a limit -39 dBm/MHz for band 34. Uplink center frequency was 1955 MHz and therefore the uplink aggregated channel bandwidth was contained in frequency range 1940 MHz – 1970 MHz. Simulation results for contiguous and non-contiguous allocations are shown in Figures 5.13 and 5.14.

From Figure 5.13 it can be seen that with contiguous allocation up to 11 dB A-MPR is required. With carrier aggregation A-MPR is not added on top of MPR and therefore it equals the required PA backoff. The region for this high A-MPRs is very narrow though and there are a lot of allocations which do not require any backoff. The situation is very similar to NS_07 with contiguous allocation in single carrier. However, because of the significantly wider bandwidth the intermodulation will reach much further and in this case fall on the strictly protected PHS band. When allocation is moved away from the channel edge the required A-MPR drops significantly as soon as the third order intermodulation does not reach to PHS band.

With multicluster allocation up to 15 dB A-MPR is required. Highest A-MPR is needed in cases where third order intermodulation will fall on PHS band i.e. when

Table 5.1. CA_NS_01 additional emission requirement. [20]

Frequency (MHz)	**Spectrum emission limit (dBm)**	**Meas. BW**
1884.5 – 1915.7	-41	300 kHz
2010 – 2025	-50	1 MHz

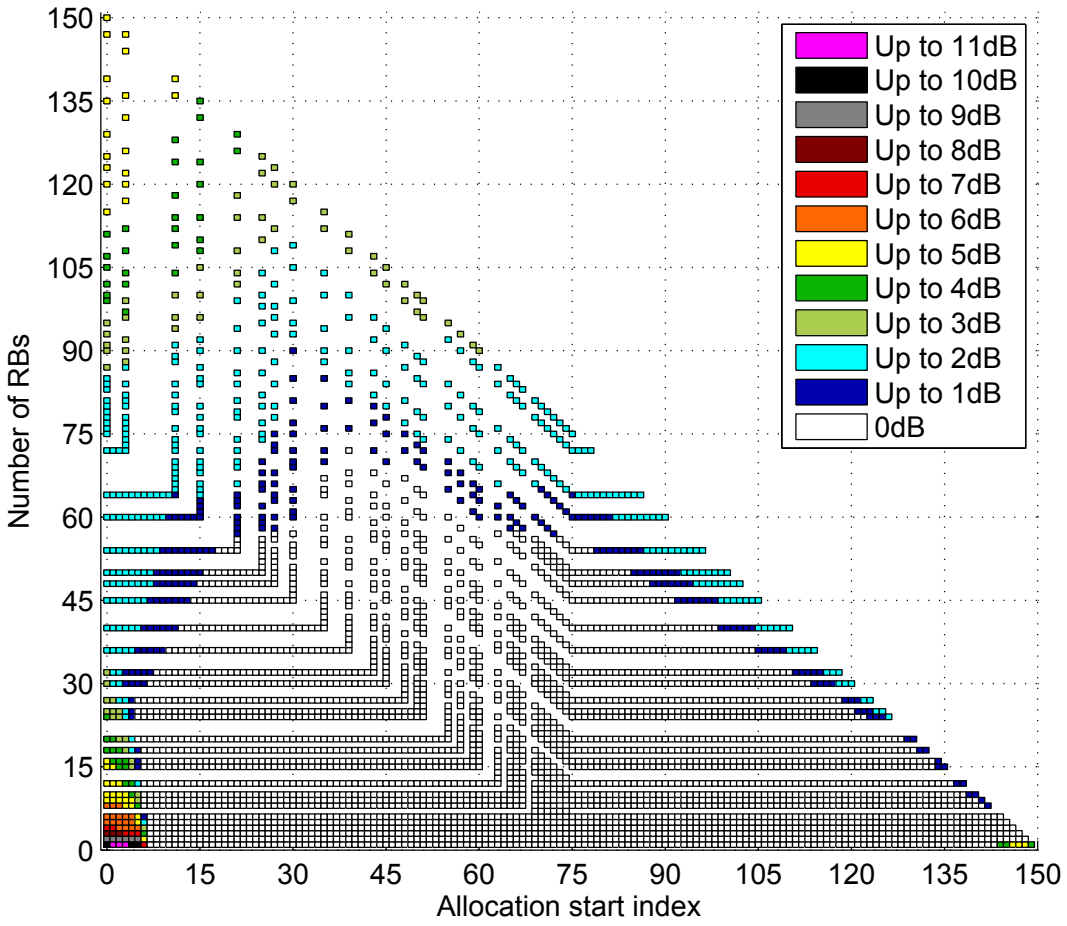

Figure 5.13. Required A-MPR for contiguous allocation in contiguosly aggregated carriers with additional emission requirement CA_NS_01.

allocations are at the outer edges of aggregated carriers. The thicker cloud which begins at 10 dB with low allocation ratio comes from allocations whose third order intermodulation does not reach PHS band but fifth order intermodulation does. Because highest MPR and A-MPR are needed to protect either spurious region or some additional requirement it would be practical to also take advantage of this information in MPR specifications.

One possible method to improve MPR specifications in a way which would result in less excess backoff is to calculate the range of low order intermodulation components for each allocation and use lower MPR when third or fifth order intermodulation does not reach the tightest requirement. With contiguous allocation this is already done in a way because the A-MPR is specified depending on both allocation start index and its size. Calculating the intermodulation range would be simple for multicluster allocation also because basically only information about the positions of outermost RBs is required. The possible gain can be seen from Figure 5.14. Instead of using the worst case A-MPR for all cases, a 5 dB improvement could be already achieved in this example by sorting out the ones where third order

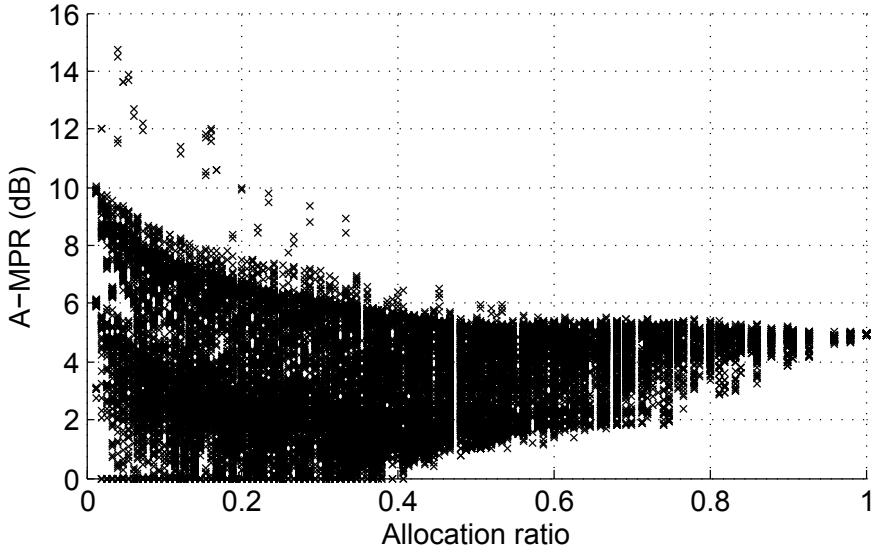

Figure 5.14. Required A-MPR for multicluster transmission in contiguosly aggregated carriers with additional emission requirement CA_NS_01.

intermodulation falls on PHS band. The gain comes at a cost of increased complexity which may be too much if different channel bandwidths and center frequencies would have to be studied separately.

5.4 Non-contiguous Transmission in Single Carrier (rel. 11)

Non-contiguous transmission in single carrier is introduced in release 11. The scheme is principally similar to multicluster transmission with contiguously aggregated carriers and also the specified MPR for does not greatly differ. The main difference is that the maximum absolute number of RBs is smaller than with carrier aggregation. This results in stronger intermodulation components with the same allocation ratio when compared to release 10. This is illustrated in Figures 5.15 and 5.16 which have allocations resulting in same allocation ratio of 0.25.

It can be seen in Figures 5.15 and 5.16 that very similar kind of allocations which are both gated by $\mathrm{UTRA}_{\mathrm{ACLR2}}$ result in slightly different MPR. This is the key property which explains the difference in multicluster masks in release 10 and 11 which are shown together in Figure 4.6.

The maximum MPR for multicluster transmission within a single carrier is 8 dB. It was verified with measurements that this is enough. An example spectrum showing the worst case allocation with 1 RB allocated at opposite edges of 20 MHz carrier is shown in Figure 5.17. 7 dB MPR was applied to signal which resulted in breaching the spurious emission limit by 0.3 dB. With 8 dB MPR the spurious emissions margin was already +1.6 dB.

When it comes to additional emission requirements multicluster transmission in single carrier is in many cases easier for the transmitter than multicluster in aggre-

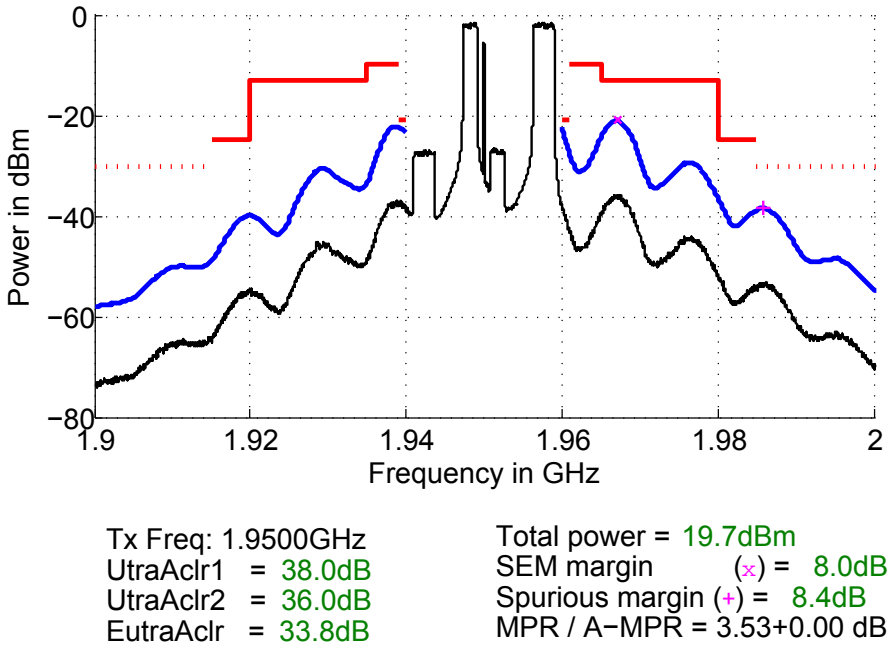

Figure 5.15. A release 11 signal: transmission power is limited by $\text{UTRA}_{\text{ACLR2}}$ and required MPR is 3.53 dB.

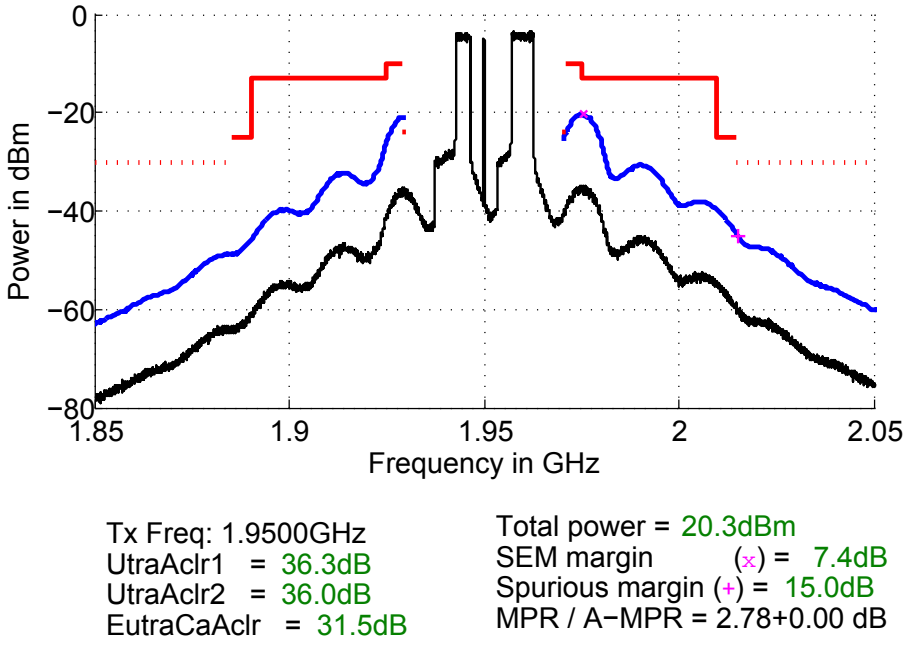

Figure 5.16. A release 10 signal: transmission power is limited by $\text{UTRA}_{\text{ACLR2}}$ and required MPR is 2.78 dB.

gated carriers. Main reason for this is that intermodulation will be closer to the wanted channel. However, if there are additional requirements present near the wanted channel then a lot of backoff may be required. The NS_07 requirement, which was discussed already in section 4.1, is one example of this kind of situation

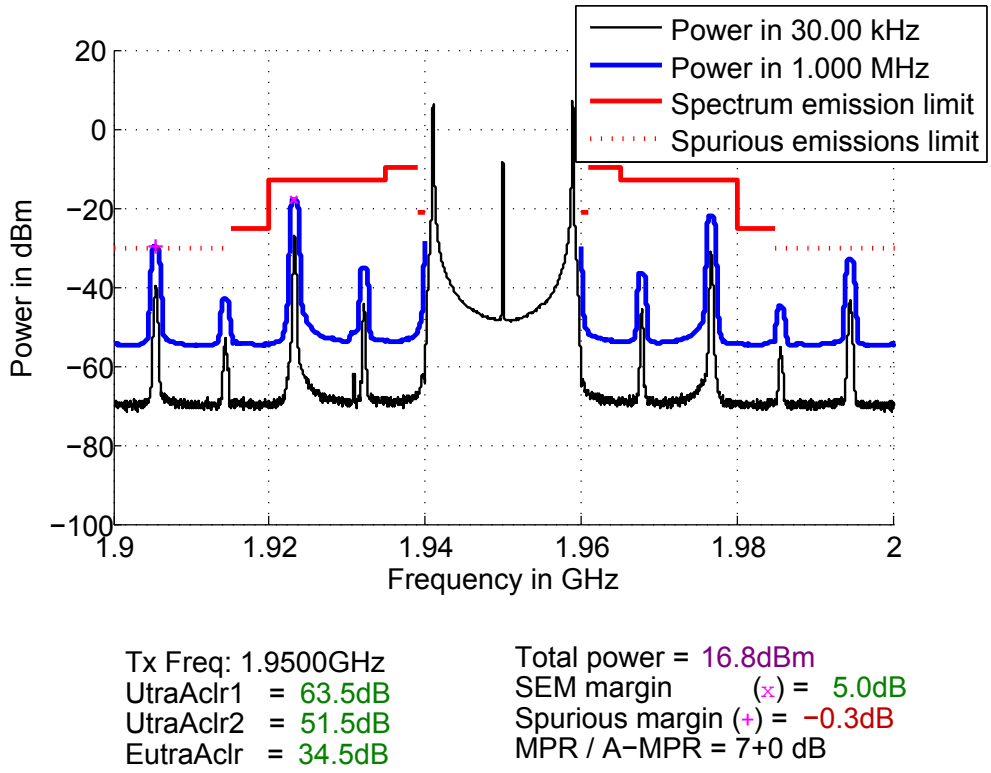

Figure 5.17. Measured spectrum of a multicluster signal having 1 RB allocated at opposite edges of 20 MHz carrier. 7 dB MPR is not enough to fulfill spurious emission requirement.

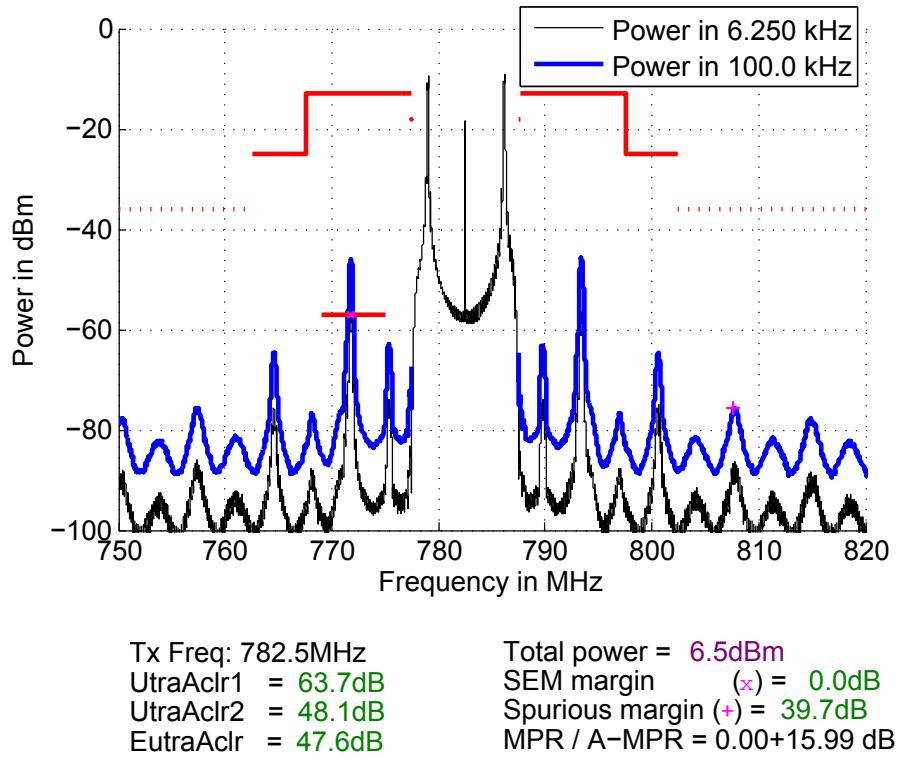

Figure 5.18. Spectrum of a multicluster signal with two 1 RB clusters together with NS_07 emission requirement. 16dB A-MPR is required to fulfill emission requirements.

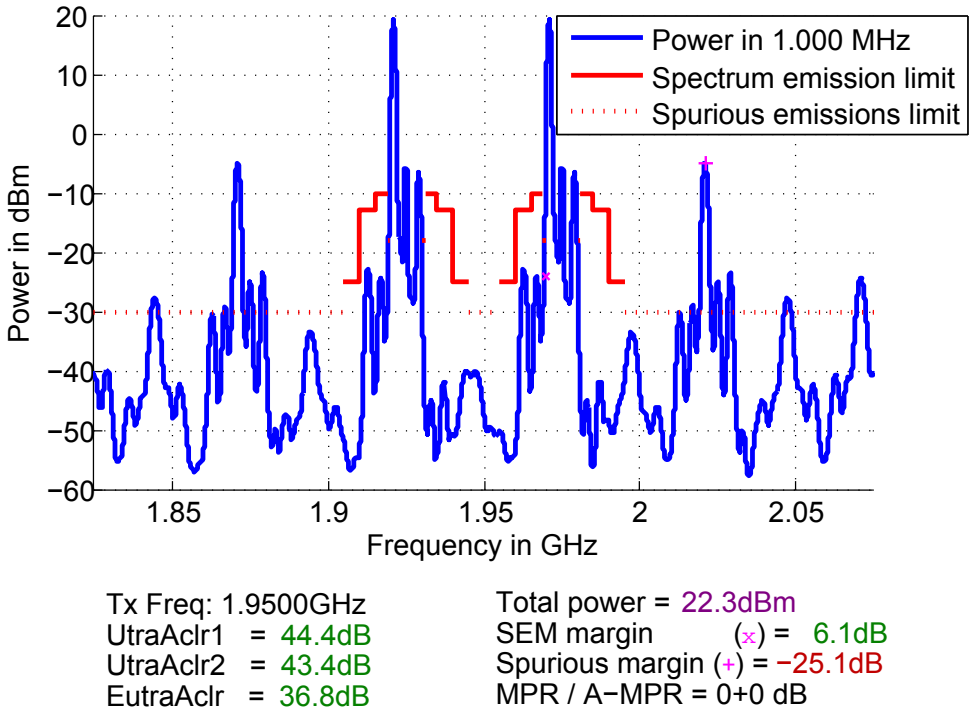

Figure 5.19. 5 RBs allocated in each 10 MHz sub-block. Third-order intermodulation products rise 25 dB above spurious emissions limit.

and an example of A-MPR requirement is shown in Figure 5.18.

It can be seen from Figure 5.18 that required A-MPR is almost 16 dB when the transmission consist of two 1 RB clusters. In practice it means that the maximum output power of an UE would be 5 mW in this scenario and the feasibility of multicluster transmission is questionable. Even though the possibility to allocate RBs non-contigously allows more flexibility and enables e.g. a way to avoid notches in channel response, the transmitter nonlinearity may be too big an obstacle in this kind of situations. Multicluster transmission within single carrier has not yet been specified with additional requirements.

5.5 Intra-band Non-contiguous Carrier Aggregation (rel. 12)

Non-contiguous carrier aggregation within a single E-UTRA band will became part of the uplink capabilities in release 12. It is a very challenging scenario because intermodulation components will fall very far from the wanted channels if the sub-block gap is wide. Using the single-PA architecture presented in Figure 4.7 means that the PA has be able to handle signals with a very wide gross bandwidth. Because of the variety of possible bandwidth combinations and different sub-block gap bandwidths it is not straightforward to specify MPR in a way which would cover all the scenarios with limited excess backoff.

When the sub-block gap bandwidth is wide third-order intermodulation will fall

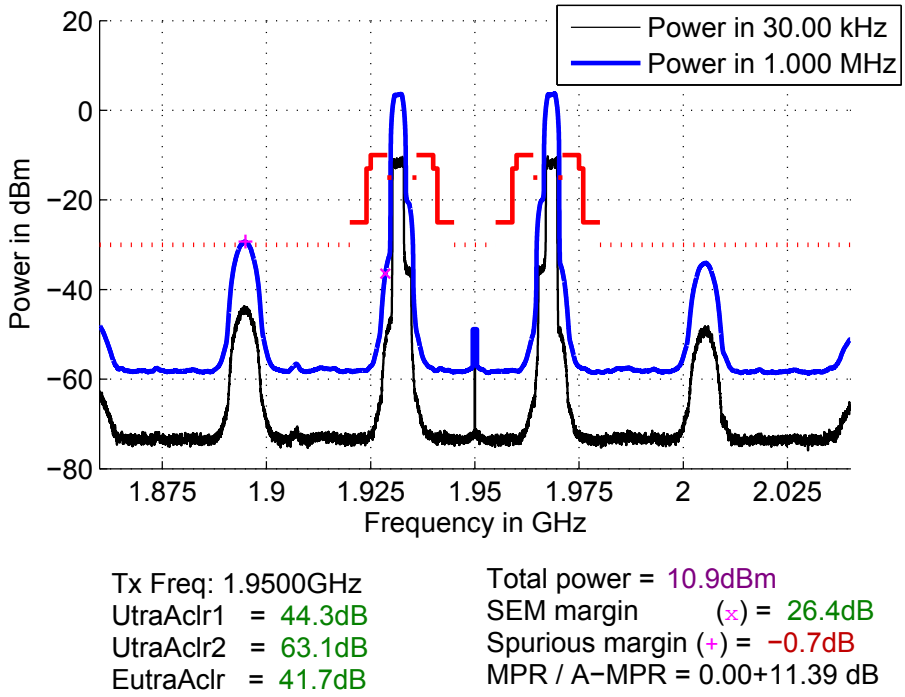

Figure 5.20. Measured spectrum of two fully allocated 5 MHz channels with 30 MHz sub-block gap.

on spurious region. This inherently means that the required backoff will be greater than in previous releases. Because of the used transmitter architecture each sub-block has its own IQ-image and carrier leakage. The final output spectrum therefore consists of several different components which will both degrade the own transmit signal quality and also cause interference to other users. An example spectrum is shown in Figure 5.19.

In Figure 5.19 the spurious emissions limit is exceeded by over 25 dB. Approximately 11 dB backoff was required to reach the emission limits even though there are no additional requirements present. When the allocation size increases PSD will get lower and the power in intermodulation components will disperse into wider bandwidth. Therefore the required MPR will diminish similarly as in other non-contiguous allocation schemes.

Because of the wide bandwidth memory effects, i.e. frequency selectivity, of the PA are also significant. The quasi-memoryless model used in simulations cannot model them which causes some inaccuracies in simulations. With real PA the emission spectrum can be asymmetric even though the allocation is symmetric. This is demonstrated in Figure 5.20 which shows two fully allocated 5 MHz carriers with 30 MHz sub-block gap.

In Figure 5.20 IMD3 component is significantly stronger below the wanted channels. The carrier leakage seen at 1.95 GHz comes from the VSG. If the total power in intermodulation components stays constant the uneven division of power leads

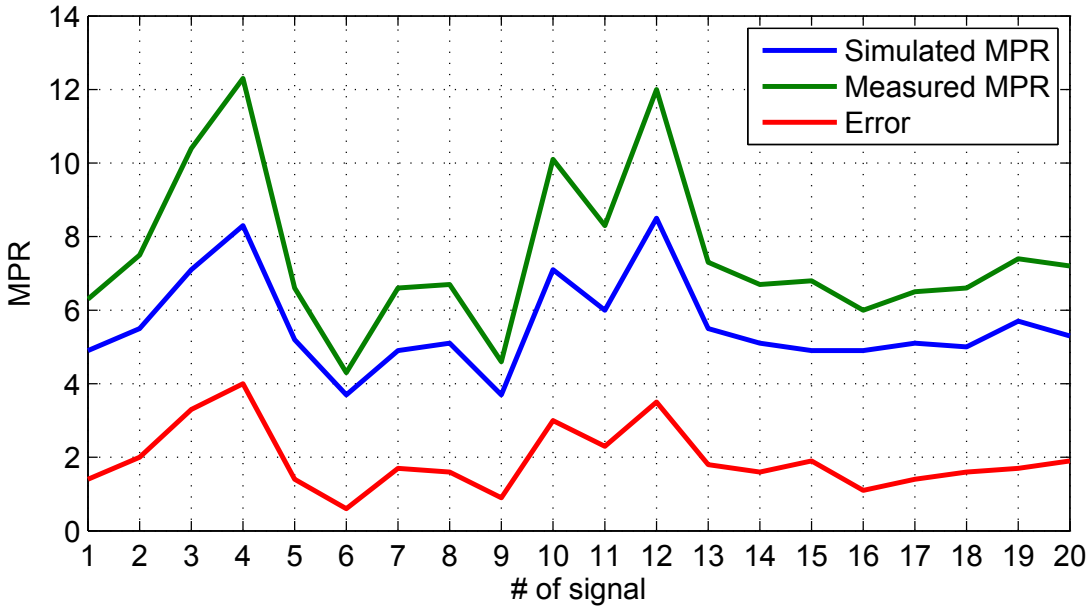

Figure 5.21. Difference between measured and simulated MPR with non-contiguous intraband carrier aggregation.

to higher MPR. Therefore the memory effects should be taken into account also in simulations. This means that the used PA model should be more complex which leads to longer simulation times. The error between simulations and measurements was studied with a group of different allocations which had one contiguous RB cluster placed in each sub-block. The used channel configuration was 5 + 5 MHz with 30 MHz sub-block gap bandwidth. The measured and simulated MPR and the difference between them are shown in Figure 5.21.

It can be seen in Figure 5.21 that the error between measurements and simulations is approximately 1-4 dB and measured MPR is consistently higher than simulated. Otherwise simulation and measurement results follow each other well and the allocatios requiring highest MPR are the same for both. The simulation model is behaving similarly as the real PA, but it is able to capture only the memoryless nonlinearity and therefore the results do not perfectly match. In practise this means that the quasi-memoryless PA model is not sufficient to accurately model the intermodulation distortion generated in intraband non-contiguous carrier aggregation transmission.

5.6 Own Receiver Desensitization (rel. 11)

One additional problem with non-contiguous intraband carrier aggregation is that the intermodulation components may fall on the own downlink band and desensitize own receiver. This happens because the effective duplex gap gets significantly

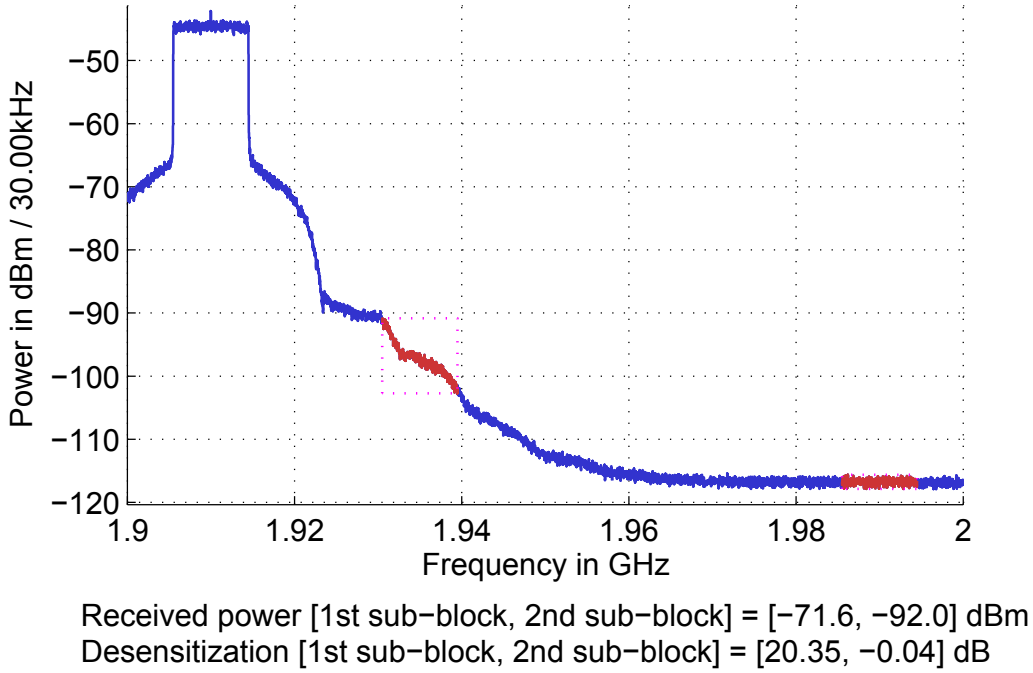

Figure 5.22. Received spectrum with fully allocated 10 MHz uplink and no downlink signal. Own uplink transmission causes over 20 dB desensitization on the sub-block nearer to the uplink.

narrower when the additional sub-block is introduced as shown in Figure 4.10. In practice the desensitization means that own reception is impaired when the received signal power is already low, e.g. when path loss between base station and UE is large and transmitter has to use high power levels.

The desensitization of the own receiver was studied using band 25 as an example. The simulation configuration was adopted from release 11 where non-contiguous intraband carrier aggregation can be used in downlink and the duplex gap can taper down to a minimum of 15 MHz. An example of a received spectrum is shown in Figure 5.22 where a fully allocated 10 MHz uplink is transmitted and no downlink signal is present. The isolation between transmitter and receiver chains is assumed to be 50 dB, which is a realistic duplexer isolation taking also parasitic coupling into account. First the received spectrum is analyzed with only background noise present. This defines the reference sensitivity for the receiver. Then uplink is activated and the difference in received power on the downlink channel is the desensitization. When a 10 MHz downlink channel is placed at the minimum duplex gap distance of 15 MHz the receiver suffers from over 20 dB desensitization.

The effect of sub-block gap bandwidth and allocation size on self-desensitization was studied using 5 + 5 MHz and 10 + 10 MHz bandwidth configurations with RBs allocated only to the uplink channel which is closer to downlink. The uplink allocation was always placed to the worst case position, i.e. the upper edge of the

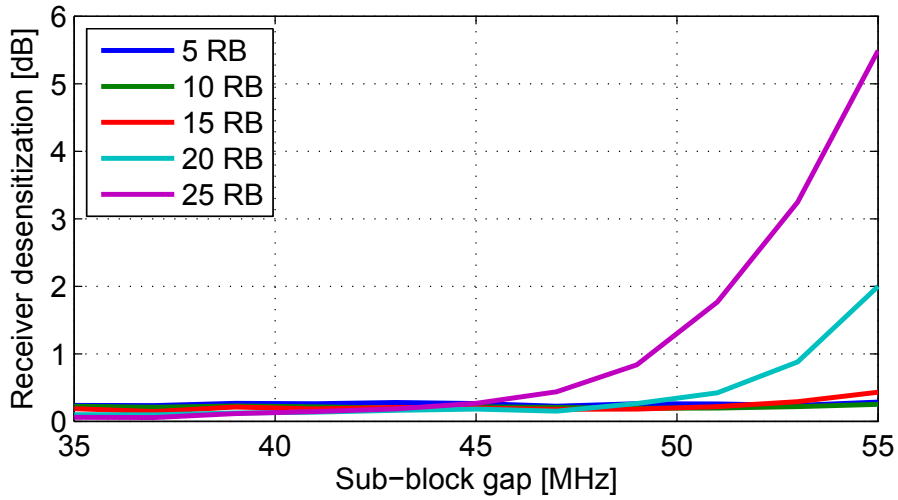

Figure 5.23. Receiver desensitization with 5 + 5 MHz channel configuration.

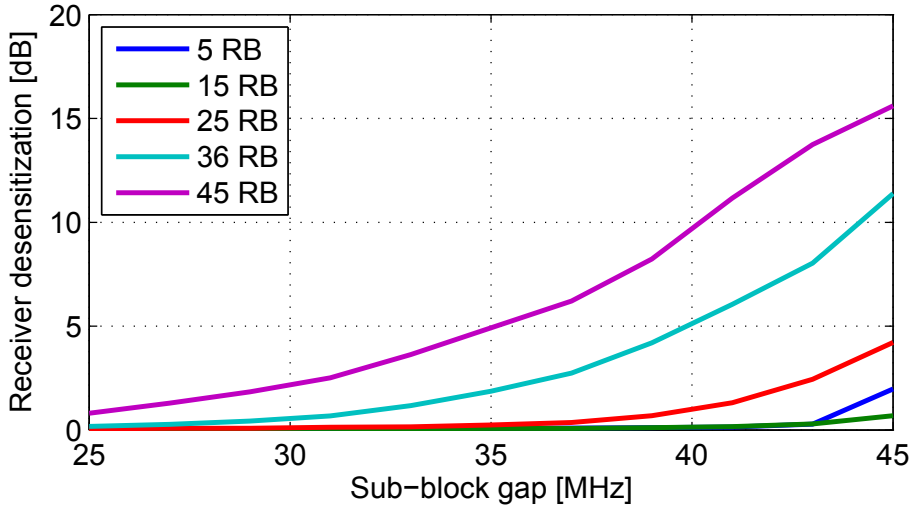

Figure 5.24. Receiver desensitization with 10 + 10 MHz channel configuration.

channel. The sub-block gap bandwidth was swept with different allocation sizes and desensitization was calculated. Because only one uplink carrier is active the used MPR for uplink transmission was applied according to release 8 specifications. The simulation results are shown in Figures 5.23 and 5.24.

It can be seen in Figure 5.23 that with 5 + 5 MHz channel configuration there is no severe desensitization when the sub-block gap bandwidth is 45 MHz or narrower regardless of allocation size. When the allocation size is 15 RB or smaller less than 0.5 dB desensitization will occur regardless of sub-block gap bandwidth. When the channel configuration is changed to 10 + 10 MHz the desensitization is much more severe as seen in Figure 5.24. To be able to transmit 45 RB allocation with less than 1 dB desense the sub-block gap must be smaller than 25 MHz. On the other hand desensitization with 5 RB allocation is also near to 1 dB with the

widest possible sub-block gap. If the used channel bandwidths were increased the situation would became more and more problematic. If no performance degradation is allowed the channels would have to be organized almost similarly as in intra-band contiguous carrier aggregation. When the second uplink carrier is activated the power of intermodulation components falling on own downlink frequencies will increase significantly. Therefore intraband non-contiguous carrier aggregation is a very challenging scheme for both mobile transmitter and receiver and it should be carefully studied which E-UTRA bands are suitable for it.

6. CONCLUSIONS

In this thesis linearity requirements of LTE-Advanced mobile transmitter has been addressed. First LTE and the basic mathematical models for transmitter nonlinearities were introduced. Then the evolution of LTE to LTE-Advanded up to release 12 was discussed considering the new features which are essential from the linearity point of view. Simulation and measurement results of the transmitter performance in those transmission schemes were also presented.

The main purpose of the thesis was to illustrate how transmitter nonlinearities affect the transmitted spectrum and how this has to be taken into account in the system specifications. The linearity requirements of the transmitter can be considered from different perspectives. On one hand linearity requirements do not change if spectrum emission limits stay constant. On the other hand the transmitted waveform may require higher linearity from the transmitter so that regulatory limits can be fulfilled. In this thesis the analysis is made from the latter point of view.

It was seen that with small, cheap, efficient and mass-producible mobile transmitters the maximum transmission power has to be lowered with certain waveforms to reach the regulatory emission requirements. In practice this is done by lowering the PA input level and therefore making the response of the PA more linear. In basic release 8 scenarios maximum of 2 dB MPR is needed. However, when carriers are aggregated and non-contiguous frequency domain resource allocation is used the amount of required PA backoff increases significantly, meaning that the scenario is more difficult to the transmitter from the linearity point of view. When additional spectrum emission requirements are present over 15 dB A-MPR is needed. Lower maximum transmission power affects link quality and forces the PA to operate in a less power efficient bias point. Still it is essential that the interference levels are kept in control so that the none of the coexisting wireless systems suffers from overwhelming performance degradation. In practise there must a working balance between cost and size of the mobile transmitter, emission requirements and additional relaxations on transmitter requirements. Therefore spectrum emission limits and relaxations on maximum transmission power requirements have to be carefully considered in system specifications.

Overall the frequency domain flexibility of LTE-A is very challenging to the transmitter and transmitter nonlinearities may also impair own reception. This sets high

requirements for the transmitter and the isolation between transmitter and receiver chains. PA designs should be able to handle bandwidths up to 100 MHz while maintaining both efficiency and linearity. One additional challenge will be the multiband and multimode operation. Because different frequency bands and different technologies are used in different geographical areas, mobiles should be able to use wide variety of them which makes the optimization of components more difficult. The analysis of nonlinearities in transmitters and e.g. the gating factors in reaching emission requirements may be used in this process.

One way to enable using efficient and nonlinear transmitters is cancelling the effects of nonlinearity. This can be done e.g. by predistorting the digital baseband in such a way that the total response of the transmitter is as linear as possible. Digital predistoring becomes more and more attracting option as computing power in mobiles increase. To be able to perform predistortion the transmitter response has to be accurately modeled. This is a great motivation for developing more accurate simulation models also.

The analysis performed in this thesis can be used to help the standardization process. MPR specifications are one part of the radio performance which is the main concern of 3GPP TSG RAN WG4. Simulation results are needed to evaluate different scenarios which may be added to the standard.

Additionally the analysis presented in this thesis may be used in developing intelligent RRM and scheduling algorithms. When the most difficult scenarios in linearity sense are known they can also be avoided. If channel state information is available in scheduling then linearity requirements can be taken into account when assigning resources. Also in cognitive radio the flexible spectrum usage will be in an important role and it is essential to understand how our own transmission will interfere others.

Future Outlook

The next major improvement in uplink capabilities of LTE-A will be interband carrier aggregation where two carriers placed in different E-UTRA bands are transmitted simultaneously. Interband carrier aggregation may became a very popular scheme in real implementations because it corresponds well the actual spectrum resources which mobile operators have. Therefore interband carrier aggregation may offer a more visible improvement to traffic capacity and throughput than the previous updates.

However, interband carrier aggregation also has its own challenges. Because the frequency separation between E-UTRA bands can be large a two PA transmitter architecture will most probably be used. This means that the intermodulation generated in a single PA will not be as severe as in e.g. intraband non-contiguous carrier

aggregation. However, the outputs of the two PAs introduce intermodulation which may degrade receiver performance. Because the frequency separation between the carriers can be very large the intermodulation may also fall between the carriers, which has not been the case before. If the PAs are placed in a common enclosure the leakages between PAs have to be controlled.

Another major trend has been moving up to higher and higher frequencies because there is more spectrum available. Higher frequencies are better suited for shorter distances and they can be used e.g. indoors in so called home-eNodeBs. The idea is to have one or more base stations in a building and use it to offload traffic from macrocells. In addition small cells can be used in machine-to-machine communications and create networks between devices in the building. Also LTE and wireless local area network integration is under planning to increase capacity indoors which will be needed as internet-of-things becomes reality.

In the future also the role of MIMO will become more and more important. In addition to reusing resources and increasing throughput, MIMO can be used to control interference via beamforming. Beamforming can also be used in cognitive radio concept e.g. to minimize interference towards primary users and aiming the antenna beam towards the wanted transmission. One of the challenges in using MIMO will be placing several uncorrelated antennas to mobiles.

REFERENCES

[1] International Telecommunication Union, World Telecommunication/ICT Indicators Database. [WWW] available http://www.itu.int/ITU-D/ict/statistics/, referenced 12.9.2012

[2] K. Mallinson, 2020 Vision for LTE, [WWW] available http://www.3gpp.org/IMG/pdf/wiseharbor.pdf, referenced 12.9.2012

[3] K. David, S. Dixit and N. Jefferies, The Wireless World Research Forum Looks to the Future, IEEE Vehicular Technology Magazine Volume 5 Issue 3, Sept. 2010

[4] H. Holma & A. Toskala, LTE for UMTS, OFDMA and SC-FDMA Based Radio Access. West Sussex, John Wiley & Sons Ltd., 2009

[5] Nokia, R1-072261 LTE Performance Evaluation – Uplink Summary, [WWW], available http://www.3gpp.org/ftp/specs/html-info/TDocExMtg--R1-49--26034.htm, referenced 18.10.2012

[6] Ericsson, R1-072578 Summary of Downlink Performance Evaluation, [WWW], available http://www.3gpp.org/ftp/specs/html-info/TDocExMtg--R1-49--26034.htm, referenced 18.10.2012

[7] H. Holma and A. Toskala, WCDMA for UMTS - HSPA evolution and LTE, 4th edition. est Sussex, John Wiley & Sons Ltd., 2007

[8] S.C. Cripps, Advanced Techniques in RF Power Amplifier design. Norwood, MA: Artech House Publishers, 2002

[9] V. Lehtinen, T. Lähteensuo, P. Vasenkari, A. Piipponen, M. Valkama, Gating Factor Analysis of Maximum Power Reduction in Multicluster LTE-A Uplink Transmission, In proceedings of IEEE RWW2013

[10] C. Gessner, Long Term Evolution - A concise introduction to LTE and its measurement requirements. Munich, Rohde & Schwarz GmbH & Co., 2011

[11] E. Dahlman, S. Parkvall and J. Sköld, 4G LTE/LTE-Advanced for Mobile Broadband. Amsterdam, Elsevier Ltd., 2011

[12] S. Sesia, I. Toufik and M. Baker, LTE – The UMTS Long Term Evolution, From Theory to Practice, est Sussex, John Wiley & Sons Ltd., 2008

[13] 3rd Generation Partnership Project, LTE. [WWW], available http://www.3gpp.org/LTE, referenced 6.10.2012

[14] 3rd Generation Partnership Project, Releases. [WWW], available http://www.3gpp.org/Releases, referenced 6.10.2012

[15] 3rd Generation Partnership Project, The Partners. [WWW] available http://3gpp.org/Partners, referenced 6.10.2012

[16] 3rd Generation Partnership Project, Specification Groups. [WWW], available http://3gpp.org/Specification-Groups, referenced 18.10.2012

[17] 3rd Generation Partnership Project, Calendar. [WWW], available http://3gpp.org/Calendar, referenced 18.10.2012

[18] 3rd Generation Partnership Project, Specifications. [WWW], available http://3gpp.org/Calendar, referenced 18.10.2012

[19] 3GPP, Overview of 3GPP Release 8 V0.2.8 (2012-09), [WWW], available http://www.3gpp.org/ftp/Information/WORK_PLAN/Description_Releases/, referenced 20.10.2012

[20] 3GPP, Evolved Universal Terrestrial Radio Access (E-UTRA); User Equipment (UE) radio transmission and reception. [WWW], available http://www.3gpp.org/ftp/Specs/html-info/36101.htm, referenced 23.11.2012

[21] D. Schoolar, LTE TDD Goes Mainstream, WinWin Magazine issue (11/2012), Huawei. [WWW], available http://www.huawei.com/en/static/HW-196686.pdf, referenced 18.11.2012

[22] 3GPP, Evolved Universal Terrestrial Radio Access (E-UTRA); LTE physical layer; General description. [WWW] available http://www.3gpp.org/ftp/Specs/html-info/36201.htm, referenced 23.11.2012

[23] Nokia Siemens Networks, The impact of latency on application performance. [WWW], available http://www.nokiasiemensnetworks.com/system/files/document/LatencyWhitepaper.pdf, referenced 18.11.2012

[24] M. Sauter, Beyond 3G - Bringing networks, terminals and the web together, West Sussex, John Wiley & Sons Ltd., 2009

[25] S. Hämäläinen, H. Sanneck and Cinzia Sartori, LTE Self-Organizing Networks (SON): Network Management Automation for Operational Efficiency. West Sussex, John Wiley & Sons Ltd., 2012

[26] C. Shannon, A Mathematical Theory of Communication, Bell System Technical Journal vol. 27, 1948. [WWW] available http://cm.bell-labs.com/cm/ms/what/shannonday/shannon1948.pdf, referenced 19.11.2012

[27] H. Schulze and C. Lueders, Theroy and Applications of OFDM and CDMA: Wideband Wireless Communications. est Sussex, John Wiley & Sons Ltd., 2005

[28] S. Saunders and A. Zavala, Antennas and Propagation for Wireless Communication Systems, 2nd edition. est Sussex, John Wiley & Sons Ltd., 2007

[29] M. Bruno, J. Cousseau, A. Shahed Hagh Ghadam and M. Valkama, On high linearity - high efficiency RF amplifier design. Proceedings of the Argentine School of Micro-Nanoelectronics, Technology and Applications 2010, Montevideo, 2010

[30] 3GPP, Evolved Universal Terrestrial Radio Access (E-UTRA); Physical channels and modulation. [WWW] available `http://www.3gpp.org/ftp/Specs/html-info/36211.htm`, referenced 23.11.2012

[31] A. Carlsson, Communication Systems: An Introduction to Signals and Noise in Electrical Communication, 4th edition. New York, McGraw-Hill Companies Inc., 2002

[32] J. Vuolevi and T. Rahkonen, Distortion in RF Power Amplifiers, Norwood, MA: Artech House Publishers, 2003

[33] J. Proakis, Digital Communications, 4th edition. New York, McGraw-Hill Companies Inc., 2000

[34] S. Sen, S. Devarakond and A. Chatterjee, Phase Distortion to Amplitude Conversion-Based Low-Cost Measurement of AM-AM and AM-PM Effects in RF Power Amplifiers, IEEE Transactions on Very Large Scale Integration (VLSI) Systems, Issue 99, pp. 01-13, 2011

[35] L. Anttila, Digital Front-End Signal Processing with Widely-Linear Signal Models in Radio Devices, Ph.D. dissertation, Dept. Information Technology, Tampere Univ. Technology, Tampere, Finland, 2011

[36] K. Martin, Complex Signal Processing is Not – Complex. in IEEE Transactions of Circuits and Systems, vol 51, no. 9, Sept. 2003

[37] S. Haykin, Communication Systems, 4th edition. est Sussex, John Wiley & Sons Ltd., 2001

[38] J. Marttila, Quadrature Sigma-Delta ADCs: Modeling and Signal Processing, M.Sc. Thesis, Dept. Information Technology, Tampere Univ. Technology, Tampere, Finland, 2010

[39] B. Razavi, RF transmitter architectures and circuits. Proceedings of the IEEE 1999 Custom Integrated Circuits, 1999.

[40] Cisco Systems Inc., Digital Transmission: Carrier-to-Noise Ratio, Signal-to-Noise Ratio, and Modulation Error Ratio. [WWW] available http://www.cisco.com/en/US/prod/collateral/video/ps8806/ps5684/ps2209/prod_white_paper0900aecd805738f5.pdf, referenced 25.1.2013 sed Transceivers. est Sussex, John Wiley & Sons Ltd., 2012

[41] 3GPP, Evolved Universal Terrestrial Radio Access (E-UTRA); Base Station (BS) conformance testing. [WWW] available http://www.3gpp.org/ftp/Specs/html-info/36141.htm, referenced 23.1.2013

[42] L. Smaini, RF Analog Impairments Modeling for Communication Systems Simulation: Application to OFDM-ba

[43] Ericsson, High efficiency power amplifiers. [WWW] available http://www.ericsson.com/in/ericsson/corpinfo/publications/review/2006_03/files/1_pa.pdf

[44] Agilent Technologies Inc., PNA-X Application: Power-Added Efficiency (PAE). [WWW] available http://cp.literature.agilent.com/litweb/pdf/5989-7293EN.pdf

[45] Y. Jeon, J. Cha and S. Nam, High-Efficiency Power Amplifier Using Novel Dynamic Bias Switching. IEEE Transactions on Microwave Theory and Techniques, Vol. 55, no. 4, April 2007

[46] A. A. Abidi, Direct-Conversion Radio Transceivers for Digital Communications, IEEE Journal of Solid-State Circuits, Vol. 30 No. 12, Dec. 1995

[47] 3GPP, Feasibility study for Further Advancements for E-UTRA (LTE-Advanced). [WWW] available http://www.3gpp.org/ftp/Specs/html-info/36912.htm, referenced 8.1.2013

[48] J. Weldon, High Performance CMOS Transmitters for Wireless Communications, Ph.D dissertation, University of California, Berkeley, 2005

[49] M. Ryan, M. Frater and M. Pickering, Fundamentals of Communications and Information Systems, Argos Press, 2011

[50] Ke. Du, M. Swamy, Wireless Communication Systems From RF Subsystems to 4G Enabling Technologies. Cambridge University Press, Cambridge, 2010

[51] A. Shahed, Contributions to Analysis and DSP-based mitigation of Nonlinear Distortion in Radio Transceivers, Ph.D. dissertation, Dept. Information Technology, Tampere Univ. Technology, Tampere, Finland, 2011

[52] G. Tong Zhou, H. Qian, L. Ding and R. Raich, On the Baseband Representation of a Bandpass Nonlinearity. IEEE Transactions on Signal Processing Vol. 53, issue 8, Aug. 2005

[53] C.Rapp, Effects of the HPA-nonlinearity on a 4DPSK/OFDM signal for a digitals ound broadcasting system, Conf. Rec. ECSC'91, Luettich, Oct. 1991

[54] Agilent Technologies Inc., AM-PM Conversion. [WWW] available `http://na.tm.agilent.com/pna/help/WebHelp7_5/Tutorials/AM-PM.htm`, referenced 21.1.2013

[55] J. Pedro & N. Carvalho, Intermodulation Distortion in Microwave and Wireless Circuits, Norwood, Artech House Inc., 2003

[56] Fujitsu, R4-125738 Band 1 PA model. [WWW] available `http://www.3gpp.org/ftp/tsg_ran/WG4_Radio/TSGR4_64bis/Docs/`, referenced 21.1.2013

[57] L. Ding, Digital Predistortion of Power Amplifiers for Wireless Applications, Ph.D. dissertation, School of Electrical and Computer Engineering, Georgia Institute of Technology, Georgia, USA, 2004

[58] J. Pedro and S. Maas, A Comparative Overview of Microwave and Wireless Power-Amplifier Behavioral Modeling Approaches, IEEE Transactions on Microwave Theory and Techniques, Vol. 53, no. 4, April 2005

[59] M. Valkama, Advanced I/Q Signal Processing for Wideband Receivers: Models and Algorithms, Ph.D. dissertation, Tampere Univ. Technology, Tampere, Finland, 2001

[60] International Telecommunication Union Radio Communication Sector, Recommendation ITU-R SM.329-12 Unwanted emissions in the spurious domain. [WWW] available `http://www.itu.int/dms_pubrec/itu-r/rec/sm/R-REC-SM.329-12-201209-I!!PDF-E.pdf`, referenced 25.1.2013

[61] Motorola, R1-062061, Uplink DC subcarrier distortion considerations in LTE, [WWW], available `http://www.3gpp.org/ftp/tsg_ran/WG1_RL1/TSGR1_46/Docs/`, referenced 22.02.2013

[62] Y. Li, R. Zhu, D. Prikhodko, Y. Tkachenko, LTE power amplifier module design: Challenges and trends, 10th IEEE International Conference on Solid-State and Integrated Circuit Technology (ICSICT), 2010

[63] Nokia Corporation, R4-121205, Way forward for non-contiguous intraband transmitter aspects, [WWW], available http://www.3gpp.org/ftp/tsg_ran/WG4_Radio/TSGR4_62/Docs/, referenced 10.02.2013

[64] Nokia Corporation, R4-110955, MPR for LTE multi cluster transmission, [WWW], available http://www.3gpp.org/ftp/tsg_ran/WG4_Radio/TSGR4_58/Docs/, referenced 10.02.2013

[65] Nokia Corporation, R4-124353, Non-contiguous intra-band reference transmitter architecture, [WWW], available http://www.3gpp.org/ftp/tsg_ran/WG4_Radio/TSGR4_64/Docs/, referenced 10.02.2013

[66] Nokia Corporation, R4-124353, Non-contiguous intraband unwanted emission, [WWW], available http://www.3gpp.org/ftp/tsg_ran/WG4_Radio/TSGR4_64/Docs/, referenced 10.02.2013

[67] Nokia Corporation and ZTE, R4-124922, Non-contiguous intraband CA ACLR, [WWW], available http://www.3gpp.org/ftp/tsg_ran/WG4_Radio/TSGR4_64/Docs/, referenced 10.02.2013

[68] Ericsson and ST-Ericsson, R4-123796, UE reference sensitivity requirement with one UL carrier, [WWW], available http://www.3gpp.org/ftp/tsg_ran/WG4_Radio/TSGR4_64/Docs/, referenced 15.02.2013

[69] Ericsson and ST-Ericsson, R4-123797, UE reference sensitivity requirement with two UL carriers, [WWW], available http://www.3gpp.org/ftp/tsg_ran/WG4_Radio/TSGR4_64/Docs/, referenced 15.02.2013